THE DECELLULARIZED HUMAN UMBILICAL VEIN (HUV)

AS AN ALLOGENEIC SCAFFOLD FOR VOCAL FOLD TISSUE ENGINEERING

APPROVED BY SUPERVISORY COMMITTEE

_____

Roger W. Chan, Supervising Professor

_____

Robert Eberhart

_____

Karen Pawlowski

THE DECELLULARIZED HUMAN UMBILICAL VEIN (HUV) AS AN ALLOGENEIC SCAFFOLD FOR VOCAL FOLD TISSUE ENGINEERING

by

Maritza Lizette Rodriguez

THESIS

Presented to the Faculty of the Graduate School of Biomedical Sciences

The University of Texas Southwestern Medical Center at Dallas

In Partial Fulfillment of the Requirements

For the Degree of

MASTER OF SCIENCE

The University of Texas Southwestern Medical Center at Dallas

Dallas, Texas

August, 2007

ACKNOWLEDGEMENTS

I would like to express my gratitude to the entire biomedical engineering program faculty at the University of Texas Southwestern Medical Center at Dallas as well as at the University of Texas at Arlington for sharing their time and knowledge. Thanks to my advisor Dr. Roger W. Chan for providing me the opportunity to work on a project that was not only challenging, but interesting. I could not have completed this without his guidance, patience, and knowledge.

I would like to thank the members in my lab, Chet Xu, Min Fu, and George Adams for their assistance with the experiments and data processing; as well as Dr. Karen Pawlowski and Paula Johnstone for their vital participation with the histological staining and analysis. Thanks to Dr. Eberhart for his thesis advice and materials, and for always taking the time to help me understand his class material. Also, thanks to Dr. Peter McFetridge from the University of Oklahoma for sharing his knowledge and for supplying the necessary samples to conduct these experiments. Kay Emerson, thank you for always having an open door and a listening ear, for always watching over all her students, and for always giving the most caring advice.

I would also like to thank my family; my mother, my father, and my brother for giving me the support I need to pursue my educational goals. I thank my mother always talking to me and encouraging me even when I am completely exhausted. I thank my father for giving me sound advice as well as comedic relief when I need it the most. I thank my brother for listening to me when I really need to talk.

Most importantly I would like to thank God for blessing me with my family, my experiences, and with all of the opportunities I have received thus far. This study was supported by the National Institutes of Health, NIDCD Grant R01 DC006101.

Maritza L. Rodriguez

August, 2007

THE DECELLULARIZED HUMAN UMBILICAL VEIN (HUV)

AS AN ALLOGENEIC SCAFFOLD FOR VOCAL FOLD TISSUE ENGINEERING

Maritza Lizette Rodriguez

The University of Texas Southwestern Medical Center at Dallas, 2007

Supervising Professor: Roger W. Chan, Ph.D.

The human umbilical vein (HUV) has great potential for use as a biological tissue engineering scaffold. Thus far, it has been used as an extracellular matrix (ECM) scaffold for cardiovascular tissue engineering applications due to its many structural and biomechanical advantages. Since the HUV is vascular derived, the chemical and physical environment from which it came allows it to be more conducive to cell adhesion and ECM remodeling than currently available synthetic scaffold materials. The connective tissue component of the HUV is primarily the Wharton's Jelly (WJ), a gelatinous connective tissue surrounding the umbilical cord vessels. It is rich in peptide growth factors, glycosaminoglycans (GAGs), and proteoglycans, many of which are similar to those present in the vocal fold lamina propria. The vocal fold undergoes vibrations at relatively large amplitudes (1-2mm) and relatively high frequencies (100- 300Hz), thus requiring a scaffold that could endure such mechanical stimuli. The lamina propria consists of proteoglycans, glycosaminoglycans (especially hyaluronic acid), and fibrous proteins (collagen and elastin) that are optimally designed to withstand the unique mechanical stimuli. The natural biological constituents of the human umbilical vein, its structural stability, and the novel method for preparing uniform specimens make this tissue potentially useful as a vocal fold scaffold. Also, as a potential allograft, the possibility of interspecies viral infectivity is low. Native HUV tissue is obtained with an automated dissection method developed by Daniel et al. (2005), where HUVs are dissected from umbilical cords

within two to three minutes, with uniform and repeatable dimensions using a custom built steel-cutting machine. Preliminary experiments were conducted to determine the optimal decellularization protocol. Once this was determined, 15 cords were obtained to further examine the potential of the HUV as an acellular scaffold. Three cords from different donors (each sliced into 3 sections or scaffolds) were examined as follows: manually dissected, in the native state, decellularized, decellularized and cultured (controls), and recellularized. In these experiments, the HUV obtained was sliced into scaffolds of uniform dimensions (10-12mm x 17-20mm x 1-2mm), decellularized, recellularized with primary-culture human vocal fold fibroblasts, and cultured for 21 days. At the end of the 21 days, each scaffold was sliced into 3 sections, subjected to biomechanical testing, scanning electron microscopy (SEM) and histology. Using a custom-built linear simple shear rheometer, the viscoelastic properties of each scaffold section were determined. Preliminary experiments determined the optimal decellularization protocol based upon: the extent of decellularization, the depth of cellular infiltration, and their shear modulus (G') and dynamic viscosity (η') as compared to those of the human vocal fold. Recellularized scaffolds were determined to have G' and η' values similar to those of the human vocal fold cover obtained from a 79-year-old male and a 53-year-old female. Scanning electron microscopy (SEM) showed that viable fibroblast cells, as characterized by a lighter shade of gray and an elongated shape, attached to the abluminal surface of the scaffold. Native tissue, decellularized tissue, and control tissue all appeared to have an intact ECM protein network structure as shown by the scanning electron micrographs. Histological staining with hematoxylin and eosin, Alcian blue with and without hyaluronidase, Periodic acid-Schiff's reagent, Safranin-O, and Masson's Trichrome were used to examine cellular attachment, depth of cellular infiltration, the structure of the tissues and the scaffolds, and the expressions of various proteins and GAGs, including glycogen, hyaluronic acid, chondroitin sulfates A, B, and C, keratosulphate, mucins, sialomucins, and sulphated sialomucins. Results showed the presence

of these proteins and GAGs in the native HUV tissue, varying extent of decreases in protein and GAG densities for the decellularized scaffold, and large decreases in protein and GAG densities for the control scaffold. However, the recellularized scaffold was able to regain some of the proteins and GAGs after 21 days of culture. Cell recovery results showed that the seeding of one million cells on each scaffold (with a seeding density of about 5,000 cells/mm^2) led to an initial cell attachment of 1.7-1.8%, a faster proliferation than similar previous studies, and an average final cell count of around 480,000 cells per scaffold. These findings provided preliminary support to the potential of the acellular HUV scaffold as an allograft for the repair of vocal fold lamina propria lesions. The HUV consists of proteins conducive to cellular attachment and proliferation, has viscoelastic properties similar to those of the human vocal fold cover, demonstrates deep cellular infiltration, and can support the growth and recovery of a relatively large number of viable cells within a short period of time. Further studies involving a larger number of samples are needed to verify and extend the present findings.

Table of Contents

List of Figures

List of Tables

CHAPTER 1

Introduction

1.1. Anatomy of the Human Vocal Fold

The human vocal fold is a layered structure designed to facilitate vibration and voice production. As shown in Figure 1.1, the outermost layer is the epithelium, which is made of a thin layer of stratified, squamous cells. The lamina propria is located between the epithelium and the muscle layer. It is a three-layered system of connective tissue: superficial, intermediate and deep layers. The superficial layer (around 0.5mm thick) is comprised mostly of loosely organized elastin and collagen fibers allowing for ample deformation during vocal fold vibration. These fibers are surrounded by interstitial proteins and fluids. The intermediate layer is also mostly made of elastin and collagen fibers, but the fibers in this layer are somewhat more organized; mainly they are uniformly oriented in the anterior-posterior (longitudinal) direction. The deep layer is primarily collagen fibers that are organized and also oriented in the anterior-posterior direction. The intermediate and deep layers together are collectively known as the vocal ligament (about 1 to 2mm thick), where the fibrous proteins can limit the elongation. Below the lamina propria lies the thyroarytenoid or vocalis muscle, being 7 to 8mm thick, and organized in fascicles (Titze, 2000). Aside from fibrous, organized proteins such as collagen and elastin, the vocal fold also contains interstitial proteins, including proteoglycans and glycosaminoglycans (GAGs), particularly hyaluronic acid (HA).

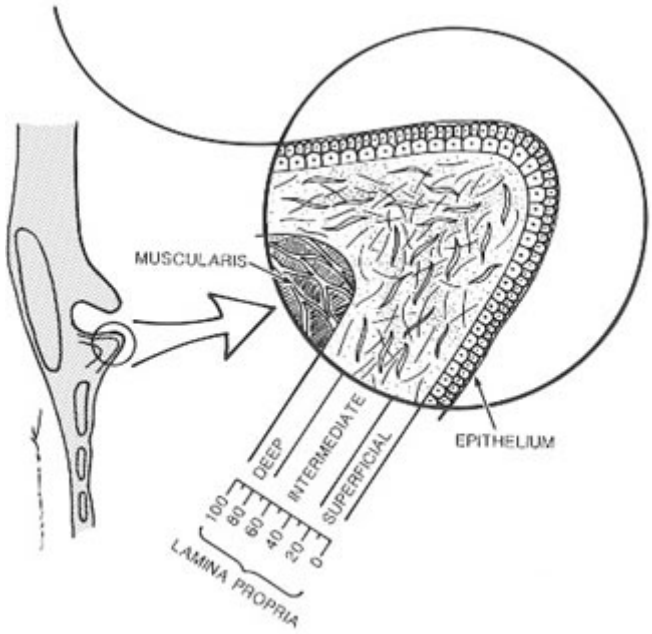

Figure 1.1: Schematic of the human vocal fold at the mid-coronal section (Gray et al., 2000)

The human vocal fold tissues naturally undergo vibrations that range from 100Hz to 1000Hz. Regular conversational voice ranges from 150-200Hz for men and 200-300Hz for women. The high end of the range, about 1000Hz, can be obtained by soprano opera singers. According to Titze et al. (2003), these tissues may experience accelerations of 200-300G for periods of 1-2 hours. The vocal fold can also undergo amplitudes of vibration up to 4mm. Under this set of mechanical stimuli, vocal fold tissues are subjected to high magnitudes of acceleration, stress and strain. It is assumed that the extracellular matrix (ECM) of the vocal fold lamina propria develops special biological and biomechanical properties to support the tissue in this unique micromechanical environment (Titze et al., 2003).

The acoustic characteristics of voice production such as pitch and loudness are dictated by the fundamental frequency and the amplitude of vibration of the vocal fold. For example, an increase in fundamental frequency will increase the vocal pitch, and an increase in the amplitude of vibration will increase vocal intensity or loudness.

1.2. Laryngeal Pathologies

In addition to traumatic injury, disturbed patterns of regulation and expression of proteins in the lamina propria can cause various laryngeal pathologies such as scarring, vocal nodules, polyps, and cysts. These pathologies affect vocal fold vibration and the resulting voice quality. Vocal fold scars are a result of trauma, surgery, burns, or inflammation and consist of dense collagenous fibers. Scarring causes the vocal fold mucosa (lamina propria) to become much stiffer than normal tissue. It occurs mainly in the lamina propria, but can also occur anywhere in the vocal fold. Nodules and polyps both develop around the vocal fold edge at the middle of the membranous vocal fold, and the lesion occurs in the superficial layer of the lamina propria. In their early stages, nodules and polyps are a reddish edematic mass; in later stages they are a whitish, stiffer mass. Such benign lesions could increase the mass and stiffness of the vocal fold cover. For example, vocal nodules and polyps increase the vocal fold mass; but can increase or decrease the stiffness of the vocal fold. Cysts occur in the superficial layer of the lamina propria and increase both the mass and stiffness of the vocal fold cover. Vocal nodules, polyps, and cysts interfere with the vibratory movements of the vocal fold. These pathologies result in abnormal voicing and are normally addressed using phonosurgical techniques, such as intrafold injection. When surgery is performed, tissue is removed, especially for vocal fold scarring. Yet it cannot be adequately replaced by current phonosurgical approaches; and as mentioned earlier, surgeries may cause scarring or further aggravate existing scar tissues (Colton et al., 1996, Benninger et al. 1996).

1.3. Tissue Engineering Approach and Rationale

Although phonosurgical techniques such as injection laryngoplasty may resolve many problems in voice disorders, they cannot often adequately replace lost tissue and could even lead to scarring and further injury. The tissue engineering approach attempts to address this problem. The rationale for engineering a tissue for vocal fold implantation or replacement is that the tissue can be designed with very specific features. When engineering a vocal fold scaffold, the dimensions of the tissue can be tailored to those necessary for the location of the implant. Also, with an acellular scaffold, the types of cells to be seeded can also be determined according to the needs of the implant location. For example, this study uses primary human vocal fold fibroblasts to populate the scaffold, since the objective is to fabricate a potential implant for the lamina propria. It is reasoned that fibroblasts will grow and differentiate most effectively for this purpose. Furthermore, it is important to choose a material that will provide an ECM similar to that being replaced, particularly for the vocal folds that would facilitate vibration and sound production. This study will examine the human umbilical vein (HUV) as a possible acellular scaffold for engineering the vocal fold lamina propria.

1.4. Requirements for an Acellular Vocal Fold Scaffold

Given the rationale presented in Section 1.3, there is a need to develop an implantable, acellular scaffold that is a close substitute to the natural vocal fold lamina propria. Certain requirements must be satisfied in order to obtain this acellular vocal fold scaffold. First, the tissue that will be used as a scaffold should contain the natural biological macromolecules, such as proteoglycans, glycosaminoglycans, and fibrous proteins, all of which are present in native vocal fold tissue. It would be difficult to engineer a scaffold out of synthetic materials that

would contain these molecules in their natural proportions whilst maintaining natural function. Using undenatured tissue as a scaffold will provide a natural ECM already containing the molecules needed to facilitate cellular growth and tissue remodeling. These molecules are of particular interest for use as a potential graft for the vocal fold lamina propria, since the vocal fold ECM contains fibrous proteins (collagens and elastins), interstitial proteins (proteoglycans and glycoproteins), and other molecules (lipids and carbohydrates). As indicated in Section 1.1, the fibrous proteins contribute to the shape and form of the vocal fold, allowing it to sustain tensile, shear, and vibrational stresses. Interstitial proteins of the ECM regulate tissue viscoelasticity, water content, collagen fiber size and density, and tissue size (Gray et al., 2000).

The second factor for consideration is that the substitute scaffold must be biocompatible to be considered as an implant. An advantage of using a natural tissue is that it is biodegradable, meaning it can be degraded naturally by the body. This avoids problems such as toxicity and chronic inflammation which can occur when a foreign material remains in the body for long periods of time.

Allogeneic acellular scaffolds offer an attractive option because they typically trigger a less severe inflammatory reaction, since they originate from the same species. An alternative acellular scaffold approach is the use of xenogeneic scaffolds. However, they have natural antibodies that if not suitably denatured, might cause hyperacute rejection, occurring within minutes (Abbas et al., 2005) if not properly processed. Allografts and xenografts have already been successfully used in soft tissue engineering applications, such as those for heart valves, urinary bladder, and blood vessels (Walles et al., 2004; Schmidt et al., 2000; McFetridge et al., 2004; Dardik, 1995; Dardik et al., 1988; Dardik & Dardik, 1973; Dardik et al., 1976). Xu et al. (2007) developed an acellular xenogeneic extracellular matrix scaffold from the bovine vocal fold lamina propria, demonstrating its potential as a xenograft for the human vocal fold. Another

biocompatibility concern is the immune response since an allogeneic scaffold might possibly pass on an infectious disease.

The final requirement for consideration is the biomechanical properties of the acellular scaffold. The tissue must facilitate repetitive vibrations for long durations, which are normal conditions of vocal fold vibration. In the present study, the scaffolds will be tested at amplitudes of 1-2mm and frequencies of 100-300Hz, which are within the range of the normal speaking voice. Furthermore, the scaffold should have dynamic viscoelastic properties similar to those of the vocal fold lamina propria, in order to facilitate vibration. Key factors to consider are the elastic shear modulus (G') and the dynamic viscosity (η') of the tissue. The viscoelastic properties are critical when studying vocal fold tissues since they can be used to predict tissue forces, tissue deformation, and the threshold conditions for the vocal folds to oscillate and remain in oscillation (Chan & Titze, 1999). They are also important in phonosurgery, for determining the type of implant (biological or synthetic) to be used for vocal fold repair. Measuring the shear properties is essential since the oscillation of the vocal folds is driven by the propagation of a shear wave on the surface of the vocal fold. The phonation threshold pressure, the minimum lung pressure required for vocal fold oscillation to begin and to be sustained, increases with increasing dynamic viscosity (Titze, 2000). It is important for the HUV scaffold to have a dynamic viscosity similar to the human vocal fold in order to be able to oscillate under normal conditions (Chan & Titze, 2006). This study will examine the human umbilical vein (HUV) as a possible acellular scaffold for engineering the vocal fold lamina propria.

1.5. Human Umbilical Cord

To support the proposed use of the HUV as a tissue engineering scaffold, the properties of the human umbilical cord should be first considered. The human umbilical cord (Figure 1.2) contains two arteries, one vein, and the extracellular matrix that constitutes the remaining portion of the cord, known as Wharton's Jelly (WJ).

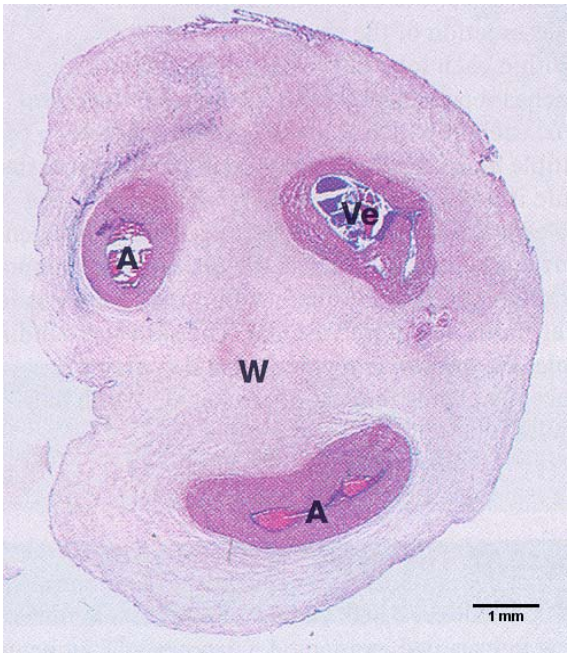

Figure 1.2. Hematoxylin & Eosin (H&E) staining of the Human Umbilical Cord (Young et al., 2006)

There are many advantages in using the human umbilical vein as an acellular vocal fold scaffold. First, it is derived from a vascular source, and has been successful in cardiovascular tissue engineering applications. Since it is from a vascular source, its original chemical and physical environment allows it to be more conducive to cell adhesion and extracellular matrix remodeling than any synthetic scaffold materials available. Another advantage is that Daniel et al. (2005) have created an automated dissection technology that can reliably dissect uniform umbilical vein samples from the umbilical cord. Their studies have found this tissue to be uniform, mechanically sound, and they have confirmed that it maintains a biphasic stress-strain relationship. Uniaxial tension tests showed the tissue's compliance, burst pressure, suture

holding capacity. The main advantage of using the human umbilical vein is that the dissected vein has Wharton's Jelly on its abluminal surface. Wharton's Jelly is a gelatinous connective tissue surrounding the umbilical vessels and is formed by the mesenchymal stem cells embedded in the ECM. Wharton's Jelly is rich in peptide growth factors, glycosaminoglycans (GAGs), and proteoglycans, all of which tend to stimulate cellular proliferation and differentiation and ECM synthesis and remodeling. Providing a rich ECM environment for the cells will allow for better cellular infiltration and will assist and stimulate the cells to synthesize extracellular matrix proteins. Also, since HUV is an allograft, the possibility of interspecies viral infectivity is low.

1.5.1. Peptide Growth Factors and Proteoglycans

Studies have shown that the Wharton's Jelly contains such peptide growth factors as insulin-like growth factor I (IGF-I), fibroblast growth factor (FGF), transforming growth factor β (TGF-β), platelet-derived growth factor (PDGF) and epidermal growth factor (EGF) (Sobolewski et al., 2005). These growth factors are thought to determine the rate of cellular proliferation, differentiation, ECM synthesis and remodeling, as well as control the production of collagen and glycosaminoglycans in large quantities. Also, Wharton's Jelly contains a large amount of hyaluronic acid (HA) (70% of total GAG content) which is responsible for the tissue being well-hydrated; HA also influences tissue viscoelasticity, cellular proliferation, cellular migration, and cell surface receptor interactions. Wharton's Jelly also has a large amount of collagen (50% of weight of defatted, dry tissue) which is responsible for its strong structural makeup, tissue viscoelasticity, and cellular activity. The proteoglycans found in Wharton's Jelly include decorin, biglycan, and versican (Gogiel et al., 2003). These proteoglycans affect the HUVs mechanical properties, affect the matrix organization of collagen, contribute to cell-cell interactions or cell-ECM interactions, and also bind the growth factors mentioned earlier. The

collagen fibril characteristics such as diameter and organization are regulated by decorin, which binds particularly to these fibrils. Biglycan is thought to affect the migration of endothelial cells to due its location close to the cell surfaces. Versican can assist the growth and proliferation of cells, and it also destabilizes their ability to adhere to the ECM (Gogiel et al., 2003).

1.5.2. Structure and Composition of the Umbilical Cord ECM

Nanaev et al. (1997) differentiated the human umbilical cord into three zones: subamniotic stroma, Wharton's jelly, and the vessels' adventitia. It was found that all zones contained collagen types I, III, and VI along with the basement membrane molecules collagen type IV, laminin and heparin sulphate proteoglycan. Immunohistochemistry was used to study the distribution of ECM molecules in human umbilical cords of different gestational age. This study also used electron microscopy to study the stromal cell ultrastructure, ECM composition, and the relationship between stromal cells and the extracellular matrix.

Immunohistochemistry using Texas-red immunofluorescence showed that collagen types I, III, and VI had a network-like pattern composed of thick bundles of coarse fibers in the subamniotic zone. It is also noticeable that the density of these fibers increases closer to the amniotic epithelium. The basement membrane of the amniotic epithelium showed collagen type IV in a spot-like arrangement. Other molecules also present in the basement membrane were laminin and heparan sulphate proteoglycan. Also, these three molecules were present in the subamniotic stromal layer as well as the mentioned amniotic epithelium. Collagen type VII was present only in the basement membrane of the amniotic epithelium.

Texas-red immunofluorescence also showed collagens type I, II, and VI were homogenously distributed throughout Wharton's Jelly. Surrounding the cleft-like areas of the ECM were isolated regions rich in collagen type IV, laminin, and heparan sulfate proteoglycan.

When examining the electron micrograph of Wharton's Jelly, a granular material was apparent, and was thought to be collagen type IV, based on its granular appearance with the immunohistochemical stains of the subamniotic zone. Surrounding this material were coarse fibrils of collagen type I enmeshed with fine fibrils that were probably collagen type III.

The adventitia of blood vessels showed a decrease in the number of contractile cells, but an increase in ECM molecules. The main difference between this area and the ECM of Wharton's jelly is that there is an abundance of collagen type I fibrils in a circular arrangement around the vessels. Structurally, this zone does not have the channel-like spaces present in Wharton's Jelly. Immunohistochemistry also showed slight staining of collagen types I and III in the media and adventitia of the cord vessels.

Studies by Sobolewski et al. (1997) showed the following characteristics of Wharton's Jelly: amount and solubility of collagen, amount of different collagen types, the ultrastructure of the collagen fibers, and the amount of various GAGs. The amount of collagen present was about 550 mg/g of tissue, which was 50% of the weight of the defatted, dry tissue. The collagen of Wharton's jelly was not only very insoluble in neutral salt and slightly acidic solution, but also only 50% of it could be solubilized by pepsin digestion. It was suggested that the collagen insolubility could be due to the following: increase in the amount of weak forces such as Van der Waals bonds or ionic interactions, a high GAG and proteoglycans content because negatively charged sulphated GAGs and positively charged amino acids can form strong ionic bonds on collagen fiber surfaces, and a large amount of type III collagen which is known to be less soluble than type I collagen. After differential salt precipitation, four collagen types were found, three of which could be identified by sodium dodecyl sulfate polyacrylamide gel electrophoresis (SDS-PAGE) as collagen types I, III, and V. The remaining collagen was suggested to be type VII since it has been shown that fibroblast-like cells originating from Wharton's jelly can synthesize collagen type VII in vitro. The quantification of the different collagen types showed that

collagen type I was 47%, collagen type III was 40%, and collagen type V was 12% of the total collagen. Masson's trichrome staining of Wharton's jelly showed cross-striated collagen that was arranged in bundles loosely arranged in the ECM, but became a circular arrangement near the blood vessel. Also in accordance with Nanaev et al. (1997) there was the appearance of a granular material and collagen fibers surrounding mesenchymal cells. Results showed Wharton's jelly has a GAG content of about 30 UA mg/g of tissue, and of these GAGs, hyaluronic acid constitutes about 70%, with a quantity of about 23 mg UA/g. It is of interest that HA is the most abundant since it has the characteristic of keeping tissues hydrated and therefore may contribute to the maintenance of viscoelastic properties of the ECM.

Romanowicz and Sobolewski (2000) also examined the extracellular matrix components of the umbilical cord vein. Although elastin is not present in Wharton's Jelly (Meyer et al., 1982), it is an essential component contributing to the structure of the human umbilical vein. Romanowicz solubilized the elastin and used the Fastin elastin assay to determine that the elastin content of the umbilical vein was 50mg/g of the dry, defatted tissue. The insoluble elastin content was measured to be 28.5 ± 3% mg/g of the dry, defatted tissue.

1.6. Thesis Objectives

The main objective of this study is to engineer an acellular HUV scaffold with biocompatibility and proper biomechanical properties such that it could potential be used as an allograft for the surgical repair of certain vocal fold lamina propria pathologies, such as vocal fold scarring. A novel decellularization protocol, developed by Xu et al. (2007) whereby the native tissue undergoes osmotic shock (using high concentration sodium chloride), nucleic acid digestion (using a PBS/RNAse/DNAse solution), and finally dehydration (using 75% ethanol) will be employed. The decellularization protocol is optimized for HUV by changing the duration

of certain steps of the protocol in order to create a scaffold that has been completely decellularized while still maintaining an intact extracellular matrix. Seeding primary human vocal fold fibroblasts on the acellular HUV scaffold and determining their attachment, infiltration, and growth rate will help determine whether the scaffold could be a successful allograft. The extracellular matrix structure and key proteins at different stages of the experiment (native, decellularized, decellularized and cultured, recellularized) will be examined, including: glycogen, hyaluronic acid, glycosaminoglycans, mucins, sialomucins, sulphated sialomucins, and collagen. These molecules in the Wharton's jelly are important since they contribute to facilitate cellular attachment, growth and ECM remodeling. Finally, the viscoelastic shear properties of the acellular HUV scaffold will be quantified to ensure their biomechanical similarity to the human vocal fold lamina propria. Thus the aim of this research is to demonstrate that a three-dimensional, biodegradable, acellular allogeneic scaffold could be fabricated by the decellularization of native human umbilical vein tissues, and that the resulting acellular scaffold would support the attachment, proliferation, and infiltration of primary-culture human vocal fold fibroblasts. Furthermore, in vitro remodeling of the scaffold for reconstruction of the vocal fold lamina propria by these fibroblasts will be examined. The decellularization of the native HUV tissue and seeding of the acellular scaffold with primary human vocal fold fibroblasts will be analyzed in terms of changes in the functional biomechanical properties of the scaffolds, i.e., their viscoelastic shear properties including the elastic shear modulus (G') and the dynamic viscosity (η').

CHAPTER 2

MATERIALS & METHODS

2.1. Experiment I: Identifying the Preferred Decellularization Protocol

The preliminary experimental design used 15 HUV sections from newborn donors. All umbilical cords were procured from local hospitals with IRB approvals. The HUV sections were used to identify the preferred decellularization protocol that would: (1) completely remove native cells in the HUV samples, (2) preserve the three dimensional structure of the ECM, and (3) allow vocal fold fibroblasts (VFF) to proliferate and infiltrate the scaffold. The experimental techniques were: Hematoxylin and Eosin (H&E) staining, Scanning Electron Microscopy (SEM), and biomechanical testing using a linear, simple shear rheometer. The details of the experiments are shown in Table 2.1.

Three native HUV sections were tested by the same experimental techniques used for decellularized sections (unmodified). Two sections underwent biomechanical testing, whereas the third section was cut in half and used for H&E staining and SEM. For cell removal, the remaining 12 scaffolds were mounted on a plastic frame and decellularized based on the saline-based osmotic approach developed by Xu et al. (2007). Four variations of the decellularization protocol were used, each with different time durations for different steps in the protocol. Four of the scaffolds, one from each decellularization group were immediately stored and later were used for H&E, SEM, and biomechanical testing. The remaining eight scaffolds were cultured for 21 days. For each of the 4 groups, one scaffold was left acellular and the other was seeded with primary human vocal fold fibroblasts. After the 21 days of culture, each scaffold was tested using H&E, SEM, and biomechanical tests.

Experimental Technique	Native HUV	Acellular Scaffolds		Primary Human VFF Repopulated Scaffolds
		Stored after Decellularization	21 Days in Culture	21 Days in Culture
Total Number Of Scaffolds	3	4	4	4
H&E Light Microscopy	½ of one scaffold	1/3 of each scaffold	1/3 of each scaffold	1/3 of each scaffold
Scanning Electron Microscopy	½ of one scaffold	1/3 of each scaffold	1/3 of each scaffold	1/3 of each scaffold
Biomechanical Testing	2 scaffolds	1/3 of each scaffold	1/3 of each scaffold	1/3 of each scaffold

Table 2.1 Design of Experiment I used to determine the preferred decellularization protocol. (VFF = vocal fold fibroblast)

2.2. Experiment II: Examining the HUV Scaffold

Results of Experiment I suggested that the decellularization protocol used for Group 4 was preferred because it was associated with full decellularization, the 3-D structure of the ECM was maintained, and that maximum cellular proliferation and infiltration were observed. Therefore the decellularization protocol from Group 4 was used to further examine the potential of the HUV as an acellular vocal fold scaffold. Table 2.2 shows the details of the experimental design for Experiment II. In order to test whether the freezing and thawing procedure (used in the automated dissection technology) might have changed the biomechanical properties of the HUV, human umbilical veins were also manually dissected from three additional umbilical cords and their biomechanical properties were tested.

Twelve HUV specimens dissected by an automated dissection technology (Daniel et al., 2005) were obtained from Dr. Peter McFetridge of the University of Oklahoma. Four different

treatment conditions were included: native tissue (control), decellularized tissue, decellularized and cultured tissue, and recellularized tissue. In order to account for variability of different sections of the vein from the same cord, as well as for variability of different veins from different cords (or subjects), each treatment was applied to vein segments from three different umbilical cords. The three HUV tissues were each sliced into 3 sections (9 sections total) and kept in their native form. Each of these sections was cut in thirds using each slice for one of the following: histology, SEM, and biomechanical testing. The histological stains used were: Hematoxylin & Eosin (H&E), Masson's Trichrome (for collagen), Alcian Blue (for glycosaminoglycans), Alcian Blue with Hyaluronidase (for HA), Periodic Acid-Schiff's reagent (PAS), and Safranin-O (for glycosaminoglycans) (Lai et al., 2006; Wayne et al., 2001). The remaining 27 sections were mounted on a support and decellularized. After decellularization, nine sections (3 sections from each of the 3 HUV tissues) were immediately stored, and nine scaffolds were cultured as controls for 21 days alongside the nine recellularized scaffolds. All decellularized, control, and recellularized scaffolds were examined using histology, SEM, and biomechanical testing. Two extra scaffolds for each vein at each condition were used alongside the main experimental scaffolds. One extra scaffold was examined using the cell recovery method after decellularization to ensure that the scaffolds were completely decellularized. After 21 days of culture, cell recovery from the second extra scaffold was used to compare the final cell count of the recellularized scaffolds to the final cell count of the different veins used in Experiment III.

2.3. Experiment III: Cell Recovery

Three umbilical cords obtained at birth from different donors were each sliced into 9 sections. These 27 scaffolds were decellularized and recellularized with human vocal fold fibroblasts exactly as Experiment II. The recellularized scaffolds were cultured and harvested in groups of three on Days 0 (1 hour after cell seeding), 1, 3, 6, 9, 12, 15, 18, and 21, in order to count the number of cells present at various time points of culture. At each time point, one scaffold from each of the three cords was sacrificed, using trypsin.

Experimental Technique	**Manually Dissected HUV**	**Native HUV**	**Acellular Scaffolds**		**Primary Human VFF Repopulated Scaffolds**
			Stored after Decellularization	21 Days in Culture	21 Days in Culture
Total Number of HUVs from different subjects	3	3	3	3	3 + 3
Total # of Scaffolds	9	9	9	9	9 + 27
Total Number Of Scaffolds from each HUV	3	3	3	3	3 + 9
Histology Stains		1/3 of each of 3 scaffolds (one from each subject)	1/3 of each of 3 scaffolds	1/3 of each of 3 scaffolds	1/3 of each of 3 scaffolds
Scanning Electron Microscopy		1/3 of each of 3 scaffolds (one from each subject)	1/3 of each of 3 scaffolds	1/3 of each of 3 scaffolds	1/3 of each of 3 scaffolds
Biomechanical Testing	3	1/3 of each of 3 scaffolds (one from each subject)	1/3 of each of 3 scaffolds	1/3 of each of 3 scaffolds	1/3 of each of 3 scaffolds
Cell Count					27

Table 2.2 Design of Experiments II and III.

2.4. Experiment IV: Biomechanical Measurements of Native HUV Tissues

The three human umbilical vein tissues in the native condition for Experiment II did not respond to the linear, simple-shear rheometer at most frequencies. Therefore, three more human umbilical veins were obtained and three scaffolds from each vein underwent biomechanical testing in their native condition. These veins were processed exactly as the native veins in Experiment II and were used in all averaged biomechanical data.

2.5. Scaffold Preparation

Human umbilical vein samples are obtained and prepared at the University of Oklahoma in the lab of Dr. Peter McFetridge. The following is the conventional dissection procedure that was used for Experiment I. Once the umbilical cord was received, it was harvested, cleaned and stored overnight. The following day it was frozen (-80ºC) onto 6mm mandrels for two days before dissection. The automated dissection method is used to dissect the vein from the cord. This procedure requires placing the mandrel on a secured modified lathe and using a high-speed, steel cutting tool to dissect the tissue (which is frozen on the mandrel). After dissection, the tissue was kept at –20ºC for four days before shipping. The tissue is then thawed by immersion in double distilled water at 5^{o}C for 1 hour, and shipped overnight to UT Southwestern in phosphate-buffered saline (PBS) with antibiotics.

Freezing and thawing the tissue multiple times could have an effect on the structure and behaviour of the extracellular matrix. Therefore the dissection protocol was modified so that the tissue is only frozen at (-80ºC) before dissection, then thawed by immersion in double distilled water at 5^{o}C for 1 hour, and shipped overnight to UT Southwestern in phosphate-buffered saline (PBS) with antibiotics. Experiments began immediately upon tissue arrival to avoid changes in the tissue structure due to time.

The thickness of the frozen tissue after cutting is about 750μm and results in a slightly larger thickness when thawed. The small muscle layer of the HUV is the first 200-400μm (max) and the remaining thickness is the Wharton's jelly.

Scaffold preparation began with cutting off and discarding 5mm of tissue on each side of the HUV. This is to ensure that the only scaffolds used for the experiments have uniform thickness. As with any type of cutting method for soft, "floppy" tissue samples, it is difficult to maintain uniformity at the ends of the samples. The vein was then cut longitudinally, opened, and sliced into small rectangular sections of dimensions 10mm x 16-17mm. Sections that were decellularized and cultured were mounted on a plastic support that provides slight tension to the tissue as well as a secure, immobile surface for cell seeding and culturing.

2.6. Decellularization Protocol

The decellularization protocol has four main steps. Before starting the protocol, the scaffolds are washed in isotonic phosphate-buffered saline (PBS) containing 100 units/ml and 1mg/ml of the antibiotics penicillin and streptomycin (Sigma, St. Louis, MO), respectively. The first decellularization step is to soak the scaffolds in 3M NaCl (Sigma, St. Louis, MO) for 12 hours at room temperature, creating osmotic stress on the cells (endothelial cells, fibroblasts, myofibroblasts, and macrophages). Afterwards, the scaffolds are soaked in a solution containing PBS, RNAse, and DNAse for 12 hours at 37ºC in order to break down the cell membrane and remove exposed nucleic acids. The solution concentrations are 25μg/ml of DNAse (Sigma, St. Louis, MO) and 10μg/ml of RNAse (Sigma, St. Louis, MO). The third step is to soak the scaffolds in 75% EtOH for 6 hours at room temperature to dehydrate the tissue as well as to provide further osmotic stress to any remaining cells. The final step is to soak the scaffolds in isotonic PBS containing 25μg/ml DNAse and 10μg/ml RNAse at 37ºC for 12 hours. Once this decellularization protocol is complete, the scaffolds are washed in isotonic PBS/DNAse/RNAse

solution to remove remaining cellular debris along with previously added reagents. The scaffolds were stored in this solution at 4ºC until they are ready to be seeded. Before cell seeding, scaffolds are sterilized in 75% EtOH under ultraviolet (UV) light for an hour, washed in PBS antibiotic solution for 2 hours to wash out all ethanol, and soaked in media overnight.

Experiment I used three other variations of this protocol to find the preferred protocol mentioned above. The first protocol required soaking the scaffold for 24 hours in 3M NaCl, 24 hours in the PBS/RNAse/DNAse solution, 12 hours in 75% EtOH, and 12 hours in the PBS/RNAse/DNAse solution. The second protocol had a 3M NaCl soaking time of 24 hours, but only 12 hours in the PBS/RNAse/DNAse solution, 6 hours in the 75% EtOH, and 12 hours in the PBS/RNAse/DNAse solution. Finally, the third protocol required soaking for 12 hours in the 3M NaCl, 12 hours in the PBS/RNAse/DNAse solution, 6 hours in the 75% EtOH, and 12 hours in the PBS/RNAse/DNAse solution. Table 1.1 shows the different times used for each group.

STEPS	**DESCRIPTION**	**GROUP 1**	**GROUP 2**	**GROUP 3**	**GROUP 4**
Washing	Wash with PBS + antibiotics				
Saline	3M NaCl, 25ºC	24hr	24hr	12hr	12hr
Nucleases	PBS, RNAse, DNAse 37ºC	24hr	12hr	24hr	12hr
Dehydration	75% EtOH	12hr	6hr	12hr	6hr
Nucleases	PBS, RNAse, DNAse 37ºC	12hr	12hr	12hr	12hr
Washing	PBS, RNAse, DNAse 25ºC				

Table 2.3 Four variations of the decellularization protocol used for Experiment I.

2.7. Cell Seeding

For Experiment I, the twelve mounted tissues (10mm x 16-17mm x ~1mm) were divided into four groups, each using a slightly modified version of the decellularization protocol. After decellularization, the abluminal surface of the scaffold was coated with 0.5mL of a collagen gel solution and incubated at 37ºC for 45 minutes to allow partial polymerization on the scaffold surface. The collagen gel was prepared by dissolving 3mg of collagen in 1ml of 0.05M acetic acid solution. To this solution, 1.5ml of 1x Earl's Eagle Medium and 0.300ml of Reconstitution buffer were added. The Reconstitution buffer is made of 0.55g NaHCO3, 20ml of 1 N NaOH, and water to make a final volume of 25ml. Before adding the collagen to the scaffolds, it was incubated at 37ºC and 5% CO_2 for 45 minutes, not allowing it to polymerize fully. Once the scaffold was coated with collagen and incubated, the scaffold was ready to be seeded. One million vocal fold fibroblasts (VFFs) from primary culture were resuspended in 100µl of DMEM containing 10% fetal bovine serum (FBS). These cells were seeded on the abluminal surface of the scaffold on top of the collagen layer. For each group one scaffold was seeded with VFFs while the other remained acellular to be used as a control. Only the preferred decellularization protocol, Group 4, was used in Experiments II and III. Also, no collagen gel was used on the scaffold surface for Experiments II and III in order to fully utilize the characteristics of Wharton's Jelly as well as to test if the collagen matrix was slightly inhibiting the cells from traveling into the scaffold.

For Experiment I and Experiment II, the cells used were a mixture of the third and fourth passages of primary culture human vocal fold fibroblasts obtained from a 60-year-old Hispanic male who underwent a laryngectomy that did not involve the true vocal folds. The vocal fold fibroblasts used in Experiment III cell recovery were normal cells taken from the fourth passage from a 58-year-old Hispanic female, who underwent laryngectomy due to thyroid cancer not involving the true vocal folds.

2.8. Scaffold Culture

These recellularized scaffolds and control scaffolds were cultured for 21 days at 37ºC, with media changes and cell culture media supernatant collections taken every other day. Collected samples were immediately stored at 20ºC. In Experiment I, on days 7 and 21, tissues were treated with Fluorescent dyes Calcein AM and DAPI and visualized by Ziess LSM confocal microscope. However, only tissues in Group 1 underwent this process on day 7.

After 21 days of culture, the scaffolds are removed from the plastic support and each cut into three slices of equal length. The three sections from the same scaffold are examined by: histology stains, Scanning Electron Microscopy (SEM), and biomechanical testing with our custom built linear rheometer for measurement of its viscoelastic properties. The media samples taken every 48 hours were stored for future assays that will quantify soluble proteins such as fibronectin, decorin, hyaluronic acid (HA), and collagen synthesized by the fibroblasts in the scaffolds.

2.9. Histological Examination

Tissues were stored in 10% Neutral Buffered Formalin in the native, decellularized, control and recellularized conditions. Preparation for embedding required dehydrating these tissues in 35%, 50%, 70%, 80%, 95%, and 100% ethanol. Afterwards the dehydrated tissues were soaked in two changes of xylene followed by two changes of paraffin. Tissues were then embedded in paraffin, sliced into 5μm sections and baked onto a slide.

Image analysis from various stains was used to examine the properties of the HUV tissues at different conditions. Table 2.4 shows which molecular constituents can be identified based on the particular stains.

Molecular constituent	Alcian Blue (pH 2.5)	Alcian Blue (pH 2.5) with Hyaluronidase	PAS	Safranin-O
Glycogen	-	-	+	
Hyaluronic Acid	+	-	-	
Chondroitin Sulfate (A&C)	+	-	-	+
Chondroitin Sulfate (B)	+	+	-	+
Keratosulphate	+	+	-	+
Mucins	-	-	+	
Sialomucins	+	+	+	
Sulphated Sialomucins	+	+	+	

Table 2.4 Chart showing which molecules are apparent in each stain. (Culling, 1985)

The progressive method for hematoxylin and eosin (H&E) staining was used to determine cell viability and infiltration depth. First the slides were deparaffinized in three changes of xylene and dehydrated in changes of 100% and 95% ethanol. After rehydrating in tap water, the slides were soaked in hematoxylin for 2.5 minutes and quickly rinsed again with tap water. Then the slides were soaked in 0.25% ammonia water for 1 minute then placed in running water. Slides were soaked in eosin for 1 minute followed by two quick changes of 95% ethanol and three changes of 100% ethanol. After two changes of xylene, they were mounted and examined. This protocol stains the nuclei blue, and the cytoplasm and other tissue elements various shades of pink (Carson, 1997).

The Alcian Blue stain (pH 2.5) was used to determine the presence of hyaluronic acid. Sections were first deparaffinized and hydrated to distilled water. Slides were then placed in 3% acetic acid solution for 3 minutes, alcian blue solution for 30 minutes at room temperature, and

rinsed briefly in 3% acetic acid solution to remove the excess alcian blue. After running the slides in tap water for 10 minutes, they were rinsed in distilled water and counterstained in nuclear-fast red solution for 5 minutes. Slides were then placed in water and one change of 95% ethanol very quickly to avoid washing off too much stain. Finally the slides were soaked in two changes of 100% ethanol and two changes of xylene before being mounted. This protocol stains weakly acidic sulfated mucosubstances, hyaluronic acid, and sialomucins a dark blue color. The background would be a pink to red color (Carson, 1997).

Hyaluronidase extracted from ovine testes was used to remove the hyaluronic acid from the tissues. This particular hyaluronidase can remove hyaluronic acid, chondroitin-4-sulphate and chondroitin-6-sulphate from fixed tissues. Slides were deparaffinized, hydrated, and incubated overnight at 37ºC in 1.0mg of hyaluronidase enzyme per milliliter of 0.9% aqueous NaCl. Afterwards, they were washed in water and stained using the alcian blue protocol. Results for this stain show the undigested acid mucopolysaccharides and sialomucins a deep blue color, whereas the digested mucosubstances containing hyaluronic acid and chondroitin sulfates A and C had a marked loss of staining (Kiernan, 2001).

The Periodic Acid Schiff (PAS) stain was used to identify glycogen and sialomucins in the tissue. Once the slides were deparaffinized and hydrated in distilled water, they were placed in 0.5% periodic acid solution for 5 minutes. Then the slides were washed in three changes of distilled water and soaked in Schiff reagent for 20 minutes. The slides were placed in running tap water for 10 minutes to develop their full color. Then they were counterstained with hematoxylin for 1 minute, washed three times with distilled water, and soaked in bluing for 1 minute. Finally the slides were washed in three changes of distilled water, dehydrated with two changes of 95% ethanol and two changes of 100% ethanol, cleared with two changes of xylene, and mounted.

Staining with Safranin-O was used to identify glycosaminoglycans (GAGs) in the HUV scaffolds. Safranin-O was prepared by adding 2 grams of Safranin-O to 195ml of water and 5ml of methanol. Alcoholic fast green FCF was prepared by adding 1 gram of Fast green FCF to 95% ethanol. Slides were first deparaffinized with xylene, dehydrated with changes of 100% and 95% ethanol, and rehydrated with distilled water. Then they were immersed in aqueous Safranin for 1 hour, washed twice in tap water very quickly, and placed in 70% ethanol followed by 95% ethanol very quickly to avoid excess stain removal. The slides were then soaked in alcoholic fast green FCF for 30 seconds and immediately dehydrated in two changes of 100% ethanol, cleared in two changes of xylene, and mounted (Kiernan, 2001).

Masson's Trichrome stain was used to determine the relative staining intensity and percentage area fraction of collagen in the scaffolds for each condition. Slides were deparaffinized in xylene, dehydrated with 100% and 95% ethanol, and rehydrated with distilled water. Then they were immersed in Bouin's solution overnight at room temperature. The slides were then washed in running water until the water ran clear. Afterwards, the slides were placed in Weigert's iron hematoxylin solution for 10 minutes, washed briefly in running water, rinsed in distilled water, soaked in Biebrich scarlet-fuchsin solution for 10 minutes, rinsed in distilled water, and placed in phosphotungstic-phosphomolybdic acid for 10 minutes. Sections were then stained in aniline blue solution for 10 minutes, rinsed in distilled water, placed in 1% glacial acetic acid quickly, dehydrated with 95% alcohol very quickly, and placed in two changes of 100% ethanol. Finally they were immersed in two changes of xylene and mounted.

Images of this stain were analyzed by using a color threshold method, similar to that of Chan et al. (2007). On a color scale of 0 (white) to 255 (black) the intensity of the collagen in the tissue was determined using Image J software (National Institutes of Health). This average intensity was used to determine how much collagen was present in the tissue with respect to its area. One scaffold from each vein represented the collagen intensity and collagen percent of that

vein. Since some tissues were large, values from multiple images of the same scaffold were averaged and their standard deviations were reported. Three veins were analyzed and averaged as a representation of each condition. The thresholding method determined a mean intensity that represented the color of collagen (blue) in the image. The relative staining intensity of collagen was calculated by taking the mean intensity (between 0 and 255) and dividing it by the maximum intensity (255). Collagen area was determined by Image J as the number of pixels in the image with that mean intensity. The percentage area fraction of collagen was calculated by the ratio of the collagen area to the total area of the tissue.

2.10. Scanning Electron Microscopy

Scanning electron microscopy was used to examine the abluminal surface of the scaffolds. Tissues were fixed in 2.5% Glutaraldehyde solution that had been prepared with 0.1M cacodylate buffer. The processing began with rinsing the tissues in 0.1M cacodylate buffer three times, 5 minutes each time. Then the tissues were soaked in osmium tetroxide solution for one hour. This solution was made by adding 4% osmium tetroxide, distilled water, and 0.2M cacodylate buffer in a 1:1:2 ratio, respectively. Tissues were then rinsed three times, 5 minutes each time. Afterwards, they were placed in 50% ethanol for 10 minutes, 70% ethanol twice for 10 minutes, 95% ethanol three times for 10 minutes, and 100% ethanol three times for 10 minutes. Then the tissues were dried using critical point drying, mounted, and sputter coated. Images were taken at 500 X and 1000 X magnification.

2.11. Measurement of Biomechanical Properties

A custom-built linear, simple shear rheometer based on the EnduraTEC Electro Force (ELF) 3200 mechanical testing system (Bose Corporation, EnduraTEC Systems Group,

Minnetonka, MN) (Chan et al., 2005) was employed to quantify the biomechanical properties of the HUV scaffolds. This system uses linear, controlled-strain oscillatory simple shear deformation to determine the viscoelastic shear properties of tissue samples, including the elastic shear modulus (G'), viscous shear modulus (G'') and dynamic viscosity (η') (Chan and Titze, 1999). The system has been validated by identifying the frequency responses of key system components, and it was found that valid rheological measurements could be made at frequencies of up to 250 Hz (Chan et al., 2005). Figure 2.1 shows the key components of the system. Briefly, a sample is placed between two parallel plates and the linear motor vibrates the upper plate at a specified amplitude and frequency. This linear motor is connected to a linear variable displacement transducer (LVDT) which allows for precise displacement amplitudes to be obtained. Attached to the lower plate is a piezoelectric force transducer that detects the tissue force response. Located below the lower plate is another force transducer that detects the normal force created by the contact of the tissue sample between the upper and lower plates. Experimental measurements of viscoelastic properties were conducted with the specimen in a transparent acrylic environmental chamber, where a heating rod heats the water to a specified temperature (~50°C) in order to maintain an ambient air temperature of 37°C and 100% relative humidity in the chamber.

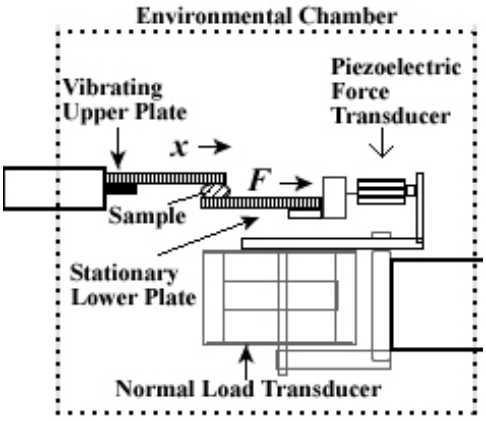

Figure 2.1 Schematic of the linear simple-shear rheometer

A photograph of the sample was taken from above the system and used to determine the area of the specimen in contact with both tissue plates. This area was used to calculate shear stress based on shear force measurements. The WinTest software (Bose Corporation, EnduraTEC Systems Group, Minnetonka, MN) specifies the frequency, displacement amplitude, and duration of the experiment. Displacement (as measured by the LVDT) and shear force (as measured by the piezoelectric force transducer) were digitized at a sampling rate of 8000 samples/sec and the resulting signals were processed by the WinTest software for calculating the viscoelastic properties of the specimen, according to the principle of linear viscoelasticity (Chan and Titze, 1999).

2.12. Statistical Analysis

The biomechanical data from two human vocal fold cover specimens were compared to those of the recellularized HUV scaffolds. Logarithmic values for G' and η' were used in this analysis. The log of the shear modulus (G') and log of the dynamic viscosity (η') of each human vocal fold specimen was plotted against those of recellularized HUV tissue. Human tissues only had one G' and η' value at each frequency (n=1) since each human vocal fold cover can only be tested once. However, three umbilical veins were recellularized (n=3), so their average G' and η' were used to compare to the human data. These plots show on average, which values are larger in comparison to each other. The unity line represents the location of equal values.

The bias is the recellularized data subtracted from the human data at each frequency which represents how different these raw values are with respect to each other across frequencies. Averages of log G' and log η' for the human and recellularized data were calculated at each frequency. The bias was plotted against the average values to show not only how different they are from each other, but how different they are from the mean as well. The

average bias depicts, in general, how different log G' and log η' values will be from equality (y=0). The standard deviation of the average bias was calculated and doubled to represent the limits where 95% of the data is predicted to be found (Bland & Atlman, 1986; Bland & Altman, 1995).

The coefficient of variation (CV) was calculated to determine how much variation exists between multiple measurements of the same condition. For the three scaffolds within a vein, the average log G' and log η' was calculated at each frequency, as well as the standard deviations associated with these measurement. The same method was used for the three veins within a condition.

CHAPTER 3

RESULTS

3.1. Experiment I - Identifying the Preferred Decellularization Protocol

3.1.1. Decellularized Scaffolds (H&E)

Figures 3.1 – 3.8 present typical H&E and SEM images, respectively, of the decellularized scaffolds according to protocols 1 – 4. For each H&E photograph, the abluminal surface is on the left and the luminal surface (endothelium) is on the right. The scanning electron micrographs show the abluminal surface of the scaffold. Examination of these photographs indicates that Group 2 was the only protocol that did not result in complete decellularization of the scaffolds. It is evident from that H&E photo that native cells would be observed across the entire scaffold.

The scanning electron micrographs of the abluminal surfaces show that for every group, an ECM structure was maintained.

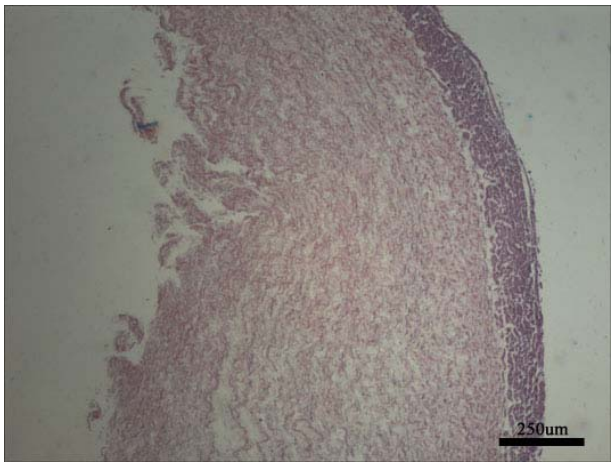

Figure 3.1. H&E Staining of Decellularized HUV Scaffold using Protocol 1. (40x Magnification. See text for details.

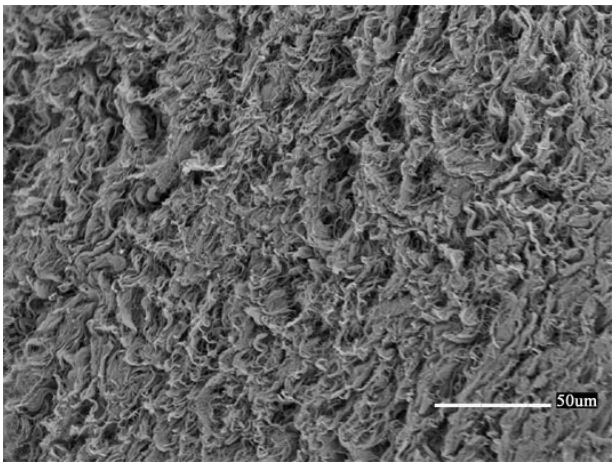

Figure 3.2. Scanning Electron Micrograph of Decellularized HUV Scaffold using Protocol 1. (500x Magnification)

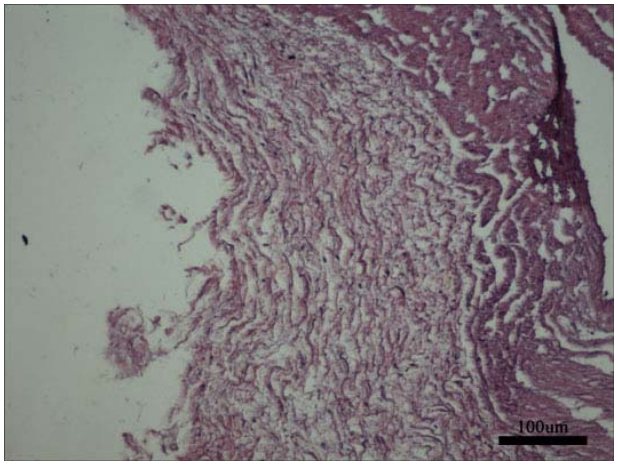

Figure 3.3 H&E Staining of Decellularized HUV Scaffold using Protocol 2. (100x Magnification)

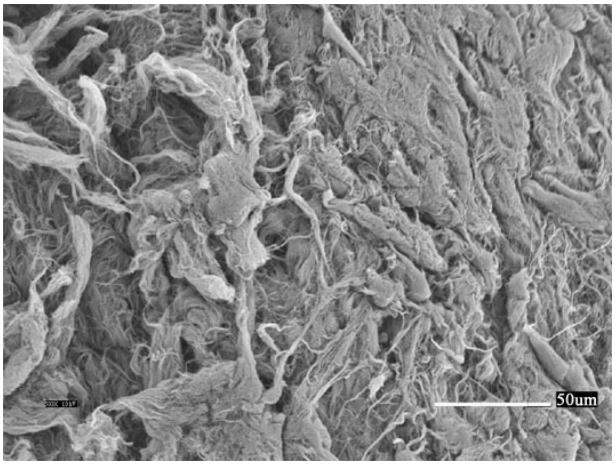

Figure 3.4 Scanning Electron Micrograph of Decellularized HUV Scaffold using Protocol 2. (500x Magnification)

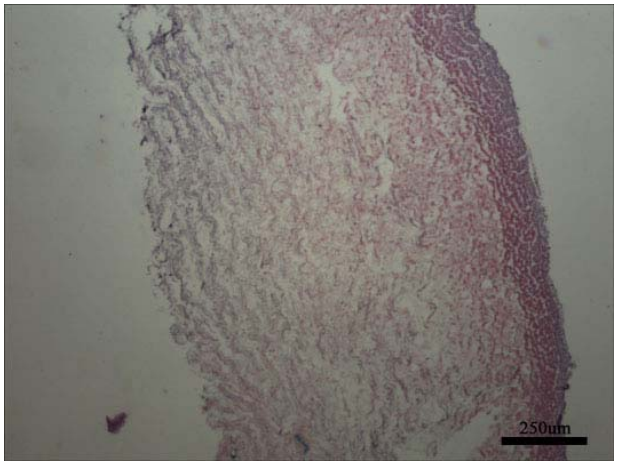

Figure 3.5 H&E Staining of Decellularized HUV Scaffold using Protocol 3. (40x Magnification)

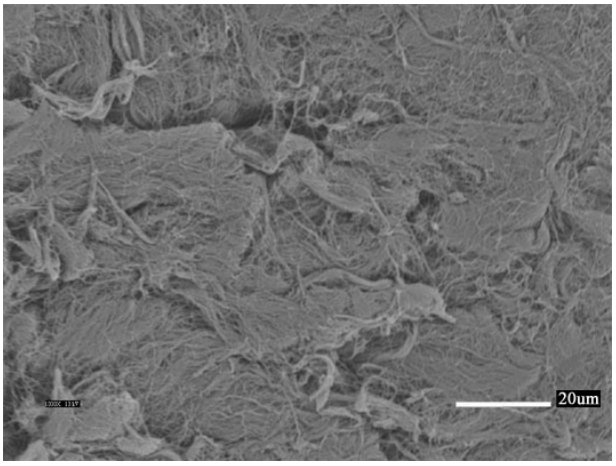

Figure 3.6 Scanning Electron Micrograph of Decellularized HUV Scaffold using Protocol 3. (1000x Magnification)

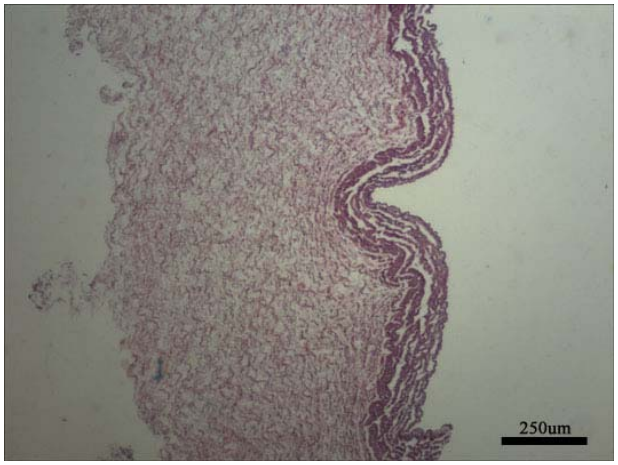

Figure 2

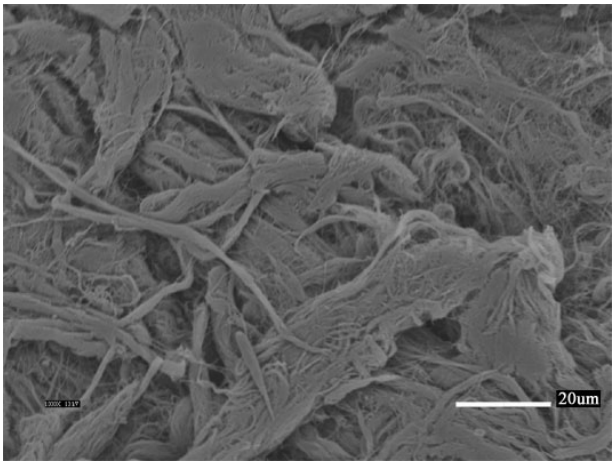

Figure 3

3.1.2. Recellularized Scaffolds (H&E)

The H&E and SEM photographs of groups 1, 3, and 4 were the only ones examined, since group 2 samples did not properly "decellularize", leaving no method to distinguish between native and seeded cells on that scaffold.

Figures 3.9 – 3.15 are the corresponding preliminary results for the scaffolds that were seeded with primary human vocal fold fibroblasts. The H&E stain results (Figs 5.9-5.10) showed that group 1 samples did not have any cells on the abluminal surface. However, a structured layer can be observed on the abluminal surface that was determined to be part of the wall of the umbilical artery that was located too close to the vein. The corresponding SEM photograph showed that the ECM was maintained even after the 21 days of culture.

For the scaffolds in group 3 (Figs 3.11-3.12), the H&E stains showed cellular proliferation, a surface layer of attached cells 1-2 layers thick, and cellular infiltration up to about 200μm. This depth remains in the area of Wharton's Jelly. The corresponding scanning electron micrograph showed cells attached onto the abluminal surface. These cells are

considered to be healthy, characterized by a lighter shade of gray, a three dimensional appearance, and an elongated shape.

The H&E photographs of the recellularized scaffolds in group 4 (Figs 3.13-3.15) show full cellular infiltration to about 700μm. Using the scale bar, it was calculated that the infiltration was about 600μm into the Wharton's Jelly and 100μm into the muscle. There are also cells attached onto the abluminal surface that are 1-2 layers thick. Similar to Group 3 results, the SEM photograph shows healthy cells that have attached and elongated.

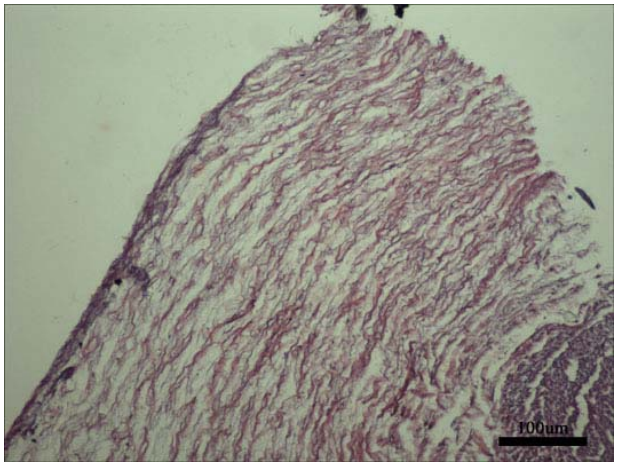

Figure 3.9 H&E staining of the Group 1 HUV Scaffold recellularized with primary human vocal fold fibroblasts. (100x Magnification)

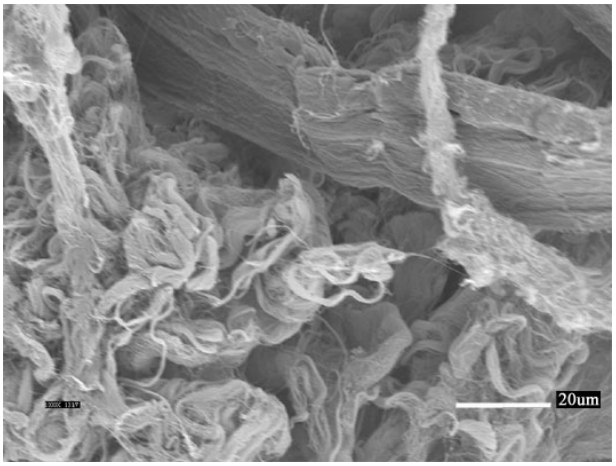

Figure 3.10 Scanning Electron Micrograph of the Group 1 HUV Scaffold recellularized with primary human vocal fold fibroblasts. (1000x Magnification)

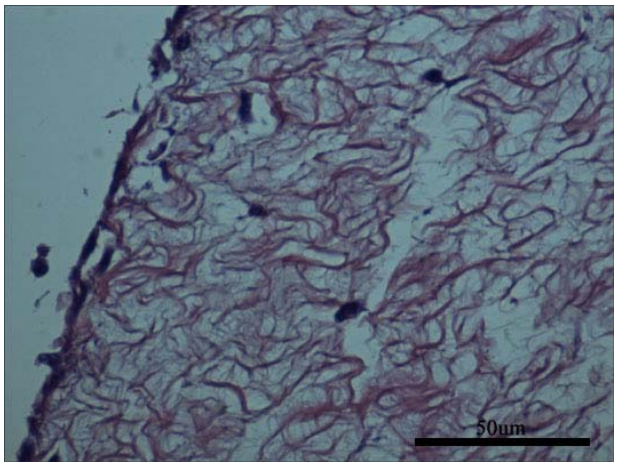

Figure 3.11 H&E staining of the Group 3 HUV Scaffold recellularized with primary human vocal fold fibroblasts. (400x Magnification)

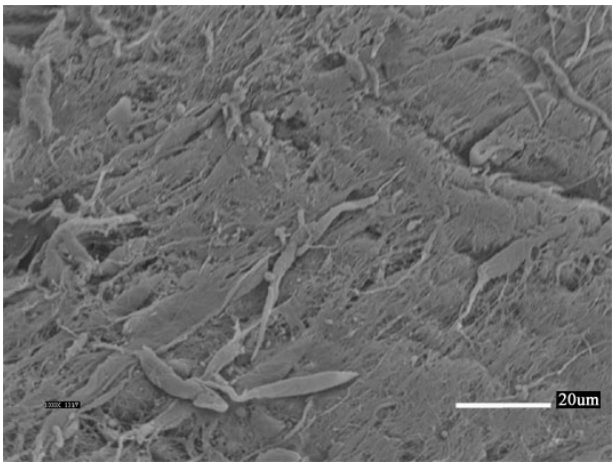

Figure 3.12 Scanning Electron Micrograph of the Group 3 HUV Scaffold recellularized with primary human vocal fold fibroblasts. (1000x Magnification)

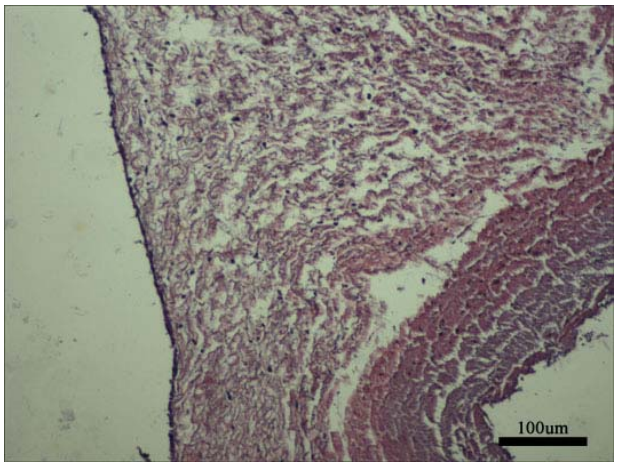

Figure 3.13 H&E staining of the Group 4 HUV scaffold recellularized with primary human vocal fold fibroblasts. (100x Magnification)

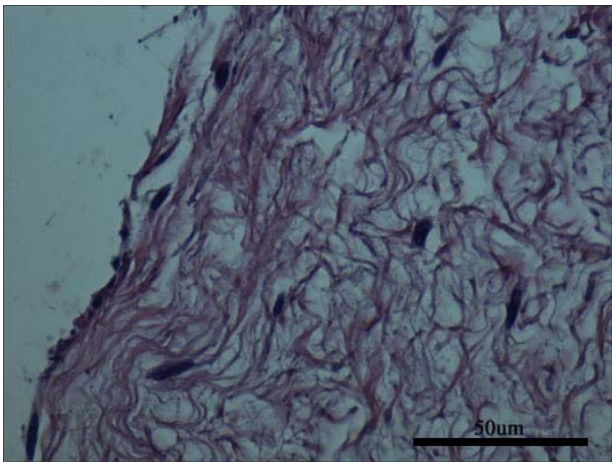

Figure 3.14 H&E staining of the Group 4 HUV scaffold recellularized with primary human vocal fold fibroblasts. (400x Magnification)

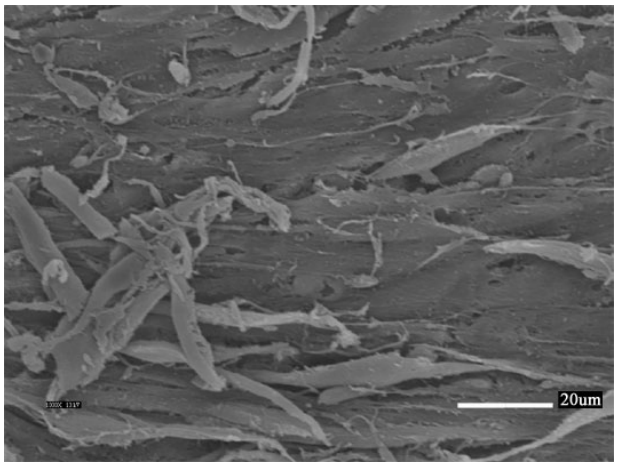

Figure 3.15 Scanning Electron Micrograph of the Group 4 HUV scaffold recellularized with primary human vocal fold fibroblasts. (1000x Magnification)

3.1.3. Biomechanical Properties

The biomechanical properties of the native HUV tissue, decellularized tissue, and recellularized tissue were compared to those of human vocal fold tissue (Fig 3.16 – 3.19). Figure 3.16 shows that the decellularized tissues (protocols 1 – 4) have in general, increasingly lower elastic modulus (G') values over the frequency range. These values are lower than those for native HUV tissue and human vocal fold tissue. However, the recellularized scaffolds (Figure 3.17) show generally higher values of G' over the frequency range than native HUV tissue and human vocal fold tissue. In this figure, Group 2 scaffolds show the highest G' values, and Group 4 scaffolds have values that are within the range of both native HUV tissue and human vocal fold values.

The dynamic viscosity (η') graphs showed a generally decreasing η' with increasing frequency (a shear thinning effect). The decellularized scaffolds (Figure 3.18) once again showed lower values than those of native HUV tissue and human vocal fold tissue. The dynamic viscosity values for the recellularized scaffolds (Figure 3.19) have higher values than the native HUV and human vocal fold tissues. Again Group 2 scaffolds had the highest values over all the groups, and Group 4 scaffolds had values within the range of the native HUV tissues as well as the human vocal fold cover.

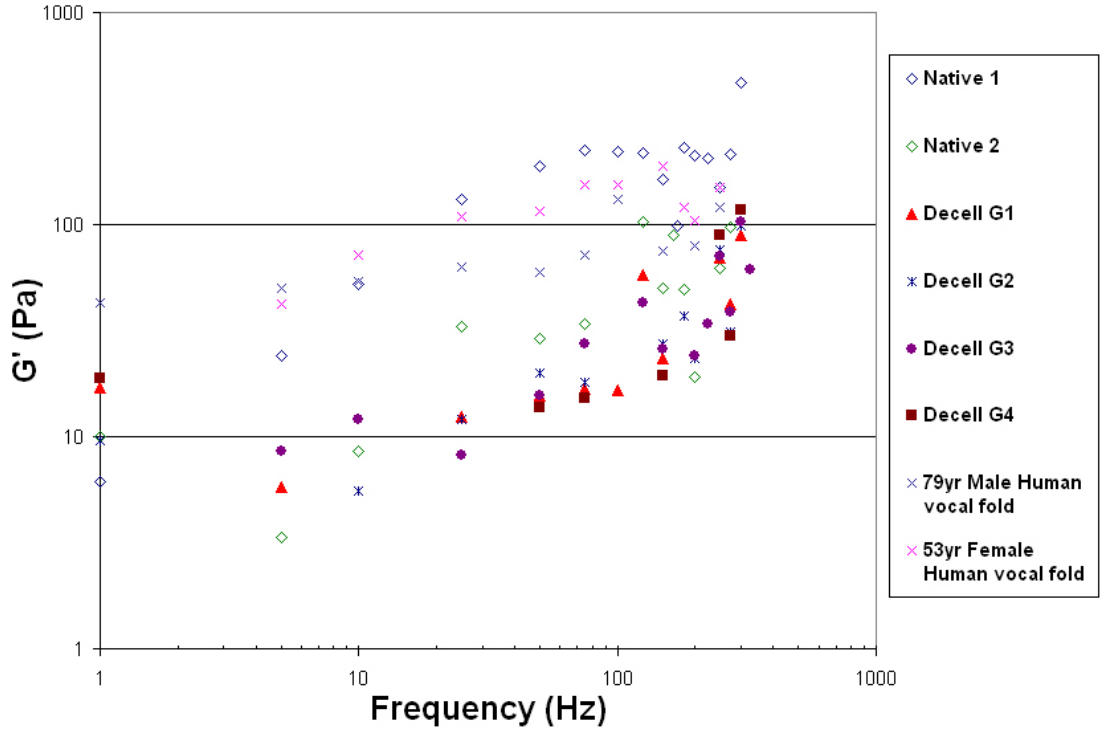

Figure 3.16 Elastic Shear Modulus (G') of Native HUV, Decellularized HUV scaffolds, and human vocal fold cover.

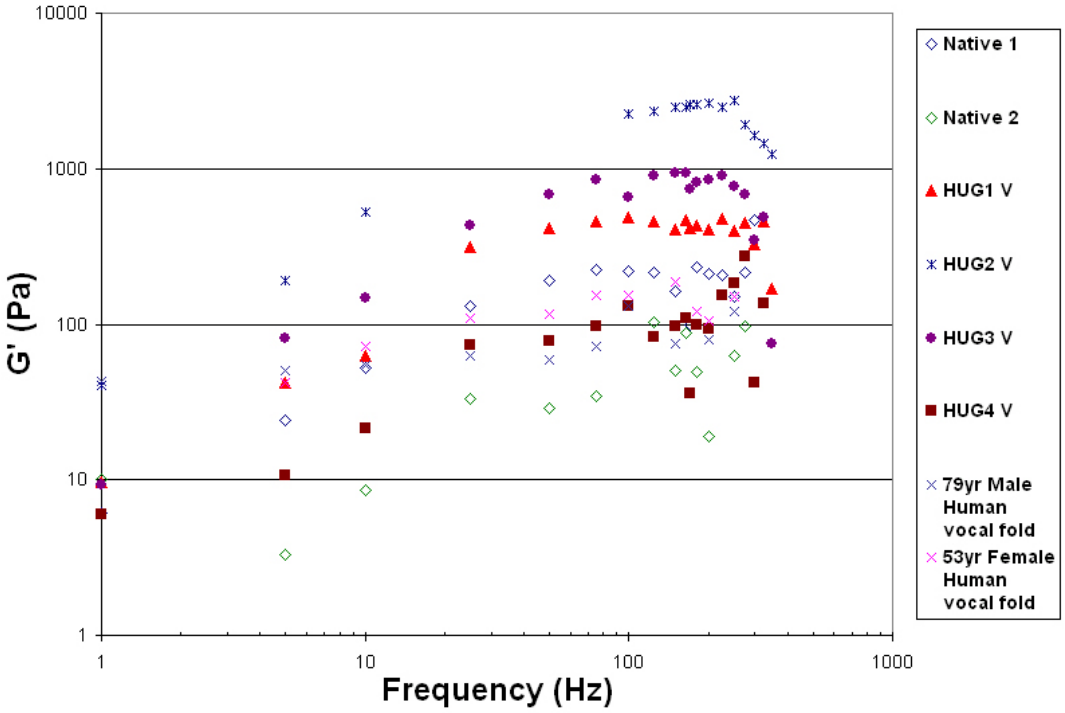

Figure 3.17 Elastic Shear Modulus (G') of Native HUV, Recellularized HUV scaffolds, and human vocal fold cover.

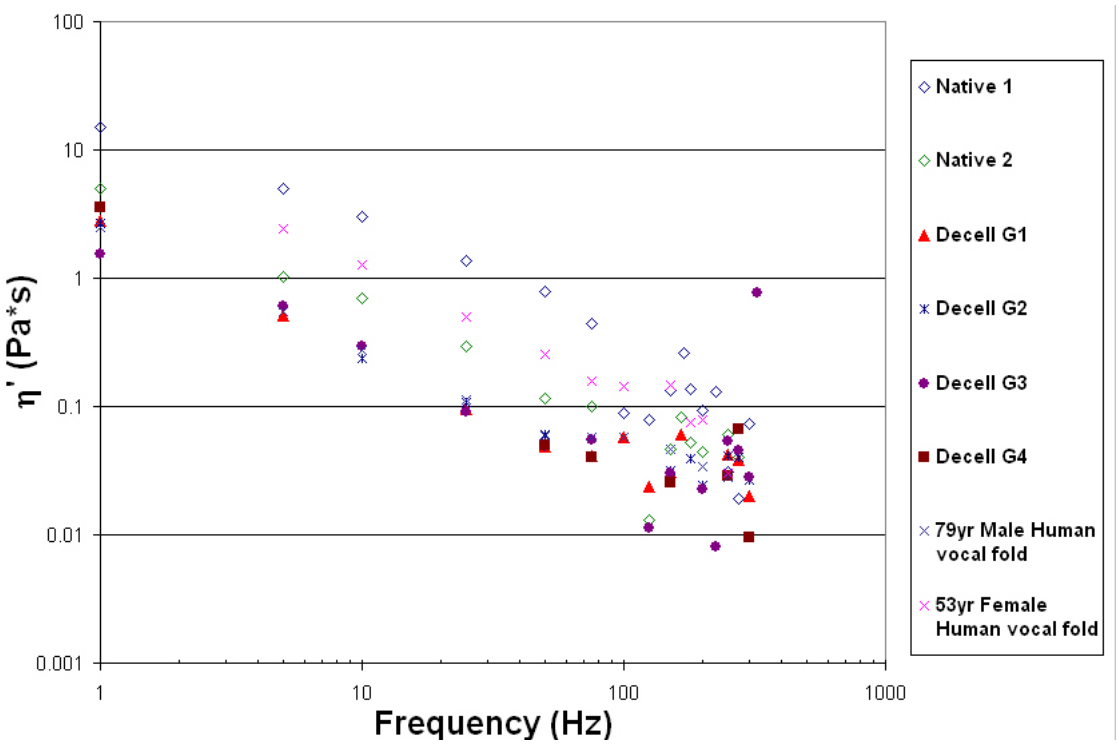

Figure 3.18 Dynamic viscosity (η') of native HUV tissue, decellularized scaffolds, and human vocal fold cover.

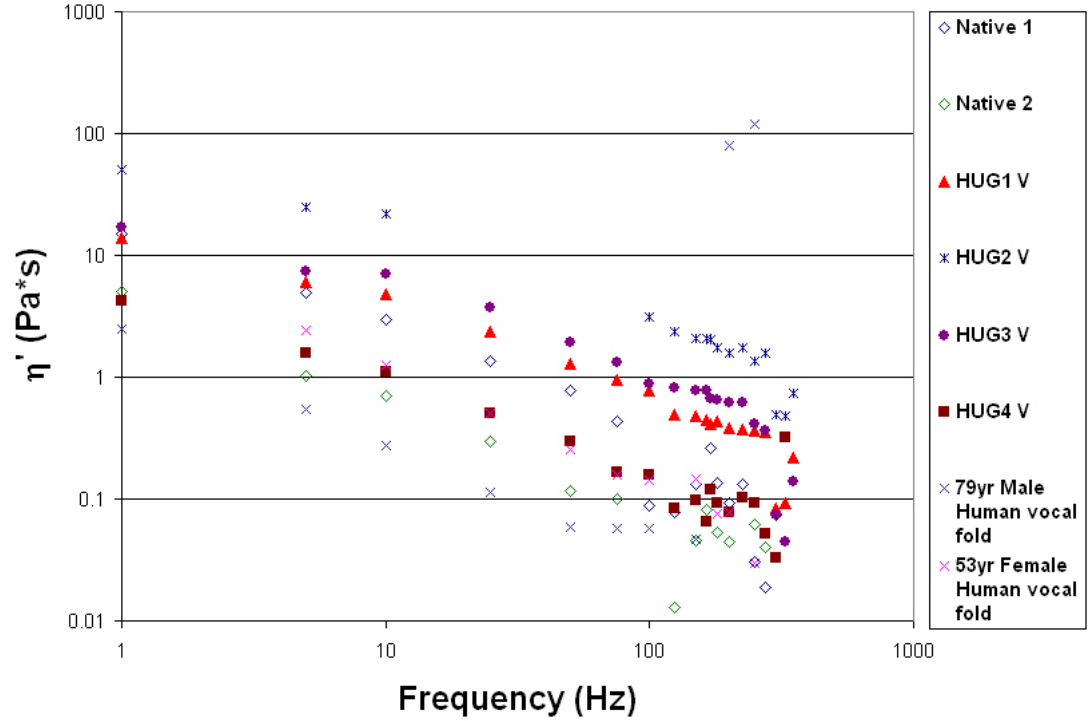

Figure 3.19 Dynamic viscosity (η') of native HUV tissue, recellularized scaffolds, and human vocal fold cover.

3.2. Experiment II – Examining the HUV Scaffold

3.2.1. Histological Staining – Native HUV Tissue

An approximate tissue thickness for the three native scaffolds was determined to be 2,650 ± 1059.58 μm using the histology photos (Table 3.1). Figure 3.20a shows the tissue stained with hematoxylin and eosin, with the entire tissue structure in its native form. The abluminal side on the left is slightly less dense than the deeper tissue. The lumen of the vein is the densest portion of the tissue (located on the right of the photo) and has the most cells. Myofibroblasts in the native tissue can be seen sparsely located throughout the abluminal side of the vein Figure 3.20b. Most of the tissue stained light blue using the Alcian Blue stain (Figure 3.20c) and the cells stained pink. Dark blue fibers representing the hyaluronic acid were also present, verified by treatment with hyaluronidase before staining (Figure 3.20d) that resulted in a drastic decrease of blue color throughout the tissue, making some practically transparent. Other molecular constituents such as chondroitin sulfates A, B, and C, keratosulphate, sialomucins, and sulphated sialomucins were also present. The Periodic Acid Schiff stain (Figure 3.20e) showed no red color, but had some areas in the tissue with dense light purple, particularly in areas around the cells. Staining with Safranin-O (Figure 3.20f) rendered most of the tissue blue-green and the cells pink/light-purple. No red or pink was seen around the cells, which would have indicated solely GAGs.

Scaffold ID	Thickness	Std Dev
	(μm)	(μm)
HUV 10-A	2960	
HUV 11-B	1470	
HUV 12-A	3520	
Average	2650	1059.58

Table 3.1 Individual and average thickness of native human umbilical veins from three different cords.

.

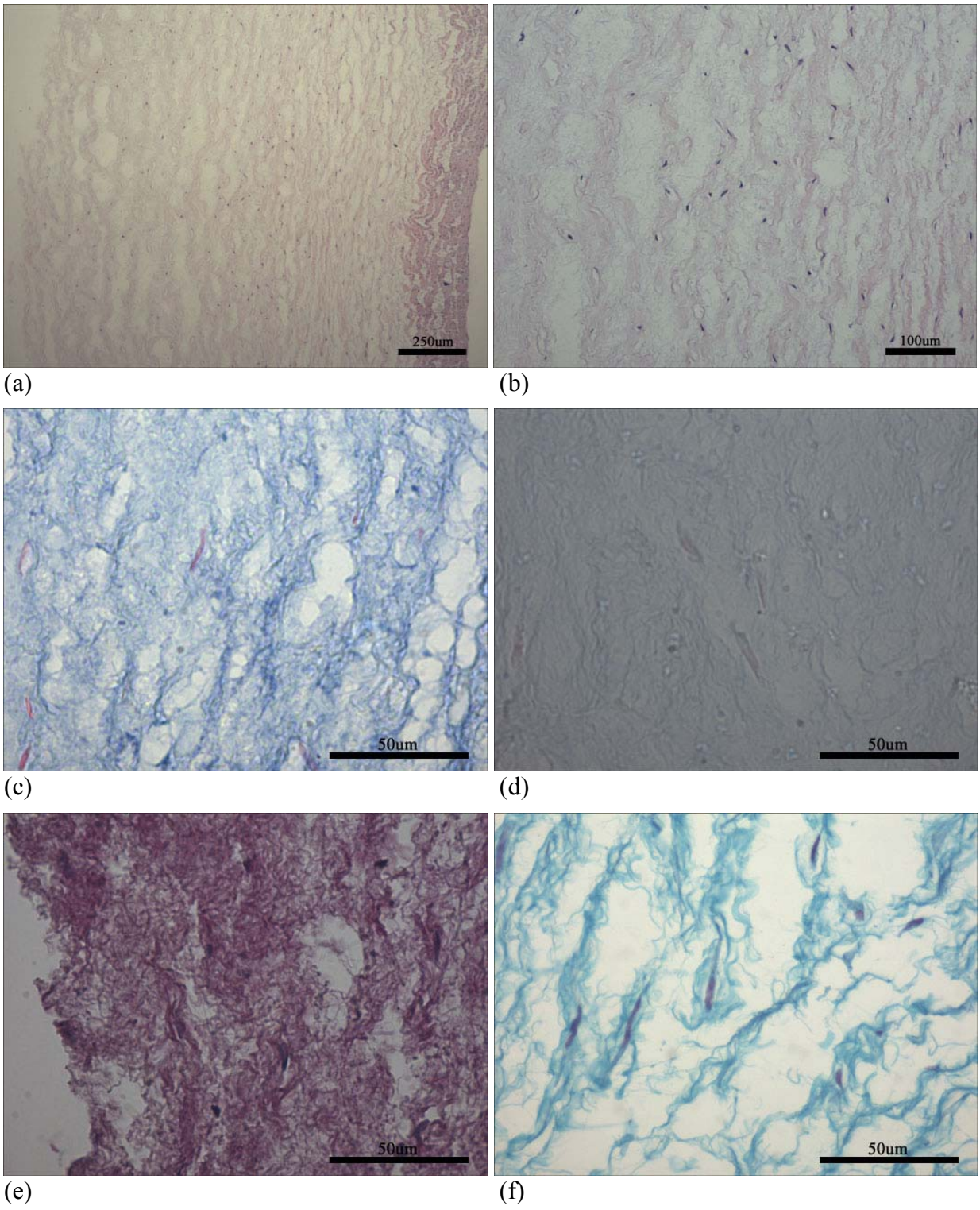

(a) (b)

(c) (d)

(e) (f)

Figure 3.20 Results of the native human umbilical vein using the following histology stains: (a) H&E (334x), (b) H&E (860x), (c) Alcian Blue (3,440x), (d) Alcian Blue with Hyaluronidase (3,440x), (e) Periodic Acid Schiff (3,440x), and (f) Safranin-O (3,440x). All photos are oriented such that the ablumen of the tissue is on the left side and the lumen on the right side.

3.2.2. Histological Staining – Decellularized HUV Tissue

Table 3.2 shows the thickness of the decellularized HUV scaffolds measured from the abluminal surface to the luminal surface. These decellularized tissues have an average thickness of 1960 ± 269.07 μm which is smaller than the thickness of the native tissue. Results from H&E stains (Figures 3.21a and 3.21b) showed the tissue density decreased slightly and the tissues were completely decellularized. Decellularized tissue stained with alcian blue (Figure 3.21c) was only slightly lighter as compared to native tissue, but still had some dark blue stain present. The hyaluronidase treated tissue lost most of the blue color (Figure 3.21d). Although the tissue was decellularized, it still maintained some of the dense light purple shown in Figure 3.21e (PAS). Similar to the native tissue results, no GAGs were detected using the Safranin-O stain (Figure 3.21f).

Scaffold ID	**Thickness**	**Std Dev**
	(μm)	(μm)
HUV 3-D	1660	
HUV 4-C	2040	
HUV 7-B	2180	
Average	1960	269.07

Table 3.2 Individual and average thickness of decellularized human umbilical veins from three different cords.

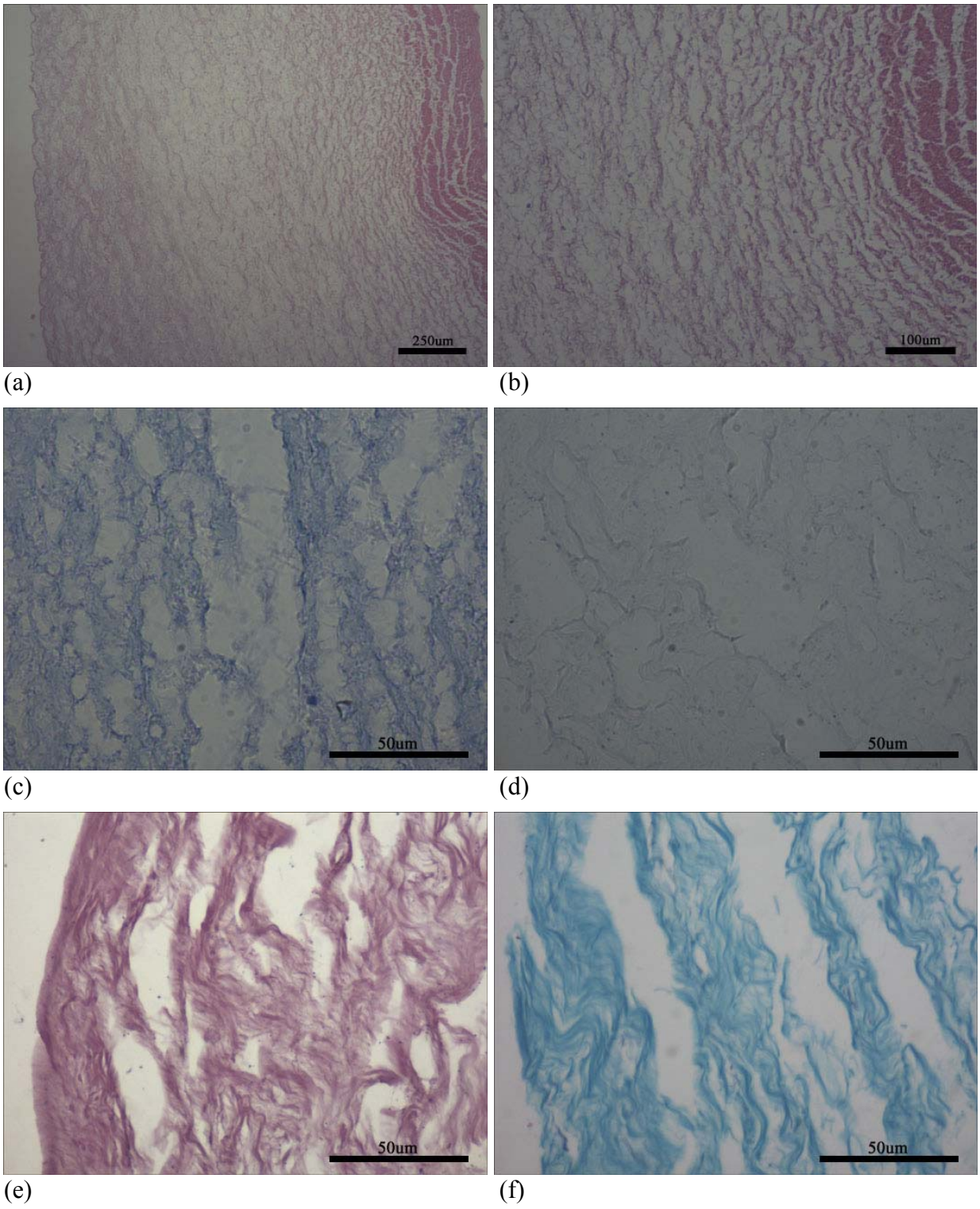

Figure 3.21 Results of the decellularized human umbilical vein using the following histology stains: (a) Hematoxylin & Eosin (334x), (b) Hematoxylin & Eosin (860x), (c) Alcian Blue (3,440x), (d) Alcian Blue with Hyaluronidase (3,440x), (e) Periodic Acid Schiff (3,440x), and (f) Safranin-O (3,440x). All photos are oriented such that the ablumen of the tissue is on the left side and the lumen on the right side.

3.2.3. Histological Staining – Decellularized & Cultured (Control) HUV Tissue

Tissue thicknesses for the control HUV tissues are shown in Table 3.3. These tissues were decellularized and cultured for 21 days which resulted in an average thickness of 1457 ± 315.33μm, smaller than the average thickness of decellularized tissue. Hematoxylin and eosin staining (Figures 3.22a and 3.22b) showed complete decellularization for most tissues except for one which had some dead cells trapped within the tissue. Also, tissue density decreased at the abluminal surface and increased deeper into the tissue. There was a significant decrease in staining intensity using alcian blue (Figure 3.22c), so a lower magnification was required to see the tissue. No significant amount of dark blue stain appeared in the tissue stained with alcian blue or in the hyaluronidase treated tissue (Figure 3.22d). PAS and Safranin-O results (Figures 3.22e and 3.22f) were negative for red and pink colors, respectively.

Scaffold ID	Thickness	Std Dev
	(μm)	(μm)
HUV 2-C	1780	
HUV 5-A	1150	
HUV 8-B	1440	
Average	1457	315.33

Table 3.3 Individual and average thickness of human umbilical veins from three different cords that have been decellularized and cultured for 21 days.

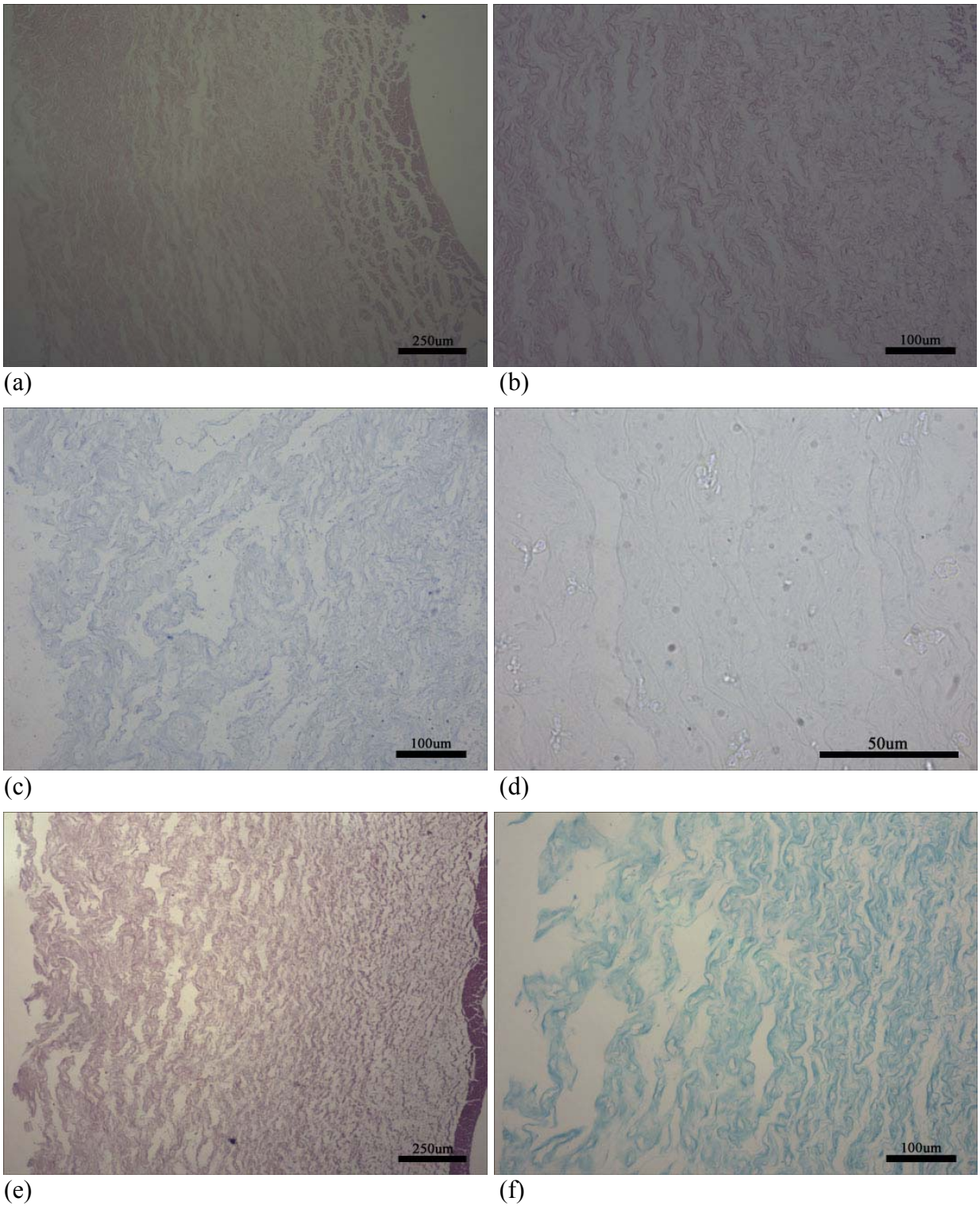

Figure 3.22 Results of the human umbilical vein that has been decellularized and cultured for 21 days using the following histology stains: (a) Hematoxylin & Eosin (334x), (b) Hematoxylin & Eosin (860x), (c) Alcian Blue (860x), (d) Alcian Blue with Hyaluronidase (3,440x), (e) Periodic Acid Schiff (334x), and (f) Safranin-O (860x). All photos are oriented such that the ablumen of the tissue is on the left side and the lumen on the right side.

3.2.4. Histological Staining – Recellularized HUV Tissue

The thicknesses of the HUV tissues seeded with human vocal fold fibroblasts are reported in Table 3.4. Two of the three tissues have a considerably smaller thickness than the control tissues, whereas HUV 6-A has a thickness in the range of the control tissue. Therefore, the average thickness of 1043 ± 523.67 μm appears to be only slightly smaller than the average thickness of the control tissues. The fibroblasts completely infiltrated the HUV scaffold and caused the abluminal surface to increase in density, i.e., becoming more compact, after the 21 days of culture (Figures 3.23a). These cells have formed several layers on the abluminal surface and have an elongated shape (Figure 3.23b). The areas of the tissue with cells were in dark blue color with the alcian blue stain, whereas the hyaluronidase treated tissues were not (Figures 3.23c and 3.23d). For these tissues, there were more dark-pink areas surrounding the cells with the PAS stain (Figure 3.23e). Also, the Safranin-O stain (Figure 3.23f) revealed shades of pink between the cells that were layered on the abluminal surface. This was the only condition for which pink shades were noticed outside the cells for staining with Safranin-O.

Scaffold ID	Thickness	Std Dev
	(μm)	(μm)
HUV 1-A	660	
HUV 6-A	1640	
HUV 9-A	830	
Average	1043	523.67

Table 3.4 Individual and average thickness of human umbilical veins from three different cords that have been decellularized, recellularized and cultured for 21 days.

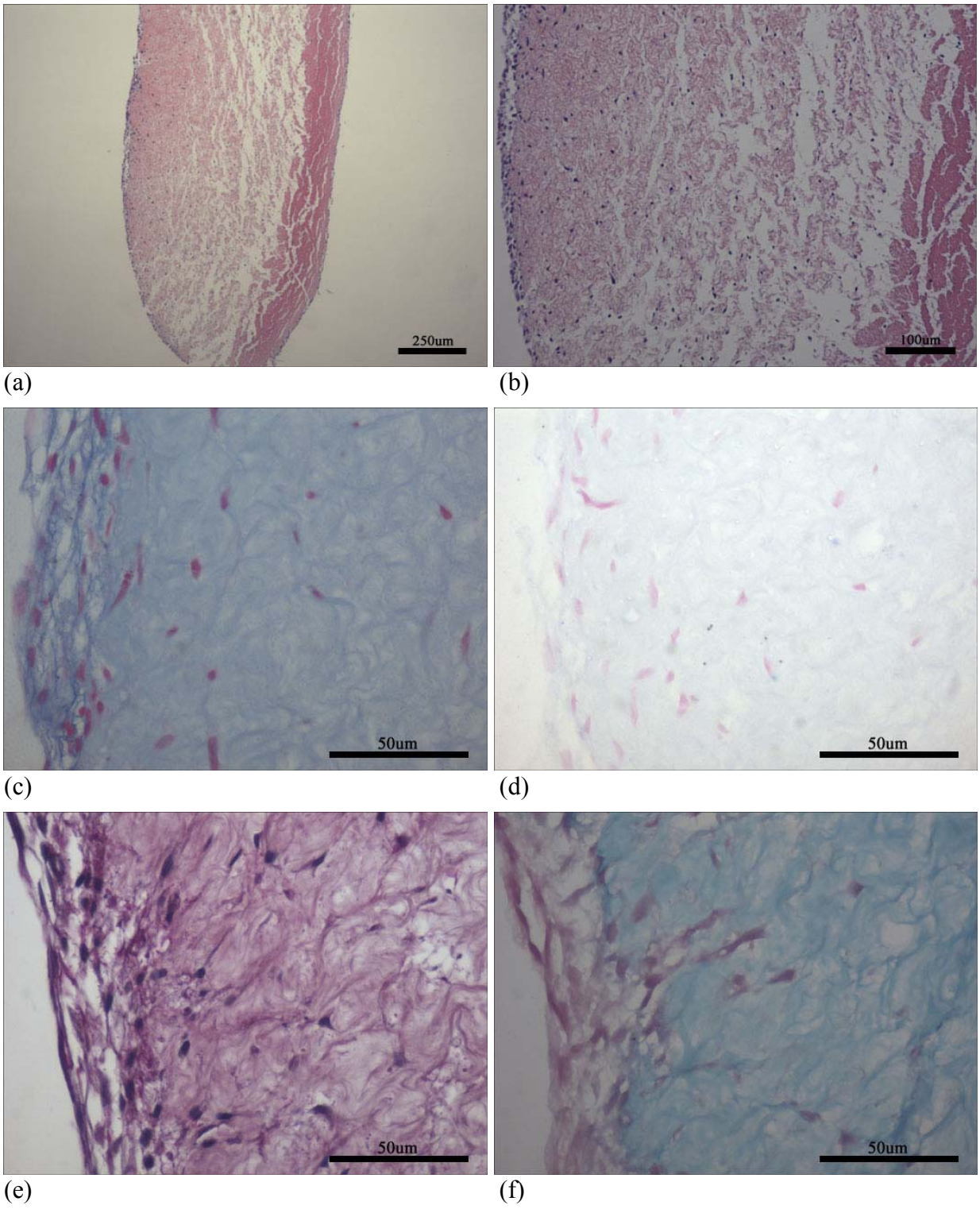

Figure 3.23 Results of the human umbilical vein that has been decellularized, seeded with cells, and cultured for 21 days using the following histology stains: (a) Hematoxylin & Eosin (334x), (b) Hematoxylin & Eosin (860x), (c) Alcian Blue (3,440x), (d) Alcian Blue with Hyaluronidase (3,440x), (e) Periodic Acid Schiff (3,440x), and (f) Safranin-O (3,440x). All photos are oriented such that the ablumen of the tissue is on the left side and the lumen on the right side.

3.2.5. Digital Image Analysis of Masson's Trichrome Images

Table 3.5 shows the image analysis results used for quantifying the relative densities of collagen in the tissue samples stained with Masson's Trichrome. For each protocol, three tissues from three different umbilical cords (n=3) were examined and the average values of their relative staining intensity and the percentage area fraction of collagen were reported. The first examination (image analysis 1) had a relatively high standard deviation for the tissue in its native condition due to the positioning of the tissue during the embedding process. Therefore a second analysis was carried out using a different scaffold from the same umbilical cord (image analysis 2). There are slight differences in the collagen area fraction for each analysis within the same processing conditions. The decellularized and control tissues had the highest collagen intensities [0.82, 0.85(1^{st}); 0.84, 0.84(2^{nd})], respectively followed by the natural tissue and recellularized tissue. However, the corresponding percentage area fractions of collagen relative to the total tissue area are the highest in the recellularized tissue (59.05% and 51.07%) and the natural tissue (57.98% and 39.49%).

	1st Image Analysis				2nd Image Analysis			
Condition	**Collagen Intensity**	**Std Dev**	**Collagen Area Fraction**	**Std Dev**	**Collagen Intensity**	**Std Dev**	**Collagen Area Fraction**	**Std Dev**
			(%)	(%)			(%)	(%)
Natural	0.75	0.13	57.98	61.27	0.82	0.01	39.49	10.71
Decellularized	0.82	0.01	38.81	2.17	0.84	0.02	32.43	13.60
Control	0.85	0.03	31.69	10.16	0.84	0.01	30.38	10.29
Recellularized	0.79	0.03	59.05	22.60	0.80	0.03	51.07	11.54

Table 3.5 Results for the Masson's Trichrome stain showing the averages of the relative staining intensities and percentage area fractions (collagen area / total area) for each condition. Both the first and second analysis used three tissues from three different cords (n=3) for each condition. See text for details.

3.2.6. Scanning Electron Microscopy

Scanning electron micrographs of the abluminal surface of each scaffold, for every condition, are shown in Figures 3.24 – 3.27. Figure 3.24 shows the typical appearance of the extracellular matrix (ECM) of the native human umbilical vein tissue. As indicated in the H&E histological slides, there were few native cells located on the abluminal surface of the native HUV; none can be seen in these SEM figures. Tissues that have been decellularized (Figures 3.25) appear to be slightly less dense and more fibrous on the surface, but the general 3-D ECM structure appears to have been maintained. The control tissues that had been decellularized and cultured for 21 days (Figures 3.26) have a similar structure to those of decellularized tissues, but seem more fibrous. Finally, the tissues recellularized with primary human vocal fold fibroblasts (Figures 3.27) are observed to have layers of cells attached to the abluminal surface. The layers shown from above (Figure 3.27a & 3.27c) have a flat appearance, whereas the layers shown at an angle (Figure 3.27b) have a bumpy appearance, thereby depicting the locations of the cell nuclei. Viable cells attached to the surface that are not part of these layers appear in a lighter shade of gray and have a three-dimensional appearance.

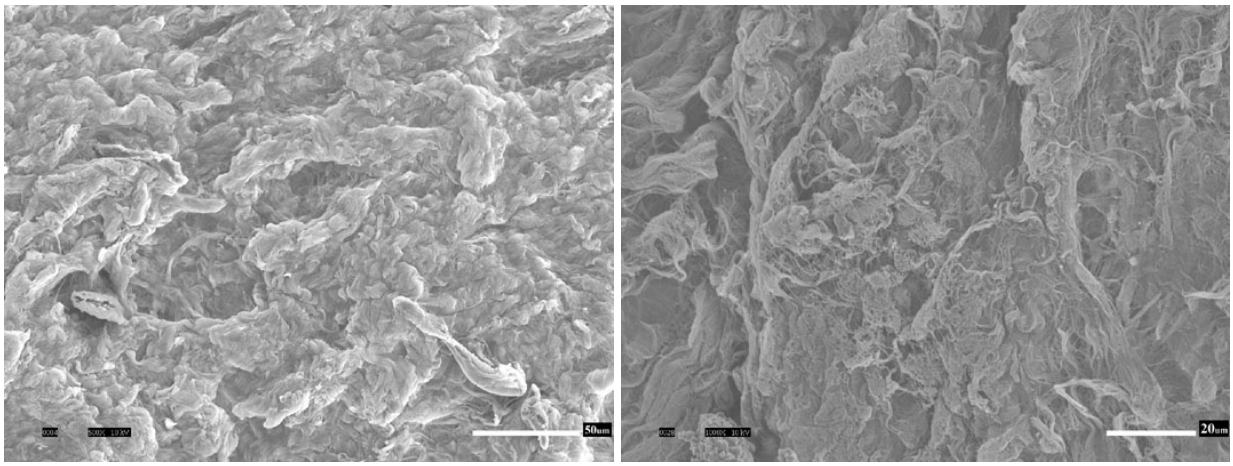

(a) (b)

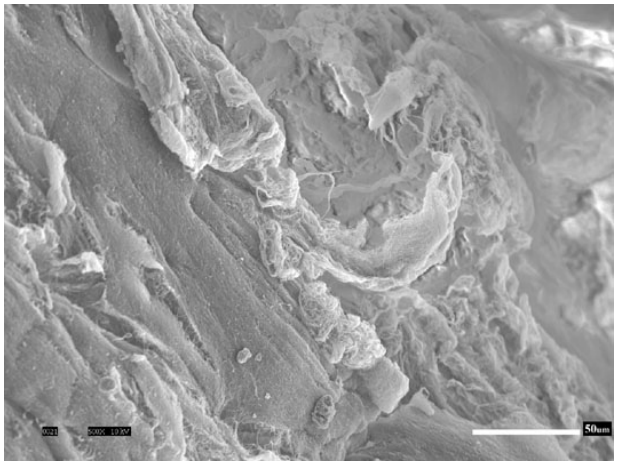

(c)

Figure 3.24 Scanning electron micrographs of native HUV tissue from three different veins at (a) 500x, (b) 1000x, and (c) 500x magnification.

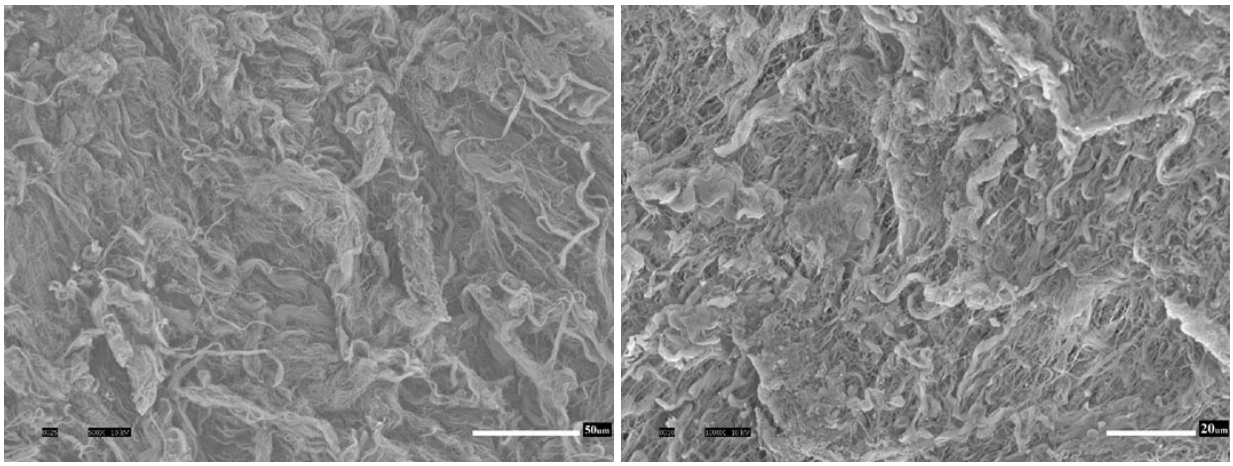

(a) (b)

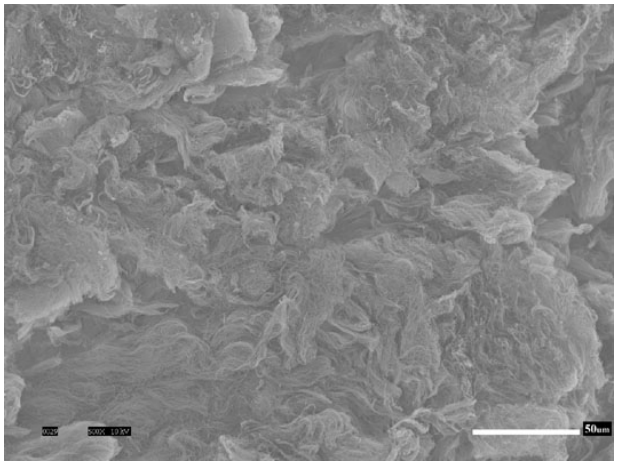

(c)

Figure 3.25 Scanning electron micrographs of decellularized HUV tissue from three different veins at (a) 500x, (b) 1000x, and (c) 500x magnification.

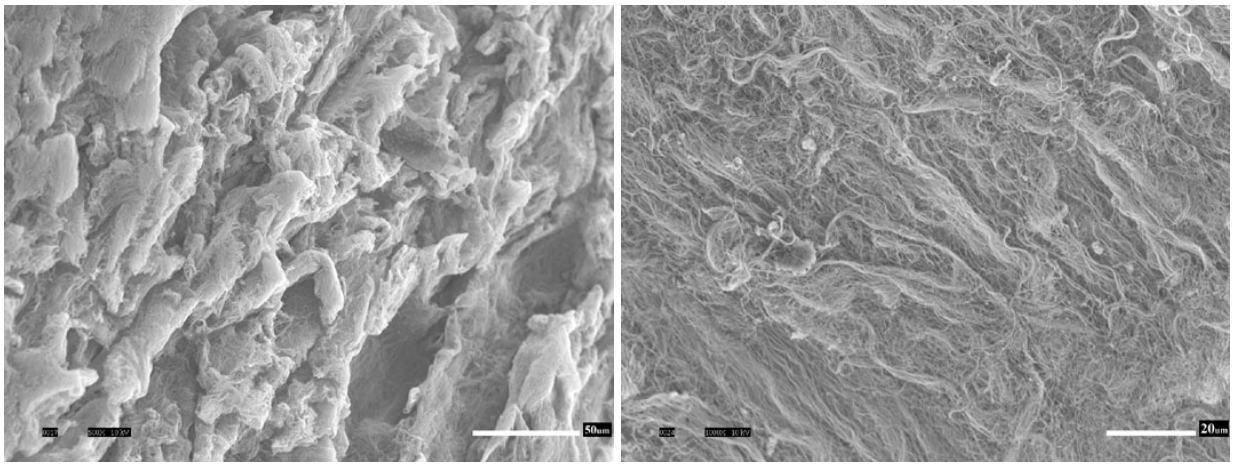

(a) (b)

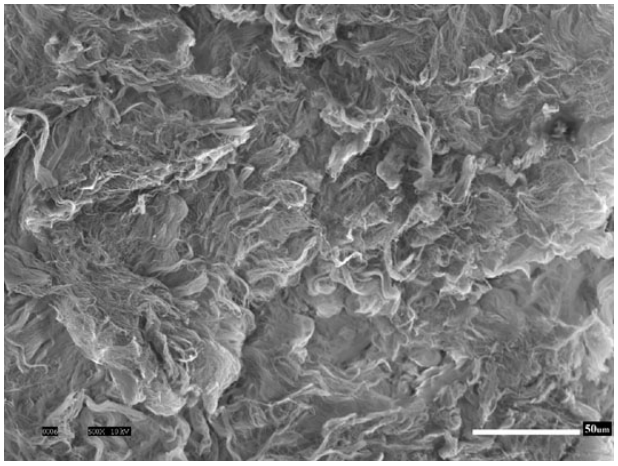

(c)

Figure 3.26 Scanning electron micrographs of control HUV tissue from three different veins at (a) 500x, (b) 1000x, and (c) 500x magnification.

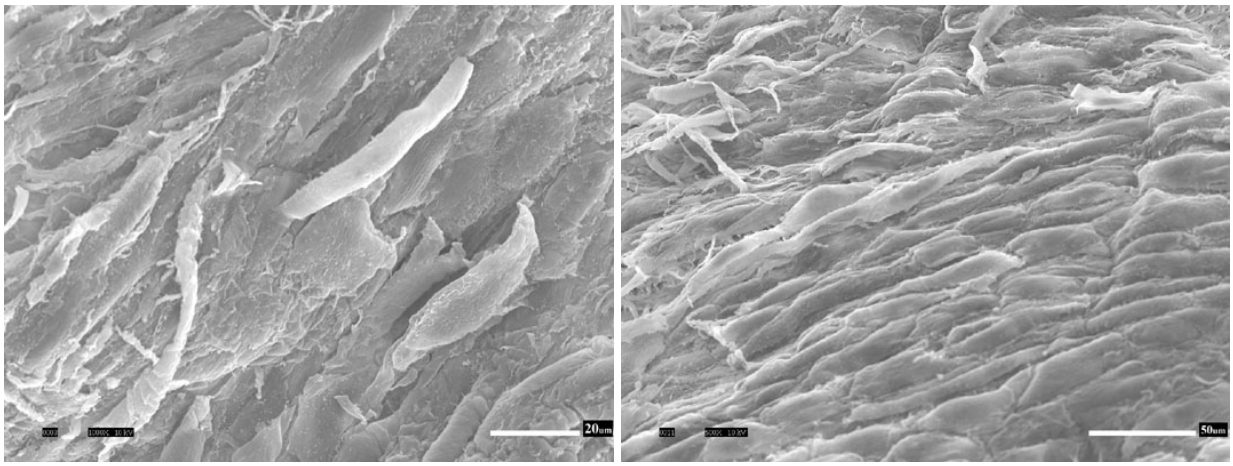

(a) (b)

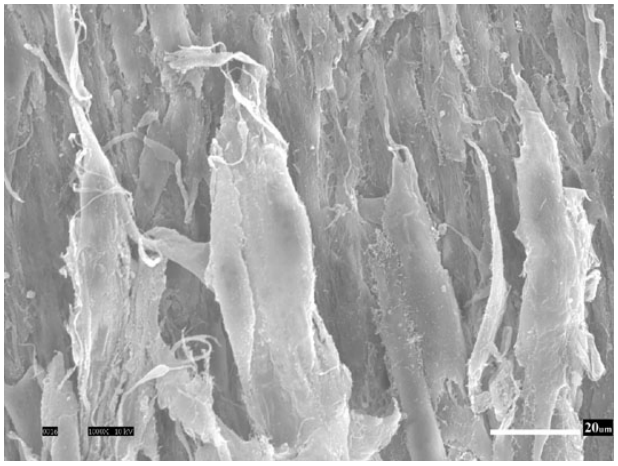

(c)

Figure 3.27 Scanning electron micrographs of recellularized HUV tissue from three different veins at (a) 1000x, (b) 500x, and (c) 1000x magnification.

3.2.7. Biomechanical Properties

The previous biomechanical measurements used native tissue that had been refrozen after dissection of the vein before being shipped to our lab. This raised the question of whether the freezing and thawing processes might have changed the mechanical properties of the native tissues. Experiment II and Experiment IV used tissues that had only been frozen at -80^{o}C before the vein dissection, then immediately refrigerated and shipped to be used. The manually dissected tissues were dissected by hand immediately after the cord was received from the hospital (within hours). Therefore, the manual tissue was in its natural state and was never frozen. Figures 3.28 – 3.33 show the results of the biomechanical tests for shear modulus for each of these native tissues. The general trend of increasing G' with increasing frequency is apparent, as before. One of the native tissues that had been refrozen had the highest values, at most frequencies. The manually dissected tissue values were slightly lower than those of the refrozen native tissue, except for the highest frequency range. The tissues that had not been refrozen (Experiments II & IV) had lower values than the manually dissected tissue. However, the other refrozen tissue had the lowest overall values. The dynamic viscosity values (Figure 3.29) for each set of tissues followed the same trends, except the values decreased with increasing frequency, similar to the shear-thinning behavior of human vocal fold tissues. Results shown in the figure are based on two samples of native tissue from Experiment I, 3 samples of manually dissected tissue, and 6 samples of native tissues from Experiments II and IV.

All conditions for Experiment II as well as the data from two human vocal fold cover samples are plotted in Figure 3.30 & Figure 3.31. Similar trends were observed for G' and η' with increasing frequency as in previous data. However, in this experiment, human vocal fold samples have the highest G' values at lower frequencies and decellularized tissues have the

highest values at higher frequencies. At these higher frequencies decellularized tissue has the highest values, followed by control tissues and native tissues. The recellularized tissues have the lowest G' values for almost all frequencies. At frequencies above 150Hz, recellularized tissues have shear modulus values very close to those of the human vocal fold cover. The shear modulus values for all conditions are relatively close to those of the human data, which can have a wide range as well. The dynamic viscosity of these tissues decreases with increasing frequency, with the decellularized tissue having the highest values again. The control tissues have values slightly lower followed by values for native tissues. Recellularized tissues have dynamic viscosities very close to those of the 53 year old female, and the 79 year old male has the lowest values over all frequencies. Figures 3.32 and 3.33 show the shear modulus and dynamic viscosity for the native, recellularized, and human vocal fold tissues. This graph gives a clearer view of how the native and recellularized tissues have similar trends to the human vocal fold tissues.

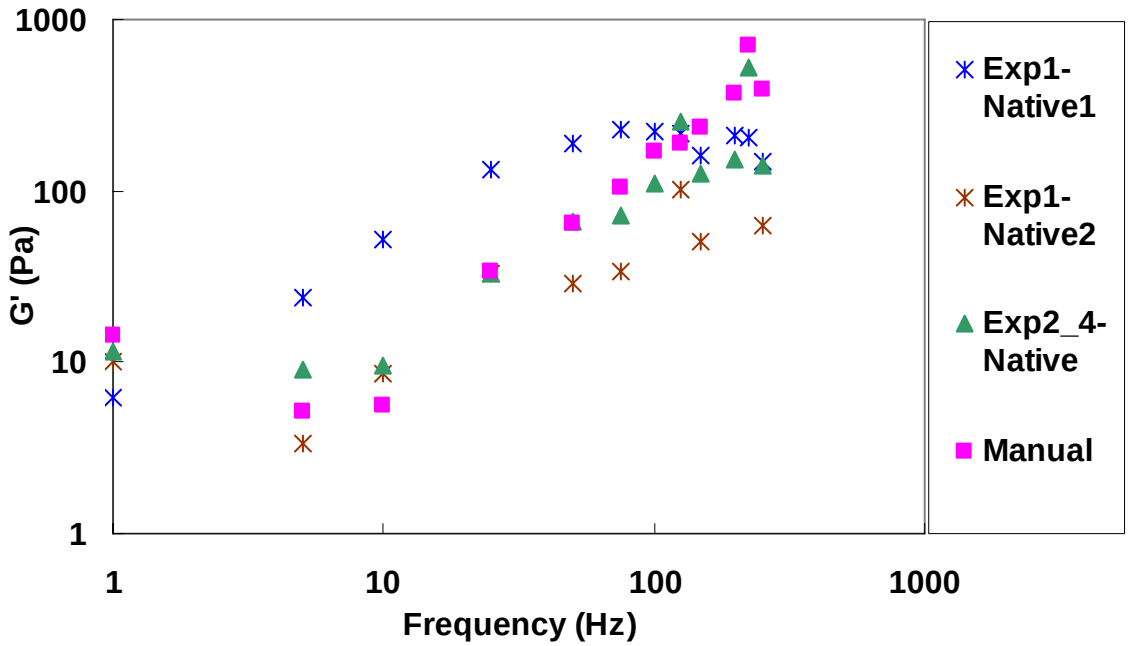

Figure 3.28 Results comparing native tissues from Experiment I (refrozen)(n=1), Experiment II & IV (not refrozen)(n=6), and manually dissected tissue (natural)(n=3).

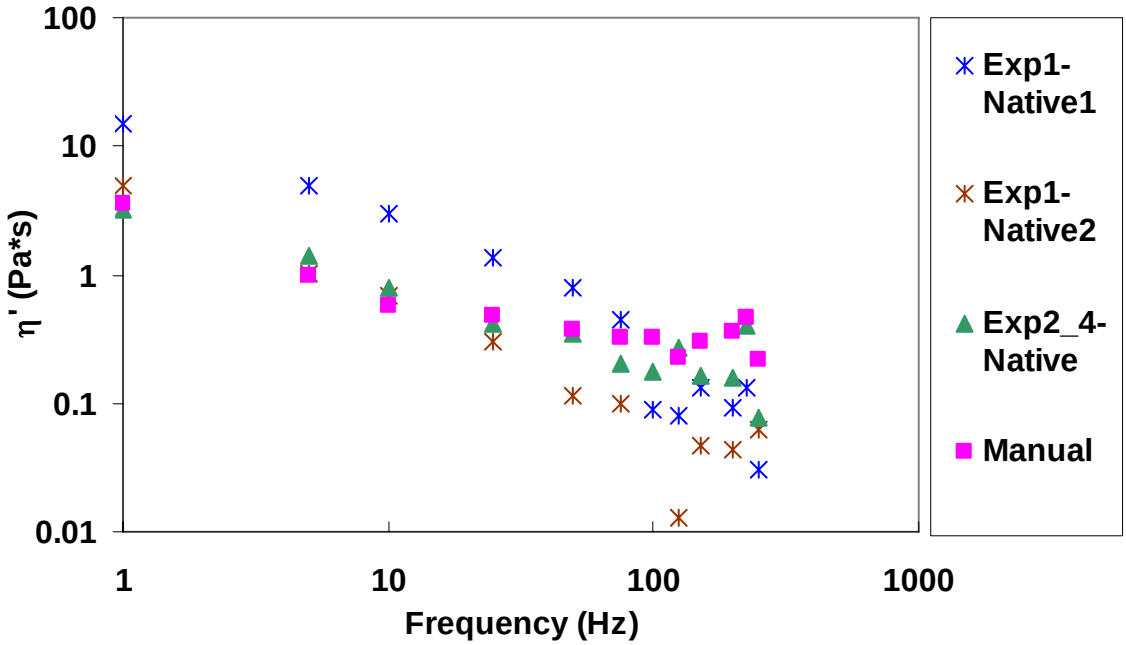

Figure 3.29 Results comparing native tissues from Experiment I (refrozen)(n=1), Experiment II & IV (not refrozen)(n=6), and manually dissected tissue (natural)(n=3).

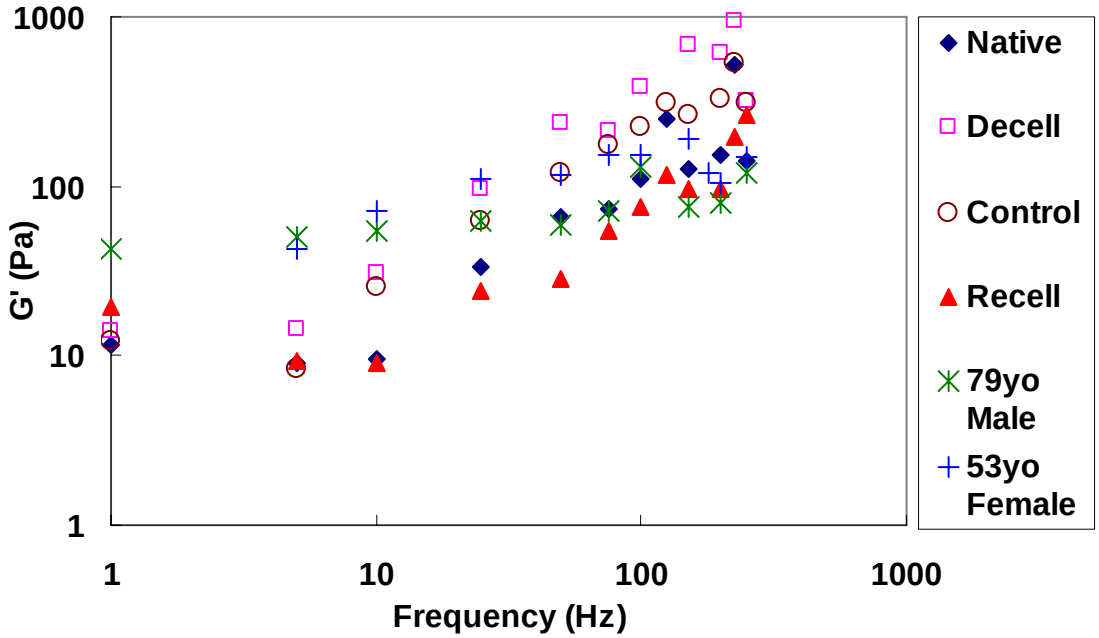

Figure 3.30 Results comparing all conditions for Experiment II as well as data obtained from human vocal folds (n=3 for decellularized, control, and recellularized data; n=6 for native tissue; n=1 for human data).

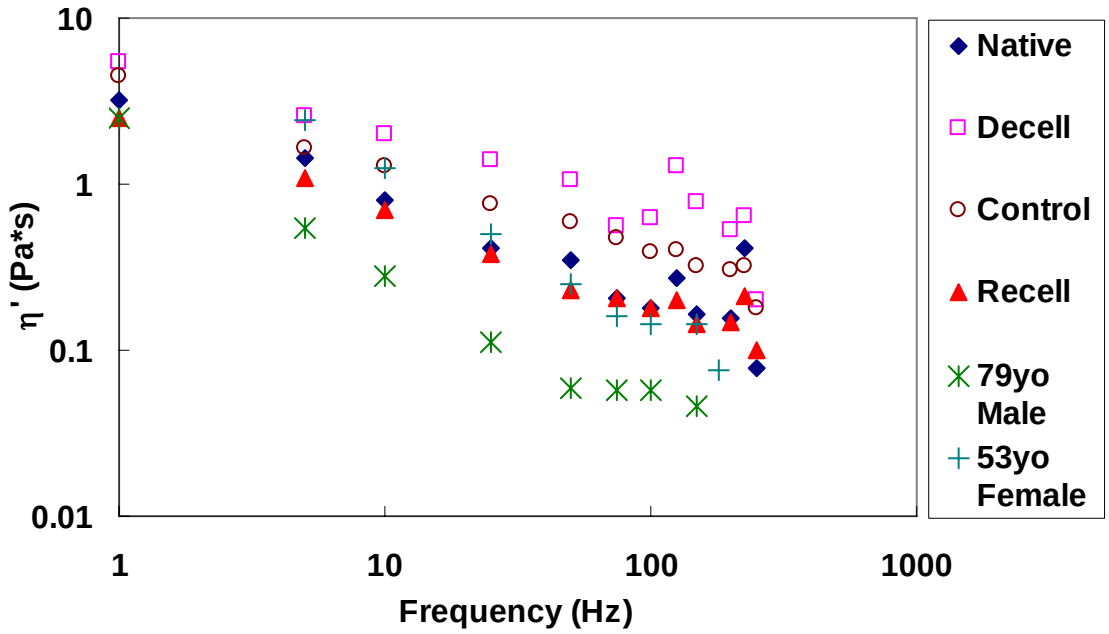

Figure 3.31 Results comparing all conditions in Experiment II across a range of frequencies: native (n=6), decellularized (n=3), control (n=3), and recellularized (n=3). Also included is data obtained from human vocal folds (n=1).

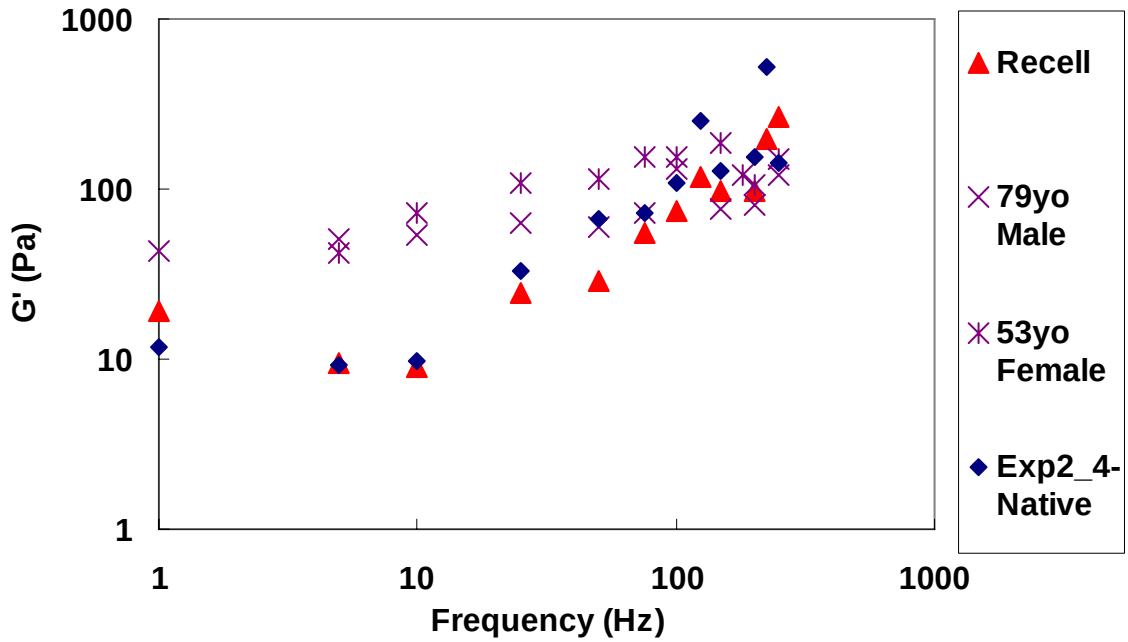

Figure 3.32 Results showing the shear modulus values of native (n=6), recellularized (n=3), and human vocal fold (n=1) tissues across different frequencies.

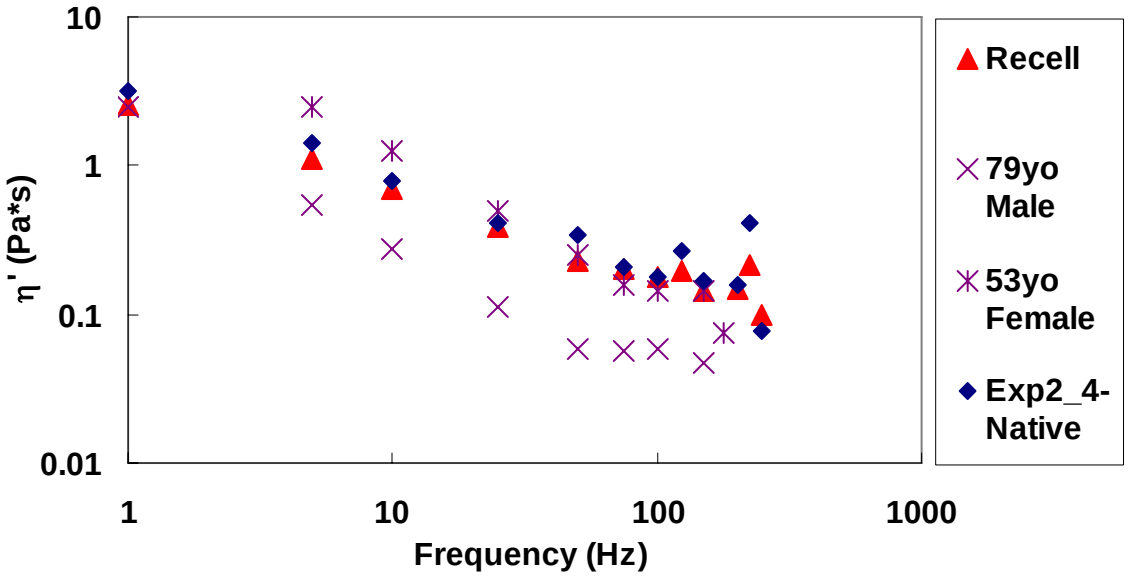

Figure 3.33 Results showing the dynamic viscosity values of native (n=6), recellularized (n=3), and human vocal fold (n=1) tissues across different frequencies.

3.3. Experiment III – Cell Recovery

The cell recovery results in Figures 3.34, 3.35 and Tables 3.6, 3.7 show the attachment and proliferation of the primary human vocal fold fibroblasts seeded onto the abluminal surface of the three-dimensional acellular human umbilical vein scaffolds. Figure 3.34 shows the individual scaffold results for the three different veins (HUV 1, HUV 2, and HUV 3). The first significant finding was that the number of cells recovered per scaffold area (mm^2) increased rapidly from day 6 to day 9. There was another increase in the number of cells at day 12, after which scaffold HUV 3 reached a plateau. Following day 12, the number of cells in scaffold HUV 1 continued to increase while the number of cells in scaffold HUV 2 increased and reached a plateau after day 15. There was a large decrease in the number of cells in scaffolds HUV 2 and HUV 3 on day 18, deviating from the general trend. Thus, monotonic behavior was not observed for any samples. The normalized average number of cells (n=3) over time (Figure 3.35) showed a similar trend, with a sharp increase from day 6 to day 9, followed by a gradual increase up to day 21, with the exception of a slight decrease on day 18, which can be explained by the individual decreases of scaffolds HUV 2 and HUV 3 in Fig. 3.34.

Results obtained from day 0 and day 1 show that of the one million cells seeded on each scaffold, an average of about 17,417 to 18,225 (1.74 - 1.82%) attached onto the abluminal surface of the acellular HUV scaffold (Table 3.6). The average final cell count after 21 days in culture was 482,292 ± 135,888 cells ranging from 382,250 to 637,000 cells. This was comparable to Experiment II, which had an average final cell count of 316,750 ± 45,102 cells ranging from 281,250 to 367,500. This finding suggested that the cellular attachment and growth in the scaffolds in Experiments II and III were comparable.

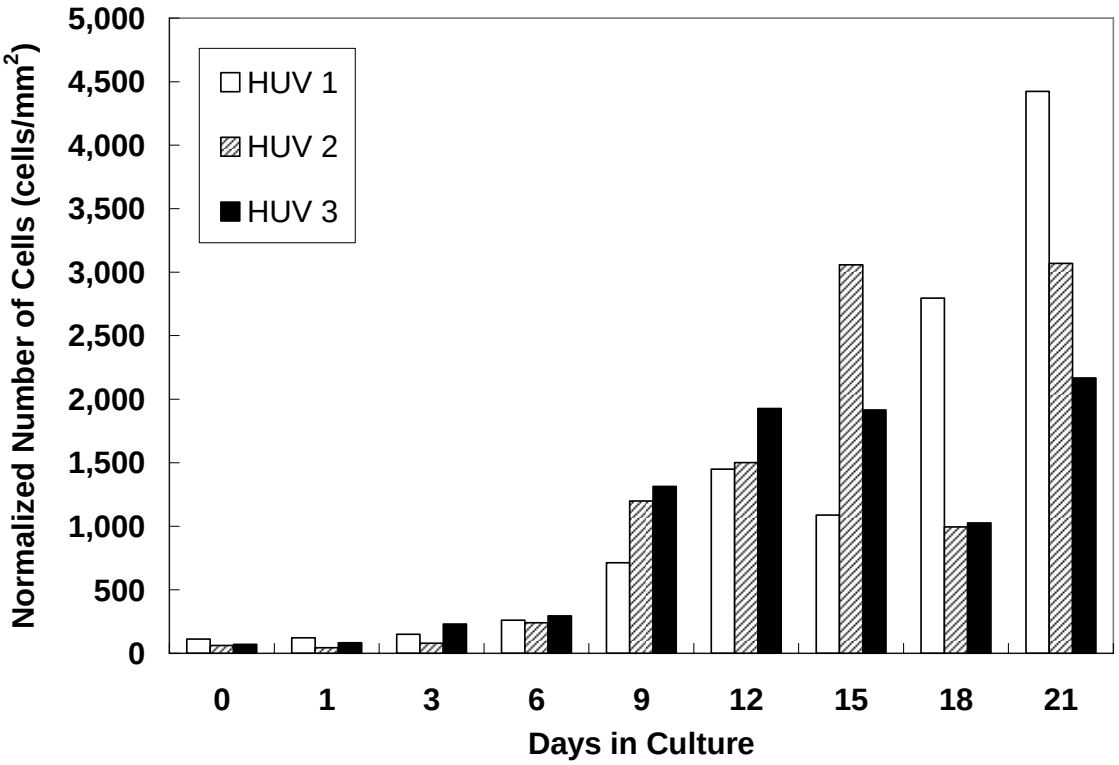

Figure 3.34 Results of cell recovery (cell counting using hemocytometer) showing the normalized number of human vocal fold fibroblasts that have attached and proliferated onto three 3-dimensional human umbilical vein (HUV) acellular scaffolds over time (n=3).

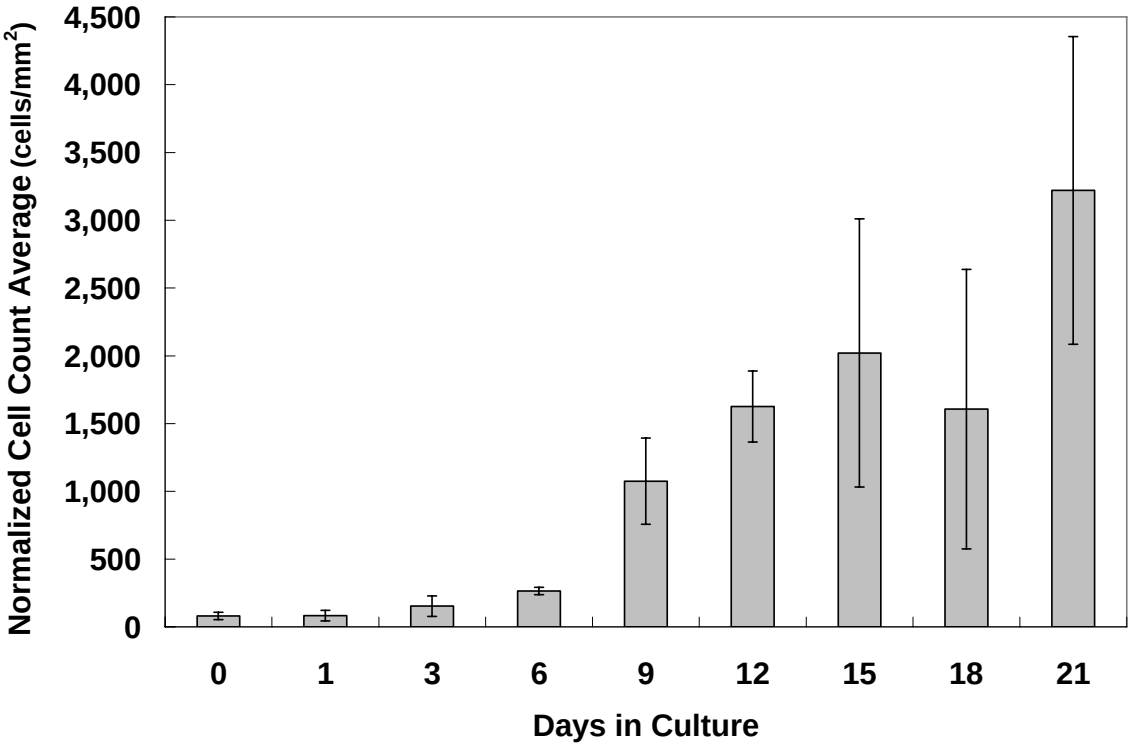

Figure 3.35 Results of cell recovery (cell counting using hemocytometer) showing the normalized average attachment and proliferation of human vocal fold fibroblasts (VFF) seeded onto three 3-dimensional human umbilical vein (HUV) acellular scaffolds over time (n=3).

Day	Average Cell Count	Standard Deviation of Average Cell Count	Average Area	Standard Deviation of Average Area
	(# of cells)	(# of cells)	(mm^2)	(mm^2)
0	17,417	5,125	217	28
1	18,225	10,220	216	24
3	38,267	18,861	250	0
6	61,250	4,394	232	8
9	236,567	70,051	220	0
12	342,933	103,818	208	28
15	382,725	155,956	202	61
18	235,067	68,026	167	48
21	482,292	135,888	153	20

Table 3.6 Results of cell recovery (cell counting using hemocytometer) showing the average attachment and proliferation of human vocal fold fibroblasts (VFF) seeded onto three 3-dimensional human umbilical vein (HUV) acellular scaffolds over time (n=3).

Scaffold	Cell Count
	(# of cells)
HUV 1	367,500
HUV 6	281,250
HUV 9	301,500
Average	316,750 ± 45,102

Table 3.7 Results of cell recovery at day 21 for the three scaffolds used in Experiment II.

3.4. Statistical Analysis

3.4.1 Bland Altman Plot

A statistical analysis was performed on the data using a Bland Altman plot. First the results for the log of the shear modulus (log G') and the log of the dynamic viscosity (log η') of the recellularized tissue were plotted against those of the two human vocal fold specimens (Figures 3.36 – 3.39). A line of identity was included to accentuate the differences in values . Most values for the human data, each representing the log G' or log η' at a particular frequency, are larger that those of the recellularized tissue. Although at certain frequencies, the recellularized tissue has greater values. Also, there are certain values that lie far from the line of equality. These correspond to the upper and lower frequencies of our system where the data are not as reliable.

Figures 3.40 – 3.43 plot the bias of the values against their average at each frequency. The average bias is plotted to show on average, how far the values are from equality. Most values lie within two standard deviations except for one value in Figure 3.42. This value corresponds to a frequency at the limit of the system as mentioned earlier.

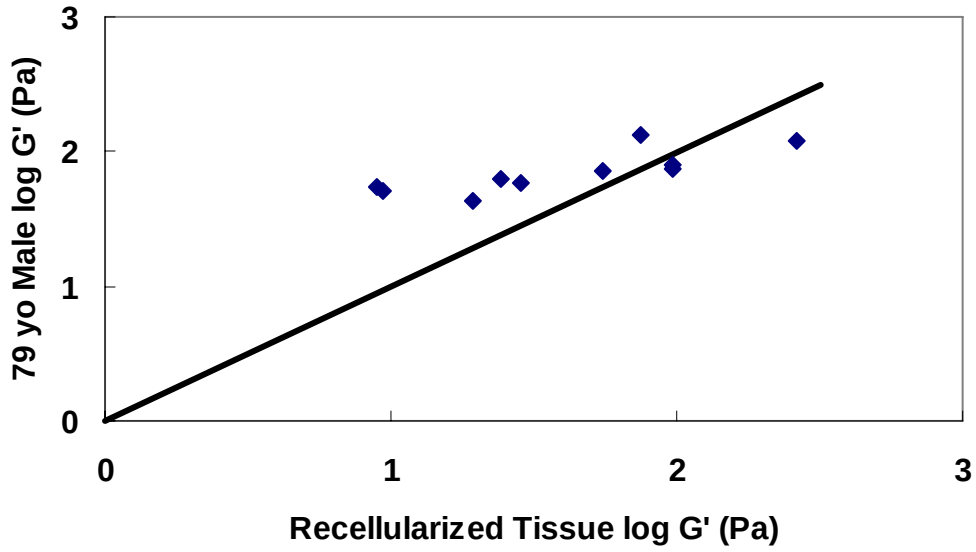

Figure 3.36 Plot of the log of the shear modulus (G') values of the 79-year-old male vocal fold cover versus recellularized HUV tissue with line of equality.

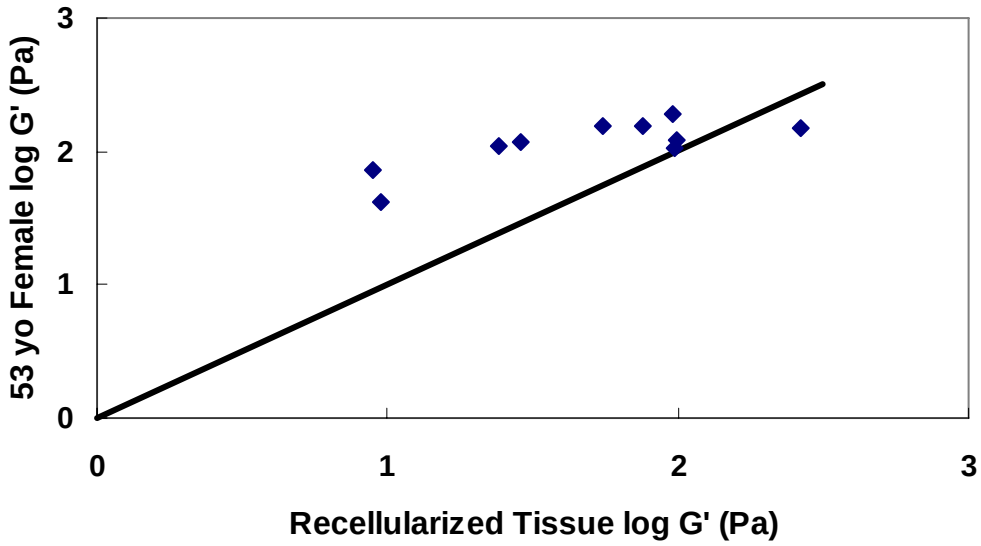

Figure 3.37 Plot of the log of the shear modulus (G') values of the 53-year-old female vocal fold cover versus recellularized HUV tissue with line of equality.

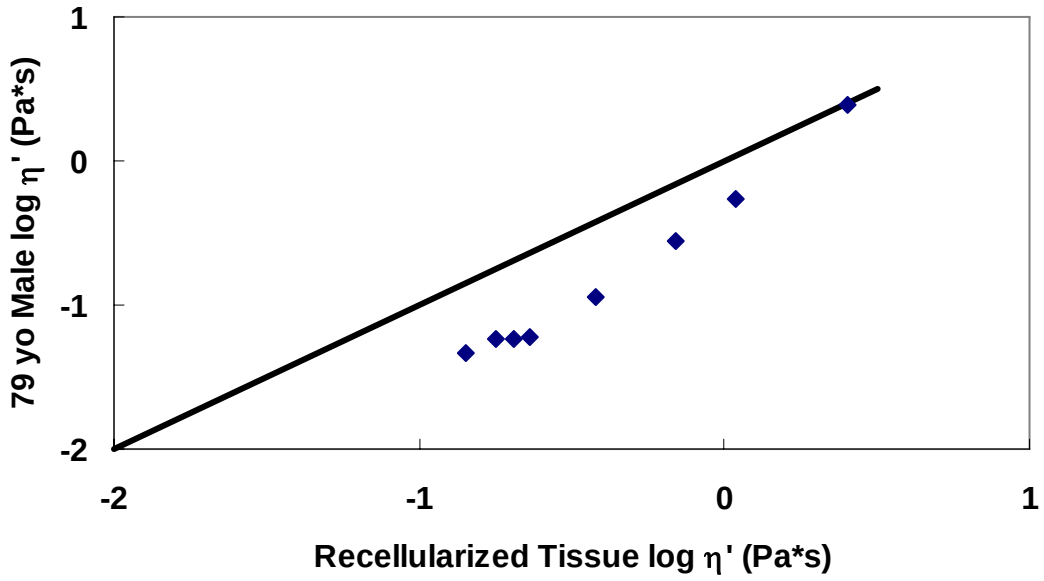

Figure 3.38 Plot of the log of the dynamic viscosity values of the 79-year-old male vocal fold cover versus recellularized HUV tissue with line of equality.

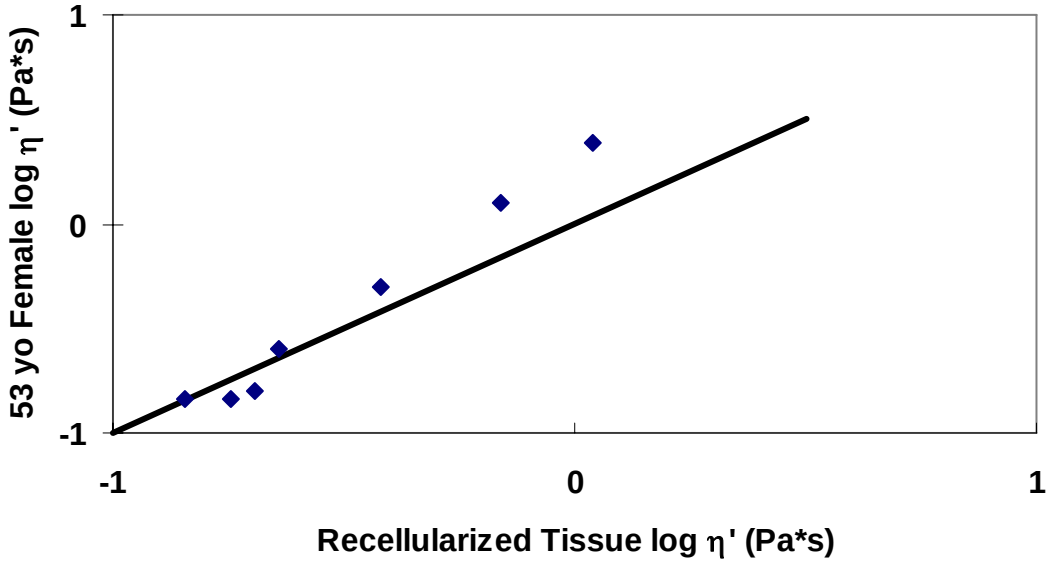

Figure 3.39 Plot of the log of the dynamic viscosity values of the 53-year-old female vocal fold cover versus recellularized HUV tissue with line of equality.

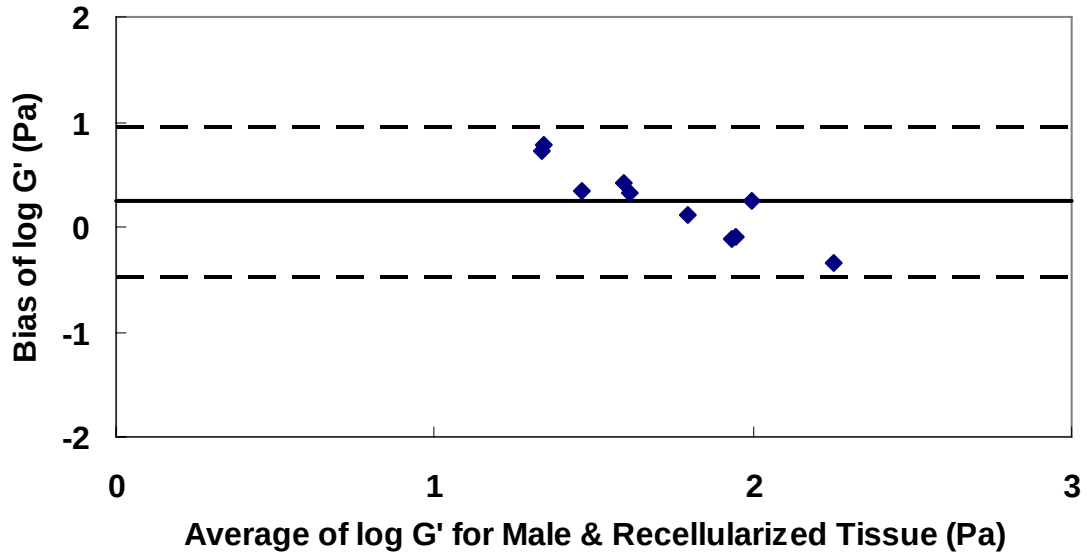

Figure 3.40 Difference in the log of the shear modulus (log G') versus the log of the shear modulus mean for each frequency (one data point represents a particular frequency) for the 79-year-old male vocal fold cover and the recellularized HUV tissue, with two standard deviations as the limits of agreement.

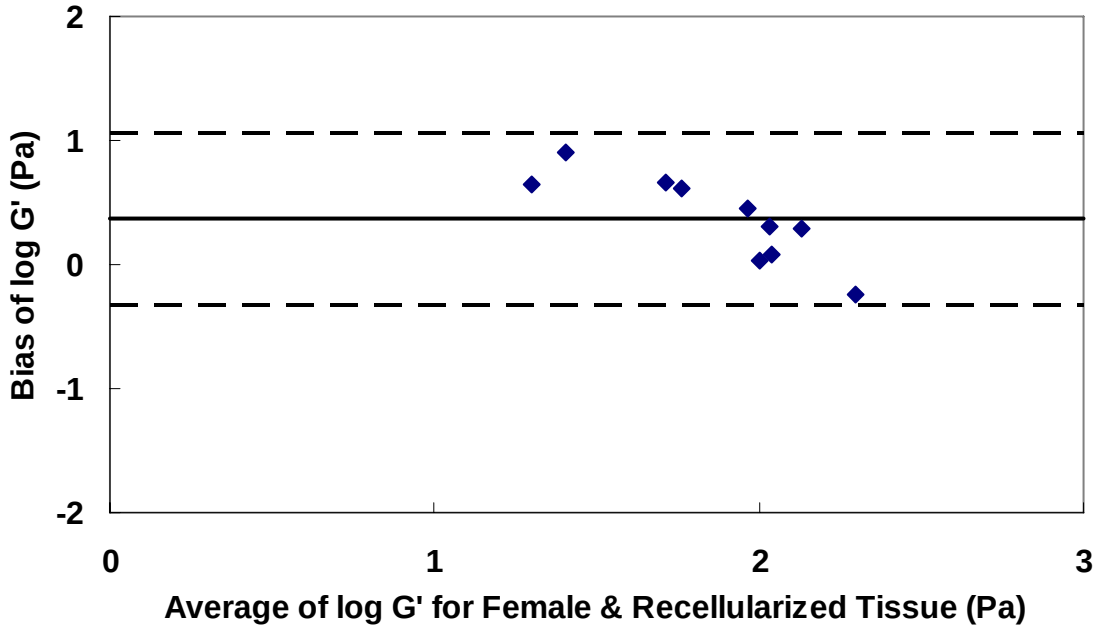

Figure 3.41 Difference in the log of the shear modulus (log G') versus the log of the shear modulus mean for each frequency (one data point represents a particular frequency) for the 53-year-old female vocal fold cover and the recellularized HUV tissue, with two standard deviations as the limits of agreement.

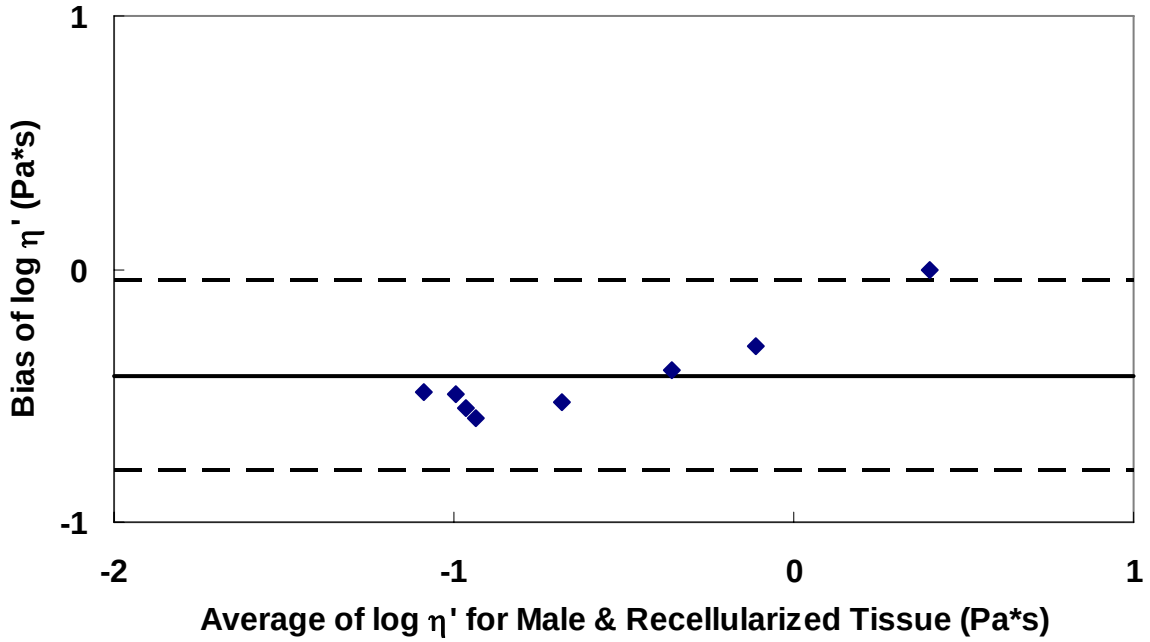

Figure 3.42 Difference in the log of the dynamic viscosity (log η') against the mean of the log of dynamic viscosities for each frequency (one data point represents a particular frequency) for the 79-year-old male vocal fold cover and the recellularized tissue, with limits of agreement.

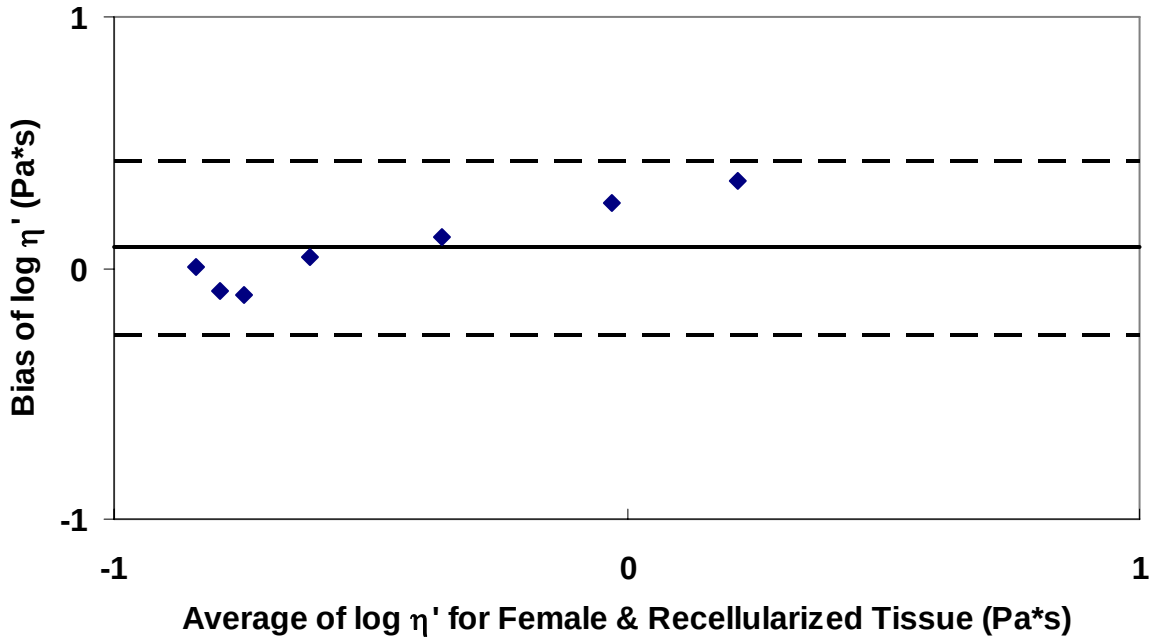

Figure 3.43 Difference in the log of dynamic viscosity (log η') against the mean of the log of dynamic viscosities for each frequency (one data point represents a particular frequency) for the 53-year-old female vocal fold cover and the recellularized tissue, with limits of agreement.

3.4.2 Coefficient of Variation

Comparisons were made between and within subjects in each condition to show the variability of the measurements. The coefficient of variation, CV (%), was calculated for the average shear modulus and dynamic viscosity of three scaffolds from the same vein (n=3) and of three veins within the same condition (n=3). For the native tissue condition, six veins were examined (n=6) because some veins did not respond to a sufficient number of frequencies. The log values of G' and η' were used in this analysis since these values are always examined on a log scale versus frequency. Coefficients of variation that have a value of zero correspond to data that only had measurements for one subject at that frequency (n=1). Coefficients of variation

that were not reported in the table correspond to frequencies that had a tissue response that could not be analyzed.

For most tissues, the CV had a wide range of values. For the veins dissected manually (Table 3.8), lower frequencies had more variation within a vein than between veins, and the opposite was seen at higher frequencies. The values of η' for HUV 1 had an unusually high CV within the vein. For native tissue (Table 3.9 and 3.10), the values for CV within the same vein were high, but values across different veins had lower CVs. Decellularized tissues (Table 3.11) showed a similar trend in CV values as the manually dissected tissue. Control tissue (Table 3.12) followed the same trend as the native tissue. Recellularized tissue had larger coefficients of variation between the scaffolds within a vein than between veins.

Frequency	Within a Vein						Between Veins	
	G'			η'			G'	η'
	HUV 1	HUV 2	HUV 3	HUV 1	HUV 2	HUV 3	Avg HUV	Avg HUV
Hz	%	%	%	%	%	%	%	%
1	2.78	14.15	5.76	52.13	31.98	5.17	4.71	14.45
5	53.21	46.95	34.50	166.24	-55.14	-431.83	9.82	-361.78
10	29.11	8.45	44.98	-180.40	-8.01	-100.25	14.31	-59.33
25	17.78	4.40	18.52	-252.99	-2.93	-79.20	21.52	-70.29
50	14.48	3.48	28.59	-153.71	-2.40	-64.80	22.63	-65.45
75	13.01	0.81	33.32	-126.21	-1.32	-59.18	22.14	-64.41
100	11.82	1.76	3.44	-115.31	-0.37	-8.50	17.84	-71.26
125	12.26	4.85	19.48	-90.36	-5.49	-57.19	23.05	-70.37
150	10.66	9.68	4.95	-106.13	-9.36	-10.52	24.01	-74.98
165	13.27	5.95	12.56	-110.87	-10.53	-4.21	25.71	-86.79
170	15.67		20.67	-117.12		-5.88	25.97	-81.92
180	14.14	13.69	4.03	-148.84	-8.83	-6.98	29.58	-76.97
200	10.08	16.98	7.83	-205.83	-6.46	-4.24	40.27	-88.33
225	7.68		3.79	-176.88		-11.76	15.00	-103.06
250	3.39	3.22	13.32	-44.10	-5.48	-32.62	18.74	-70.06

Table 3.8 Coefficients of variation for the average shear modulus and dynamic viscosity of scaffolds from within an umbilical vein, and between umbilical veins that were dissected manually (n=3).

Frequency	Within a Vein						Between Veins
	G'						G’
	HUV 10	HUV 11	HUV 12	HUV 13	HUV 14	HUV 15	Avg HUV
Hz	%	%	%	%	%	%	%
1	7.54	1.89	2.35	6.21	21.95	20.53	7.78
5	0.00		19.82	0.00	2.61	16.17	23.04
10	62.03	6.10	23.69	10.91	30.18	20.97	13.76
25	61.38	12.94	23.43	18.78	31.34	18.42	22.23
50	58.84	10.89	31.26	22.13	3.65	23.65	30.97
75	56.91	11.88	29.35	16.59	36.21	21.71	19.92
100	35.54	4.57	8.16	10.65	34.47	20.68	14.17
125	0.00			1.27	2.08	60.67	38.02
150	50.13		5.70	10.45	35.11	20.89	19.46
200	93.67		3.43	19.15	3.39	34.82	34.62
225	0.00				4.82		0.21
250	27.92	2.60	5.03	11.76	22.00	8.18	12.11

Table 3.9 Coefficients of variation for the average shear modulus within an umbilical vein (n=3) and between umbilical veins in their native form (n=6). Each Tissue ID (HUV 10 – 15) is the average value of three scaffolds from that vein.

Frequency	Within a Vein						Between Veins
	η'						η’
	HUV 10	HUV 11	HUV 12	HUV 13	HUV 14	HUV 15	Avg HUV
Hz	%	%	%	%	%	%	%
1	52.17	2.71	6.55	8.17	29.71	18.17	12.41
5	0.00		-139.41	0.00	4.43	-81.75	424.17
10	-518.72	-5.03	-58.51	-35.25	17.00	-50.74	-113.88
25	-193.97	-6.90	-33.48	-30.32	-276.91	-28.22	-45.46
50	-153.62	-8.32	-36.89	-36.30	490.14	-23.51	-58.05
75	-83.14	-9.88	-33.43	-26.57	-153.33	-24.08	-30.74
100	-77.00	-17.06	-39.93	-23.27	-133.47	-26.44	-26.30
125	0.00			-29.50	-12.54	-26.29	-78.25
150	-109.87		-0.14	-13.90	-105.56	-21.13	-26.23
200	-99.29		-1.89	-18.18	-12.03	-29.58	-39.14
225	0.00				-22.82		-49.44
250	-39.07	-3.51	-13.04	-11.20	-69.25	-30.89	-30.11

Table 3.10 Coefficients of variation for the average dynamic viscosity within an umbilical vein (n=3) and between umbilical veins in their native form (n=6). Each Tissue ID (HUV 10 – 15) is the average value of three scaffolds from that vein.

Frequency	Within a Vein						Between Veins	
	G'			η'			G'	η'
	HUV 3	HUV 4	HUV 7	HUV 3	HUV 4	HUV 7	Avg HUV	Avg HUV
Hz	%	%	%	%	%	%	%	%
1	2.53	7.58	1.61	63.91	16.54	5.15	5.06	26.41
5	17.12	23.92	9.22	305.64	-163.04	-178.45	37.93	273.19
10	70.61	23.21	8.25	419.21	-38.17	-44.85	32.32	-334.26
25	63.29	16.19	11.90	-4436.43	-32.63	-32.08	17.46	-80.73
50	76.07	12.58	12.39	-234.36	-31.25	-31.65	4.79	-19.08
75	66.37	12.78	10.60	-150.14	-26.41	-26.08	4.34	-18.27
100	58.84	0.12	8.34	-251.51	-28.19	-34.89	5.41	-22.55
125	0.00		9.64	0.00		-16.73	35.72	-340.85
150	0.00	17.37	10.14	0.00	-19.31	-24.14	39.04	-137.49
200	0.00	51.36	13.36	0.00	-14.18	-25.92	55.05	-110.60
225	0.00		11.01	0.00		-27.58	25.69	-162.56
250	43.88	7.32	5.37	-133.49	-26.13	-23.36	14.74	-33.77

Table 3.11 Coefficients of variation for the average shear modulus and dynamic viscosity of scaffolds from within and between decellularized umbilical veins (n=3).

Frequency	Within a Vein						Between Veins	
	G'			η'			G'	η'
	HUV 2	HUV 5	HUV 8	HUV 2	HUV 5	HUV 8	Avg HUV	Avg HUV
Hz	%	%	%	%	%	%	%	%
1	10.10	13.39	43.23	8.40	30.07	38.15	11.82	12.20
5	15.28	31.87	42.09	22.93	450.98	194.50	13.56	85.16
10	4.42	74.88	43.11	-65.59	-509.70	308.27	19.98	-264.19
25	34.59	46.74	26.79	-50.18	-134.25	-1518.83	25.14	-83.12
50	26.39	38.72	23.38	-46.68	-104.47	-467.66	19.95	-70.45
75	24.75	37.39	21.96	-45.07	-89.31	-241.65	18.84	-60.93
100	27.34	29.79	35.58	-51.49	-89.81	-178.75	14.24	-55.74
125	0.00	29.94	17.38	0.00	-101.52	-130.62	10.41	-38.93
150	26.13	40.31	19.18	-39.69	-73.04	-136.52	21.16	-54.70
200	55.42	56.68	14.60	-38.34	-80.65	-108.05	32.23	-53.61
225	0.00	0.00	11.81	0.00	0.00	-75.42	5.74	-23.14
250	10.58	18.16	11.77	-41.88	-51.00	-65.21	14.11	-47.11

Table 3.12 Coefficients of variation for the average shear modulus and dynamic viscosity of scaffolds from within and between control (decellularized and cultured for 21 days) umbilical veins (n=3).

Frequency	Within a Vein						Between Veins	
	G'			η'			G'	η'
	HUV 1	HUV 6	HUV 9	HUV 1	HUV 6	HUV 9	Avg HUV	Avg HUV
Hz	%	%	%	%	%	%	%	%
1	5.99	2.52	10.31	83.82	30.35	37.01	5.11	31.11
5	4.41	0.00	28.02	142.74	0.00	-90.47	26.75	-408.64
10	5.98	0.00	13.39	620.77	0.00	-50.89	26.52	-102.68
25	29.04	18.66	31.71	-128.92	-50.06	-43.25	19.00	-23.75
50	39.09	1.71	28.91	-102.03	-19.24	-42.50	20.19	-29.62
75	33.75	12.42	29.10	-93.49	-38.91	-45.91	18.82	-20.40
100	21.30	8.74	20.18	-85.48	-38.64	-45.10	15.03	-19.73
125	16.22	0.00	51.76	-75.51	0.00	-52.32	28.17	-21.84
150	33.19	18.80	32.97	-70.70	-32.82	-47.25	11.28	-8.31
200	16.44	39.23	44.28	-19.22	-27.58	-56.81	33.80	-25.62
225	9.42	0.00	25.76	-21.95	0.00	-77.31	6.39	-16.73
250	0.00	0.00	28.37	0.00	0.00	-74.86	13.89	-2.03

Table 3.13 Coefficients of variation for the average shear modulus and dynamic viscosity of scaffolds from within and between umbilical veins that have been recellularized with primary human vocal fold fibroblasts and cultured for 21 days (n=3).

3.4.3 Parametric Modeling of Viscoelastic Shear Properties (*G'* and *η'*)

The data for *G'* and *η'* for each tissue specimen or scaffold were described parametrically using the power law:

$$G' = a f^{b}$$

Equation 3.1 Power law for the elastic shear modulus (*G'*)

$$\eta' = a f^{b}$$

Equation 3.2: Power law for the dynamic viscosity (*η'*)

where *f* is the frequency and a and b are the coefficients. The corresponding coefficient of determination (R^2) was included to determine how well the data fit the model. These models were fitted to the data for the native, decellularized, and recellularized tissues over the frequency range of 10Hz – 225Hz.

Coefficients a and b and Corresponding Coefficients of Determination R^2 for Curve Fitting of Each Data Set.						
	$G' = ax^b$			$\eta' = ax^b$		
Condition	a	b	R^2	a	b	R^2
Nat 13-1	2.861	0.461	0.803	2.997	-0.890	0.988
Nat 13-2	3.305	0.564	0.557	4.504	-0.79	0.907
Nat 13-3	1.969	0.541	0.599	2.685	-0.880	0.801
Nat 14-1	4.463	0.307	0.881	1.871	-0.860	0.999
Nat 14-2	2.170	1.044	0.887	8.110	-0.590	0.891
Nat 14-3	0.649	1.349	0.848	9.776	-0.590	0.804
Nat 15-1	14.960	0.019	0.01	2.591	-0.950	0.700
Nat 15-2	1.583	0.739	0.921	2.451	-0.670	0.796
Nat 15-3	4.386	0.188	0.021	0.942	-0.700	0.981
Average	4.038	0.579		3.992	-0.769	
Std Dev	4.284	0.417		2.990	0.136	

Table 3.14 Linear regression for shear modulus (G') and dynamic viscosity (η') for all native tissues using the power law.

Coefficients a and b and Corresponding Coefficients of Determination R^2 for Curve Fitting of Each Data Set.						
	$G' = ax^b$			$\eta' = ax^b$		
Condition	a	b	R^2	a	b	R^2
Decell 3A	0.007	1.720	0.977	7.855	-1.330	0.998
Decell 3C	41.260	0.769	0.791	61.700	-0.670	0.855
Decell 3D	1.743	0.517	0.945	3.438	-1.010	0.994
Decell 4A	8.463	0.403	0.264	5.812	-0.820	0.920
Decell 4C	11.140	0.171	0.023	7.346	-1.020	0.935
Decell 4F	1.147	0.717	0.902	4.011	-0.960	0.998
Decell 7A	1.144	0.840	0.88	2.058	-0.640	0.987
Decell 7B	1.905	0.793	0.908	3.077	-0.650	0.926
Decell 7D	0.794	1.112	0.923	2.070	-0.440	0.895
Average	7.511	0.782		10.819	-0.838	
Std Dev	13.230	0.445		19.199	0.270	

Table 3.15 Linear regression for shear modulus (G') and dynamic viscosity (η') for decellularized tissues using the power law.

Coefficients a and b and Corresponding Coefficients of Determination R^2 for Curve Fitting of Each Data Set.						
	$G' = ax^b$			$\eta' = ax^b$		
Condition	a	b	R^2	a	b	R^2
Recell 1A	2.203	0.741	0.847	2.512	-0.530	0.867
Recell 1B	1.956	0.513	0.377	1.414	-0.830	0.989
Recell 1C	3.351	0.905	0.849	8.119	-0.590	0.914
Recell 6A	0.048	1.324	0.874	3.533	-1.070	0.955
Recell 6B	2.565	0.536	0.338	3.492	-0.640	0.922
Recell 6C	2.753	0.355	0.236	2.703	-0.810	0.995
Recell 9A	1.285	0.590	0.649	0.887	-0.540	0.801
Recell 9B	2.771	0.408	0.591	1.503	-0.750	0.964
Recell 9C	0.660	1.162	0.981	0.775	-0.160	0.314
Average	1.955	0.726		2.771	-0.658	
Std Dev	1.087	0.339		2.257	0.254	

Table 3.16 Linear regression for shear modulus (G') and dynamic viscosity (η') for recellularized tissues using the power law.

3.4.4 Non-Parametric Statistical Test

The Mann-Whitney *U* test was used to compare the parameters calculated from the linear regression curve-fitting with the power law, to examine if there are significant differences between the following pairs of conditions: Native versus decellularized, native versus recellularized, and decellularized versus recellularized tissues. Although earlier data have shown differences in G' and η' between different conditions, results in Table 3.17 showed that the differences were not statistically significant.

Mann-Whitney *U*								
Condition	**a**				**b**			
	G'		**η'**		**G'**		**η'**	
	Z	p	Z	p	Z	p	Z	p
Native vs. Decellularized	-0.751	0.453	-1.015	0.310	-1.015	0.310	-0.619	0.536
Native vs. Recellularized	-1.280	0.200	-0.927	0.354	-0.839	0.402	-1.283	0.199
Decellularized vs. Recellularized	-0.132	0.895	-1.810	0.070	-0.221	0.825	-1.325	0.185

Table 3.17 Mann-Whitney *U* test for significant differences between the parameters of linear regression curve-fitting for difference pairs of conditions.

CHAPTER 4

DISCUSSION

4.1. Preferred Decellularization Protocol (Experiment I)

The preliminary results showed that three of four variations of the decellularization protocol led to successful decellularization of the HUV tissue, while maintaining the 3-D protein network structure of the human umbilical vein extracellular matrix (ECM). Group 2 was the exception. Although groups 1 and 2 used the same incubation time in the first saline step, which caused osmotic stress on the cells, tissues from Group 1 were properly decellularized while those in Group 2 were not. The remaining decellularization steps for Group 2 were the same as in Group 4, yet Group 4 was properly decellularized as well. Therefore, a possible reason for the unsuccessful decellularization of tissues in Group 2 could be an error in conducting the experiments involving Group 2. Since Groups 1, 3, and 4 were able to successfully decellularize the tissues while maintaining the ECM, the preferred protocol was determined based on the depth of cellular infiltration as well as the biomechanical data. The protocol used for the tissues in Group 4 had the best results in both of these categories and was thus used for Experiments II and III.

4.2. Recellularization

For Experiment I, the scaffolds in Group 1 had no fibroblasts present after 21 days of culture, but had a structured layer present on the abluminal surface (Figure 3.9) that differed from the natural tissue ECM. This structure could possibly be bacterial contaminants since this group was removed from sterility on day 7 in order to be treated with the fluorescent dyes calcein AM and DAPI for visualization under a Ziess LSM confocal microscope. After

examining other HUV tissues with a similar layer, another possibility is that it was part of the umbilical artery located close to the vein due to natural anatomical variability between different cords. Since the automated dissection process dissects the vein from the cord at a predetermined thickness, any portion of an artery located within this range will remain on the abluminal surface of the tissue and could block cellular infiltration. Hence, for Experiments 2 and 3, all veins were visually inspected for the presence of the artery on the abluminal surface of the HUV. Due to a lack of tissue availability, some scaffolds did have the artery on the abluminal surface, but these were not used in the recellularization group, nor used for biomechanical testing. Groups 3 and 4 had the highest level of cellular proliferation and the deepest cellular infiltration into the scaffold. This was likely due to the shorter saline step in the decellularization protocol, resulting in a better pore architecture for cellular attachment and infiltration. Tissues in Group 4 had full cellular infiltration (Figure 3.13), possibly because of a shorter dehydration step than Group 3.

In Experiment II, all recellularized tissues, including three scaffolds from each of the three veins, demonstrated full cellular infiltration. Two to three cell layers are visible on the abluminal surface, with synthesis of new proteins observed histologically in the connective tissue. Figure 3.23b shows the concentrated cell layers on the tissue surface as well as the more sparsely located cells deep in the tissue. Scanning electron micrographs (Figure 3.27) showed the morphology of these cell layers for one scaffold from three different veins. The cells in these layers have a generally flat appearance, with a protrusion where the nucleus can be located. The cells on the top layer showed attachment, were elongated in shape, and were likely viable as indicated by the lighter shade of gray.

4.3. Histological Examination

Tissue thicknesses were examined using the slides with the H&E stain at a total magnification of 334X. The thickness measurements were taken at the widest part of the tissue to partially compensate for any decrease in thickness that may have occurred during histological processing of the tissue, especially during paraffin embedding and ethanol dehydration. Geometrical deformation of the tissue associated with such processing likely resulted in the large difference in thickness between the tissues within a condition. The native HUV tissue had a uniform thickness of 750μm after being dissected frozen. The native HUV tissue expanded significantly upon thawing in water, with an average thickness of 2,650 ± 1059.58 μm, about three and a half times larger than its frozen thickness. Note that not the entire tissue was this thickness and there were portions that did not expand as extensively. After the decellularization process, the average thickness decreased to 1960 ± 269.07 μm. This was a major decrease in thickness, likely due to some tissue degradation as well as the constant tension applied to the tissue while being mounted on the plastic frame. Control scaffolds that were decellularized and cultured for 21 days had an average thickness of 1457 ± 315.33μm, another considerable decrease in thickness. This was most likely due to tissue degradation in the culture media. The recellularized scaffolds had an average thickness of 1043 ± 523.67 μm, within the range of the control scaffolds. However, these recellularized scaffolds appear quite different, with a denser ECM due to the new matrix proteins produced by the human vocal fold fibroblasts.

The histological stains used in the present study were capable of detecting glycogen, hyaluronic acid, chondroitin sulphate (A,B,C), keratan sulphate, mucins, sialomucins, and sulphated sialomucins. Carbohydrates, or glycans, are made up of any of the following:

monosaccharides, disaccharides, oligosaccharides, or polysaccharides. Glycosaminoglycans (GAGs), or mucopolysaccharides, are long linear or branched chains of monosaccharides or repeating disaccharides. Glycogen is the main storage polysaccharide of animal cells and functions as a primary short term energy storage that can be quickly used when the body is in sudden need of glucose. Hyaluronic acid is an acid mucopolysaccharide. Acid muco-polysaccharides are usually composed of two types of alternating monosaccharide units, and one must have an acidic group (carboxyl or sulfuric). Hyaluronic acid is the most abundant GAG and exists in cell coats and in the ECM of connective tissues of vertebrates. Chondroitin is also a GAG with an almost identical structure to hyaluronic acid, except it contains N-acetyl-D-glucosamine residues. It is a small component of ECM, but its sulfuric acid derivates chondroitin sulphate A (chondroitin 4-sulphate) and chondroitin sulphate C (chondroitin 6-sulphate) are major structural components of cell coats and connective tissue structures. Keratan sulphate, or keratosulphate, is a sulphated GAG and is a large highly hydrated molecule mostly found in joints to cushion mechanical stress. When acid mucopolysaccharides occur as complexes with specific proteins, they are called mucins or mucoproteins. Mucins are found in body tissues including connective tissues and supporting tissues. Sialomucins are mucins that contain sialic acid. (Lehninger, 1975)

The different histological stains are used to identify particular molecular constituents by comparing certain pairs of stains. Tissues treated with Alcian Blue will stain positive for hyaluronic acid, chondroitin sulfates A, B, and C, keratosulphate, sialomucins, and sulphated sialomucins. Treatment of those same tissues with hyaluronidase followed by staining with Alcian Blue will remove the hyaluronic acid and chondroitin sulphates A and C. By comparing the loss of color intensity between the two slides, it is possible to visually observe the

constituents that were most abundant, or that were responsible for most of the color intensity. If a large amount of blue color is lost once treated with hyaluronidase, this means most of the color intensity from the original Alcian Blue stain was due to a large amount of hyaluronic acid and possibly chondroitin sulphates A and C. Therefore the following molecular constituents did not contribute much to the color intensity of the Alcian Blue stain: chondroitin sulphate B, keratosulphate, sialomucins, and sulphated sialomucins. The Safranin-O stain further confirms the abundance of HA and chondroitin sulfates A and C. An intense Safranin-O staining and Alcian Blue staining combined with a significantly less intense staining of hyaluronidase treated tissues would indicate that HA and chondroitin sulphates A and C contribute the most to the color intensity, since hyaluronidase treated tissues should stain any chondroitin sulfate B, keratosulphate, sialomucins, and sulphated sialomucins present.

Since PAS can be used to stain glycogen, mucins, sialomucins, and sulphated sialomucins, comparing this stain to the results mentioned earlier can be used to determine which of these constituents is contributing most to the stain. If the hyaluronidase treated tissues lose a significant amount of color, then there is not an abundance of sialomucins and sulphated sialomucins. Once this is determined, then the PAS stain color intensity can be attributed to glycogen and mucins.

Native HUV tissue stained with Alcian Blue (Figure 3.20c) showed a general light blue background stain, with the cells stained pink, and a significant amount of fibers stained dark blue. These fibers may represent glycosaminoglycans, particularly hyaluronic acid (HA), along with other molecular constituents such as chondroitin sulfates A, B, and C, keratin sulphate, sialomucins, and sulphated sialomucins. This finding demonstrates the large amount of HA present in the native tissue, which Gogiel et al. (2003) previously measured to be 70% of the

GAG content in Wharton's Jelly. Treatment with testicular hyaluronidase (Fig. 3.20d) removed the appearance of hyaluronic acid, and chondroitin sulfates A and C. The resulting tissue was stained extremely light blue and practically transparent due to the enzymatic digestion of these molecules. This significant change in staining color confirmed the abundance of HA and perhaps chondroitin sulfates A and C in the native HUV tissue. The PAS stained tissues (Fig. 3.20e) showed no red color, but different shades of purple, likely due to the aging of the available Schiff reagent (Carson, 1997). The native tissue has some dense regions of purple that represent glycogen, mucins, sialomucins, and sulphated sialomucins, mostly around the location of the cells. Staining with Safranin-O (Fig. 3.20f) should have been specific for glycosaminoglycans; however, it probably did not stain hyaluronic acid very strongly since the results with Alcian Blue showed intense hyaluronic acid staining. These results agreed with those of Sobolewski et al. (1997), suggesting that sulphated GAGs make up a distinctly low percent (each between 4-10%) of the total GAG content.

The decellularized tissue (Figure 3.21) showed a marked loss of dark blue fibers, depicting how much hyaluronic acid (HA) remained in the tissue. The loss can be contributed to tissue degradation as well as some HA having been washed out of the tissue. Glycogen, mucins, and sialomucins were still present as shown by the dark purple areas of the PAS stain, but there were fewer areas where this stain was apparent. As in the native HUV tissue, no GAGs were detected in the decellularized tissue, indicating that it did not stain HA very well since the Alcian Blue results indicated that abundant HA was present in the tissue. Any other GAGs that it might have stained were not apparent since they existed in much smaller quantities than HA.

The control (decellularized and cultured) tissue showed a significant loss of HA in the Alcian Blue images (Figure 3.22). After 21 days of culture, the tissue became less dense and had

slight degradation, contributing to the loss of the hyaluronic acid. Treatment with hyaluronidase showed an even lighter stain that could only be seen at a lower magnification. There were no signs of the molecular constituents specifically stained by PAS or Safranin-O. The control tissues show a significantly different stain and structure from the native and the decellularized tissue due to the 21 days of culture. Overall, there was a loss of most of the molecules of interest, a decrease in density, and a decrease in tissue thickness.

In the recellularized tissues it was apparent that the human vocal fold fibroblasts synthesized new ECM proteins, including HA (Figure 3.23). Tissues stained by Alcian Blue (Figs. 3.23c, 3.23d) showed that the amount of hyaluronic acid present was not as abundant as that of decellularized tissue, yet it was more than that of the control tissue. Therefore, only some of the HA was lost during the culture, while some HA could be attributed to the metabolic activities of the cells proliferating and infiltrating the scaffold, as part of the process of ECM remodeling. This was most apparent at the abluminal surface, where cell layers have attached and formed new ECM with dark alcian blue stain depicting the HA. Staining with PAS (Fig. 3.23e) also showed an increase in the amount of mucins, glycogen, and sialomucins, particularly at the abluminal surface where the cell layers are connected. This condition is the only one that had a positive result for GAGs using the Safranin-O stain (Fig. 3.23f). Extremely large amounts of HA and other GAGs were present in the new ECM at the abluminal surface, which was not apparent even with the native HUV tissue. These sulphated GAGs are able to bind with amino acids on the surface of collagen fibers, causing Wharton's jelly to be more compact as seen in the recellularized scaffolds.

Masson's Trichrome (Figure 4.1) stain collagen fibers in the tissue blue. Cell nuclei will appear black, and cytoplasm, keratin, muscle fibers, and intercellular fibers will appear red.

Figure 6.1 shows Masson's Trichrome staining of native, decellularized, control, and recellularized tissues. These images show blue collagen fibers on the abluminal surface (left side), a dark red/pink stain of the muscle on the luminal side (right side), and a red/pink stain of the cells and their newly formed ECM on the abluminal surface as well as within the tissue. The native tissue shows a bright blue color for collagen and a bright dark red color for the muscle on the luminal side. After decellularization, there is a noticeable decrease in the color intensity of the collagen and muscle fibers. The control tissue, which has been decellularized and cultured for 21 days, shows an even lower color intensity for collagen and muscle. However, the recellularized tissue has regained the collagen color intensity showing that new collagen is being synthesized by the fibroblasts on the surface of and within the scaffold.

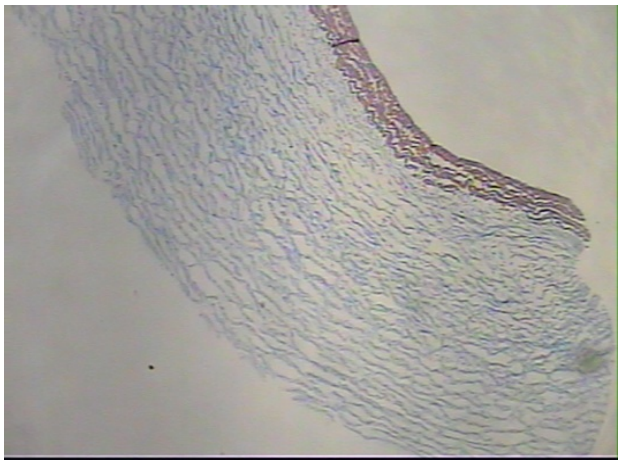

(a)

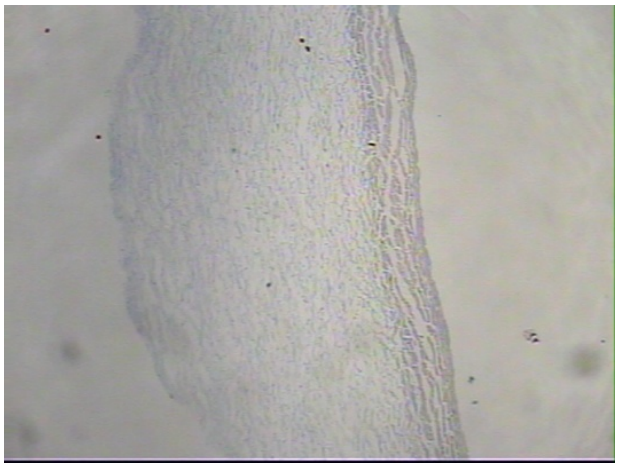

(b)

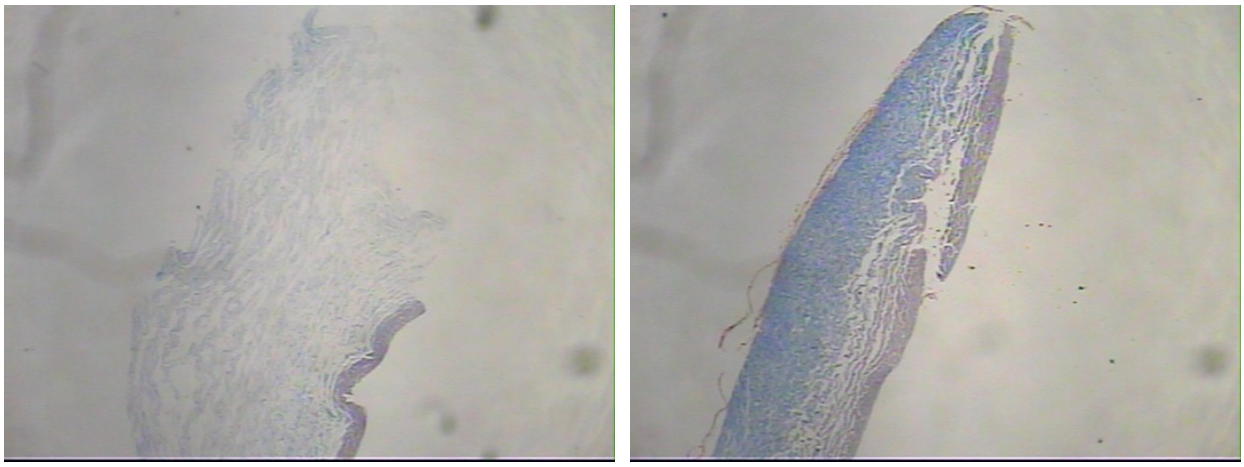

(c) (d)

Figure 4.1 Masson's Trichrome staining of (a) native, (b) decellularized, (c) control (decellularized and cultured), (d) and recellularized human umbilical veins. All photos are oriented such that the ablumen of the tissue is on the left side and the lumen on the right side.

For image analysis of the Masson's trichrome slides, the relative staining intensities of collagen for all conditions were within the same range (Table 3.5). The ranges of the relative intensities for the first and second image analysis were 75-85% and 80-84%. As mentioned before, the large range for the native tissues (75% intensity) was due to the large standard deviation that resulted from the positioning of one of the embedded tissues for one vein. A different scaffold from that same vein was used as a replacement for the second analysis, which was why the range was smaller. The amount of collagen present in each tissue decreased as they went from native to decellularized to cultured. Some collagen in the Wharton's jelly may have been removed during the decellularization process, and more collagen was removed during the culture due to tissue degradation. The seeded vocal fold fibroblasts synthesized new collagen in their new ECM during remodeling of the scaffold, causing the increase in collagen seen in the image analysis. This new collagen, along with the increase in the amount of GAGs seen in the Safranin-O stain likely contributed to the viscoelastic changes of the scaffolds, to be discussed below.

4.4. Scanning Electron Microscopy

Scanning electron micrographs of the native tissue (Figure 3.24) showed a dense abluminal surface with large fiber bundles, although it was not as dense as the tissue on the luminal side (Figure 3.20a). Some tissue surfaces appeared denser than others, and Figure 3.24c may have shown a portion of an artery that was too close to the vein. Decellularized tissue showed a looser structure throughout (Figure 3.21a, 3.2, 3.6 and 3.8), as it can be seen by the larger quantity of small fibers on the surface. The same can be said of the control tissue. All tissues demonstrated an intact 3-D protein network structure of the extracellular matrix, despite being subjected to the decellularization and culture processes. On the other hand, there might be some tissue degradation and loss of molecules such as collagen, HA, and GAGs that could not be observed in SEM, as reflected by the changes in densities and viscoelastic properties of the tissues.

4.5. Biomechanical Properties

In Experiment I, native HUV tissue and the human vocal fold tissue had similar values for the elastic shear modulus and dynamic viscosity. In general, decellularized scaffolds had lower values of G' and η' than natural HUV tissue and human vocal fold tissue, whereas recellularized scaffolds generally had higher values. The main exceptions to this trend are the recellularized scaffolds in Group 4, which had values within the range of both the native HUV tissues and human vocal fold tissues. Although Group 3 had considerable cellular proliferation on the surface, it is likely that the extensive cellular infiltration seen in Group 4 is the reason for such similar values to that of human vocal fold cover. These infiltrated cells could be producing proteins at various concentrations that may be comparable to the concentrations produced in natural tissues. The decellularized scaffolds in Group 2 had a higher G' and η' values than other

decellularized scaffolds possibly because of the native cells that remained in the scaffold after the decellularization protocol. Remaining native cells combined with the seeded vocal fold fibroblasts probably producing abnormal amount of collagen and other molecules may have contributed to the Group 2 scaffolds having the highest G' and η' values.

Biomechanical results for the second experiment differed slightly from those in the first experiment because more veins were tested per condition, giving more a more reliable representation of that condition. Also, most data from 165 Hz to 180 Hz were omitted because those frequencies are too close to the resonance frequency of the system. Data taken at above 250 Hz was discarded due to the noise limits of the system. In Experiment I, native tissue and human vocal fold tissue have higher values than those of decellularized tissue. Experiment II shows that the average values of G' and η' for decellularized tissue are larger than those of human and native tissue above 25Hz (Figures 3.30 and 3.31). This means that steps in the decellularization process caused the tissue to become stiffer. Control tissue was slightly above human and native tissue values likely because it was stiffer after the decellularization process and became less stiff in culture due to tissue degradation and a looser tissue structure. Recellularized tissue had G' and η' values slightly lower than those of human and native HUV tissue because the fibroblasts were actively producing proteins and remodeling the tissue (Figures 3.32 and 3.33). Therefore, the recellularized tissue obtained viscoelastic properties favorable for vibration, similar to those of human vocal fold tissues. The values of G' and η' versus frequency for native, decellularized, control, and recellularized tissues modeled that of the human vocal fold. Average values of the six native tissues were similar to those of the human vocal fold throughout all frequencies.

The dissection method originally used would freeze, thaw, refreeze, and thaw the tissues again before using them in an experiment (Daniel et al., 2005). This brought into question how

the natural biomechanical properties of this tissue might have changed due to the freezing and thawing processes. In order to determine the effect of such freezing and thawing, the new process of using the tissue once it has been thawed after dissection was compared to the conventional method, as well as to manually dissected native HUV tissues without any freezing (Figures 3.28 and 3.29). The G' values for the new method were in between the two values for the old method. This could possibly mean that there is a change in viscoelastic properties due to freezing and thawing. Since these values lie in between the values of the two native tissues from the old method, the direction in which the stiffness changes cannot be determined. However, the manually dissected veins, which represented the most natural state of the tissue, had higher G's than the native tissues of the new method. Therefore the freezing and thawing caused a slight decrease in the stiffness of the native tissue as compared to its natural state. Chan and Titze (2003) found that quick freezing of canine vocal fold tissues with liquid nitrogen prior to storage at -20^{o}C had similar values to fresh canine vocal fold tissues. They also found that slow freezing before storage at -20^{o}C resulted in a significant decrease in G' and η' with respect to fresh canine vocal fold tissue. The new method still has the quick freezing at -80^{o}C, but has eliminated the slow refreezing at -20 prior to dissection, which is why the values of G' and η' for native HUV tissue using the new method are very close to those of human vocal fold tissues. Other findings by Chan and Titze (2003) showed that the elastic shear modulus and dynamic viscosity of 24-hour-postmortem canine vocal fold tissues are not significantly different from those of fresh canine vocal fold tissue. The human vocal fold tissue used for comparison in this experiment was obtained within 24 hours after they were harvested.

The abnormalities in the data at higher frequencies for the manually processed tissue were likely due to the fact that the tissue did not have an even surface and was slightly thicker than tissues dissected with the automated method, since it was done by hand. The reason for the

large discrepancies in G' values for the native tissues with the automated dissection method were that the data for each of those came from only one scaffold from one vein. As seen earlier, there can be large differences in the viscoelastic properties between veins, and even within a vein.

4.6. Cell Recovery

One million cells were seeded onto each scaffold, with an average seeding density of almost 5,000 cells/mm^2. The average initial attachment was 1.74 – 1.82% of the cells seeded, which represents 17,000 to 18,000 cells (Table 3.6). Xu et al (2007) found a similar initial attachment of about 10,000-20,000 cells using a seeding density of 10,000 cells/mm^2 for their two cell recovery trials of seeding human vocal fold fibroblasts onto a bovine acellular vocal fold scaffold. This indicated that there may be a threshold in the number of cells/mm^2 after which the initial cellular attachment was no longer dependant on the seeding density. There was cellular proliferation between day 0 and day 6, but the number of cells increased dramatically from day 6 to day 9 (Figure 3.34 and 3.35), similar to what was observed on day 7 in Xu et al. Taking this into account, the highest level of cellular replication probably occurred between days 7 and 9. Xu et al.'s final cell count was about 250,000 cells per scaffold. The average number of cells per scaffold surpassed that number between days 9 and 12. This quicker cell growth was likely the result of the present primary human vocal fold fibroblasts being taken from passage 4, whereas those in Xu et al. were taken from passage 10. This was important as replicative senescence may result in a decrease in the growth rate of vocal fold fibroblasts in later passages (such as passage 10), due to unstable gene expressions in the primary cell culture. The average final cell count was about 480,000 cells per scaffold (3,000 cells/mm^2). The number of cells generally increased up to day 12, after which in some tissues it reached a plateau and in others it continued to increase. The data from day 18 is an exception to this general trend of increase. The average

final cell count for scaffolds from Experiment II was about 316,000 cells per scaffold, which lies within the range between day 18 and day 21 of the cell recovery results.

4.7. Statistical Analysis

The plots of the average log G' and log η' for native tissue versus recellularized tissue (Figures 3.36-3.39) showed how different these values were from each other. In general, G'and η' values were larger for the human vocal fold cover than for the recellularized tissues. This was seen in the biomechanical data discussed earlier. However the plots of the bias versus the average values (Figures 3.40 – 3.43) showed that most of the results for the recellularized tissue lied within two standard deviations of the G' and η' of the human vocal fold. The G' and η' values that had the largest difference corresponded to the frequencies of 5, 10, and 250 Hz, which were the limits of the rheometer system. Viscoelastic data obtained at these frequencies were not as consistent, and this explained the one point that lied outside of the two standard deviations for η' (Figure 3.42). The recellularized data at each frequency lied within two standard deviations of the human data, supporting the suggestion that they have similar biomechanical properties.

The coefficients of variation (CVs) were relatively large within and between veins (Tables 3.8-3.13). Some data showed larger variations between the samples within a vein, and other showed the opposite. This can be attributed to having a small sample size in the present study, so that any one "outlier" samples would have a tremendous effect on the average data, skewing the overall results.

The shear modulus and dynamic viscosity of individual specimens were plotted on a log-log scale as a function of frequency (10Hz – 225Hz) and were fit to power laws. The frequency range was from 10Hz to 225Hz, which is the most reliable range of the system. For the shear

modulus (G'), as seen in earlier plots, the data appeared linear on the log-log scale. Most R^2 values were in the 0.9 range, but a few values were considerably lower due to missing data points at certain frequencies where measurements could not be made. The Mann-Whitney *U* test compared three pairs of tissue processing conditions on the parameters (a and b) of the power law and no significant differences were found between the conditions. Although the plots of the shear modulus and dynamic viscosity showed general trends and differences over the frequency range for the different conditions, these differences were not significantly different from each other. The comparison between the parameters for η' of decellularized and recellularized scaffolds was closest to reaching the level of significance, with $p = 0.070$. The plot of dynamic viscosity versus frequency for all conditions showed that of these three groups, the decellularized and recellularized data have the largest difference.

CHAPTER 5

CONCLUSIONS

The objective of this study was to develop a procedure by which the human umbilical vein (HUV) could be transformed into a biodegradable, acellular allogeneic scaffold. The structure of the resulting "tissue engineered" acellular HUV scaffold was examined histologically by a variety of stains and by scanning electron microscopy. The biocompatibility of the scaffold was examined by recellularization with primary culture human vocal fold fibroblasts, and the proliferation of cells in the scaffold was assessed by cell recovery with trypsinization. The viscoelastic properties of the scaffold were also measured with a custom-built, linear simple shear rheometer system. The results of the study are summarized below:

- A preferred protocol was found for the decellularization of the native HUV tissues for fabrication of the acellular HUV scaffold. Results of Experiment I suggested that the method of Group 4 yielded better results than the other methods. This was indicated by the observations of full decellularization in the tissues, an intact 3-D ECM protein structure in the acellular scaffolds, 2-3 cell layers on the abluminal surface of the recellularized tissues, full cellular infiltration, as well as viscoelastic properties of the recellularized tissues being close to those of the human vocal fold cover.
- Native HUV tissue was rich in molecular constituents that would help cellular proliferation and infiltration. Decellularization was shown to partially remove some of these molecules, such as HA and collagen. However, they were found to be recovered through recellularization of the tissue, as shown histologically with the various stains, and also in the image analysis of the relative content of collagen.

- There was a slight decrease in the frequency averaged elastic shear modulus, G', and the dynamic viscosity, η', for the native HUV tissues obtained from the automated dissection method as compared to the manually dissected native tissue. The quick freezing process could be responsible for this difference. However, results from the quick freezing, thawing, and slow freezing conventional dissection method were both higher and lower than those of the manual dissection. The slow freezing process likely caused a more significant change in the viscoelastic properties of the native HUV tissue.
- The biomechanical properties of the native HUV tissue and the human vocal fold cover were very similar. All tissues followed the same trend for G' and η', but the decellularized and control tissues showed higher values. Recellularized tissue showed a decrease in G' and η' as compared to the decellularized and control tissues, probably as a result of the newly synthesized proteins and tissue remodeling with the seeded human vocal fold fibroblasts. Based on the small sample size of this study, Bland-Altman plots showed that the G'and η' of the recellularized tissues were comparable to those of the human vocal fold cover (within two standard deviations of the human values), suggesting that the remodeled scaffold would facilitate vocal fold vibration.
- Initial attachment of primary human vocal fold fibroblasts onto the abluminal surface of the acellular HUV scaffold was found to be low as compared to the seeding density. Fibroblasts from passage 4 proliferated faster and became more numerous than similar cells from passage 10 in previous research. In twelve days, the cell count for the HUV tissue outnumbered the final cell count (after 21 days of culture) of previous studies. These results supported the potential of the HUV as a tissue-engineered acellular allograft for the surgical repair of vocal fold lamina propria disorders. However, these results

should be considered as preliminary due to the small sample size and the large data variability. They must be corroborated by further studies with additional samples.

CHAPTER 6

RECOMMENDATIONS

Further studies involving a larger number of the HUV specimens will be necessary to provide a larger statistical power for the data analysis, given the large variability of the data observed. An experiment examining more veins should get a better estimate of the biomechanical data since the data are somewhat noisy. Also, each vein should have scaffolds examined at all conditions so that the effect of each condition is apparent within the vein. Since all veins expand to different thicknesses after dissection, there is inherent variation among thicknesses taken from the different veins. If one vein was used across all conditions, the data can be normalized with respect to that vein. Future cell recovery experiments will also need more samples since it was apparent for some scaffolds the number of cells continued to increase after day 12, while for others it reached a plateau. Also, variation of the initial cell seeding density might be useful to determine the optimal seeding density. This can be useful in the future given a limited availability of primary culture human vocal fold fibroblasts.

Further studies should also involve quantitative measurements of the soluble matrix proteins in the media samples, using biochemical assays such as ELISAs and the Sircol collagen assay, in order to track the metabolic synthesis of the proteins (including collagen, elastin, decorin, fibronectin, hyaluronic acid) by the vocal fold fibroblasts, as a function of the culture time and condition.

References

Abbas, A.K., Lichtman, A.H. (2005) *Cellular and Molecular Immunology*. 5th Edition. Philadelphia: Elsevier Saunders, pp. 369-386.

Benninger, M.S., Alessi, D., Archer, S., Bastian, R., Ford, C., Koufman, J., Sataloff, R.T., Spiegel, J.R., Woo, P. Vocal fold scarring: current concepts and management. *Otolaryngol Head Neck Surg*. 1996; **115**(5): 474-82.

Bland, J.M., Altman, D.G. Statistical methods for assessing agreement between two methods of clinical measurement. *The Lancet* 1986; p. 307–310.

Bland, J.M., Altman, D.G. Comparing two methods of clinical measurement: A personal history. *International Journal of* Epidemiology 1995; **24**(3) suppl. 1: S7–S14.

Carson, F.L. (1997) *Histotechnology. A Self-Instructional Text.* 2nd Edition. Chicago: American Society of Clinical Pathologists, pp. 95-96, 113-116, 118-121, 134-136, 138-140,

Chan, R.W., Fu, M., Young, L., Tirunagari, N. Relative contributions of collagen and elastin to elasticity of the vocal fold under tension. *Annals of Biomedical Engineering* 2007; **35**: 1471-1483.

Chan, R.W., Titze, I.R. Effect of postmortem changes and freezing on the viscoelastic properties of vocal fold tissues. *Annals of Biomedical Engineering* 2003; **31**: 482-491.

Chan, R.W., Titze, I.R. Viscoelastic shear properties of human vocal fold mucosa: Measurement methodology and empirical results. *J. Acoust. Soc. Am*. 1999; **106**(4): 2008-2021.

Chan, R.W., Titze, I.R. Dependence of phonation threshold pressure on vocal tract acoustics and vocal fold tissue mechanics. *J. Acoust. Soc. Am.* 2006; **119**(4): 2351-2362.

Chan, R.W., Lee, B., Rodriguez, M. A controlled-strain, simple shear rheometer for linear viscoelastic characterization of vocal fold tissue. Society of Rheology Meeting, Lubbock, TX. February 17, 2005.

Colton, R.H, Casper, J.K. (1996) *Understanding Voice Problems. A Physiological Perspective for Diagnosis and Treatment*. 2nd Edition. Baltimore: Lippincott Williams & Wilkins, pp. 66-74, 241-252.

Culling, C.F.A., Allison, R.T., Barr, W.T. (1985) *Cellular Pathology Technique*. 4th Edition. London: Butterworth & Company Publishing, p. 218.

Daniel, J., Abe, K., McFetridge, P.S. Development of the human umbilical vein scaffold for cardiovascular tissue engineering applications. *ASAIO Journal*. 2005; **51**:252-261.

Dardik, H. The second decade of experience with the umbilical vein graft for lower-limb revascularization. *Cardiovascular Surgery* 1995; **3**(3): 265-269.

Dardik, H., Ibrahim, I.M., Sprayregen, S., Dardik, I.I. Clinical experience with modified human umbilical cord vein for arterial bypass. *Surgery* 1976; **79**(6):618-624.

Dardik, H., Miller, N., Dardik, A., Ibrahim, I.M., Sussman, B., Barry, S.M., Wolodiger, F., Kahn, M., Dardik, I. A decade of experience with the glutaraldehyde-tanned human umbilical cord vein graft for revascularization of the lower limb. *J. Vasc. Surg*. 1988; **7**:336-346.

Dardik, I., Dardik, H. Vascular Heterograft: Human Umbilical Cord Vein as an Aortic Substitute in Baboon. *J. Med. Prim*. 1973; **2**:296-301.

Gray, S.D., Titze, I.R., Alipour, F., Hammond, T.H. Biomechanical and histologic observations of vocal fold fibrous proteins. *Annals of Otology, Rhinology & Laryngology*. 2000; **109**: 77-85.

Gogiel, T., Bankowski, E., Jaworski, S. Proteoglycans of Wharton's jelly. *The International Journal of Biochemistry & Cell Biology*. 2003; **35**:1461-1469.

Kiernan, J.A. (2001) *Histological & Histochemical Methods. Theory & Practice.* 3rd Edition. London: Arnold Publishers. pp. 236-237.

Lai, P., Chang, Y., Chen, S., Wang, C., Liang, H., Chang, W., Sung, H. Acellular biological tissues containing inherent glycosaminoglycans for loading basic fibroblast growth factor promotes angiogenesis and tissue regeneration. *Tissue Engineering* 2006; **12**(9): 2499-2508.

Lehninger A.L. (1975) Biochemistry, 2nd Edition. New York: Worth Publishers, Inc., pp. 249-273.

McFetridge, P.S., Daniel, J.W., Bodamyali, T., Horrocks, M., Chaudhuri, J.B. Preparation of porcine carotid arteries for vascular tissue engineering applications. J. *Biomed. Mater. Res.* 2004; **70A**: 224-234.

Meyer, F.A., Laver-Rudich, Z., Tanenbaum, R. Evidence for a mechanical coupling of glycoprotein microfibrils with collagen fibrils in Wharton's Jelly. *Biochimica et Biophysica Acta* 1983; **755**: 376-387.

Nanaev, A.K., Kohnen, G., Milovanov, A.P., Domogatsky, S.P., Kaufmann, P. Stromal differentiation and architecture of the human umbilical cord. *Placenta*. 1997; **18**:53-64.

Pawlicka, E., Bankowski, E., Jaworski, S. Elastin of the Umbilical Cord Arteries and its alterations in EPH Gestosis (preeclampsia). *Biology of the Neonate* 1999; **75**:91-96.

Romanowicz, L., Sobolewski, K. Extracellular matrix components of the wall of umbilical cord vein and their alterations in pre-eclampsia. *J. Perinat. Med*. 2000; **28**:140-146.

Schmidt, C.E., Baier, J.M. Acellular vascular tissues: natural biomaterials for tissue repair and tissue engineering. *Biomaterials* 2000; **21**:2215-2231.

Sobolewski, K., Bankowski, E., Chyczewski, L., Jaworski, S. Collagen and glycosaminoglycans of Wharton's Jelly. *Biology of the Neonate*. 1997; **71**: 11-21.

Sobolewski, K., Malkowski, A., Bankowski, E., Jaworski, S. Wharton's jelly as a reservoir of peptide growth factors. *Placenta*. 2005; **26**:747-752.

Titze, I.R. (2000) *Principles of Voice Production*. Second Printing. Iowa City, IA: National Center for Voice and Speech.

Titze, I.R., Svec, J.G., and Popolo, P.S. Vocal dose measures: quantifying accumulated vibration exposure in vocal fold tissues. *J. Speech Lang. Hear. Res.* 2003; **46**: 919-932.

Walles, T., Giere, B., Macchiarini, P., Mertsching, H. Expansion of chondrocytes in a three-dimensional matrix for tracheal tissue engineering. *Ann Thorac Surg* 2004; **78**:444-448.

Wayne, J.S, McDowell, C.L, Willis, M.C. Long-term survival of regenerated cartilage on a large joint surface. J. *Rehabil. Res. Dev*. 2001; **38**(2): 191-200.

Xu, C.C., Chan, R.W., Tirunagari, N. A biodegradable, acellular xenogeneic scaffold for regeneration of the vocal fold lamina propria. *Tissue Engineering* 2007; **13**: 551-566.

Young, B., Lowe, J.S., Stevens, A. & Heath, J.W. (2006) Wheater's Functional Histology: A Text and Colour Atlas. (5th ed.). Philadelphia, PA: Elsevier, pp. 385.

Vitae

Maritza Rodriguez received her Bachelor of Science degree in Chemical Engineering as well as a concentration in Spanish Language at Massachusetts Institute of Technology in Cambridge, MA in June 2003. During her undergraduate studies, she participated in the Undergraduate Research Opportunities Program and conducted research at the Biotechnology Process Engineering Center (BPEC) under the supervision of a graduate student in a lab supervised by Linda Griffith. The year following graduation, she continued to work in that lab as a lab technician while preparing for her graduate studies.

In August 2004, she started her doctorate degree in Biomedical Engineering in a joint program between the University of Texas Southwestern Medical Center at Dallas (UTSW) and the University of Texas at Arlington (UTA). Under the supervision of Dr. Roger W. Chan in the department of Otolaryngology at UTSW, she conducted her research in tissue engineering, particularly using the decellularized human umbilical vein (HUV) as an allogeneic scaffold for vocal fold tissue engineering. Maritza will receive her Master of Science in Biomedical Engineering from UT Southwestern Medical Center in December 2007.

While finishing her master's research at UTSW, she applied for the Graduate Assistance in Areas of National Need (GAANN) scholarship at the University of Oklahoma (OU) in Norman, OK. She was awarded this scholarship and transferred to the Bioengineering program at the University of Oklahoma in August 2007. She is currently conducting her doctorate research in tissue engineering under the supervision of Dr. Peter McFetridge.